Functional Modulation and Adaptive Responses to PKC Targets on Cardiac Troponin I

by

Sarah Elizabeth Lang

**A dissertation submitted in partial fulfillment
of the requirements for the degree of
Doctor of Philosophy
(Cellular and Molecular Biology)
in the University of Michigan
2014**

Doctoral Committee:

Associate Professor Margaret V. Westfall, Chair
Associate Professor Daniel E. Michele
Associate Professor Mark W. Russell
Professor Linda C. Samuelson

To my mother and father,

whose unceasing love inspired this work.

ACKNOWLEDGEMENTS

During my time as a graduate student, I have been privileged to work with wonderful people who have made my experience extremely rewarding. First and foremost, I would like to thank my mentor, Dr. Margaret Westfall for her tireless efforts during my training. I cannot convey how much I appreciate the mentorship I received during my time in lab. Your patience and guidance in improving my speaking, writing, and thinking skills has been invaluable during my development as a scientist. Your passion for the field is truly inspiring, and I look forward to continuing a scientific career with the strong skill set you have helped me build. I would also like to thank my dissertation committee, Drs. Daniel Michele, Mark Russell, and Linda Samuelson, for their insight and support during my dissertation work. Your suggestions and guidance has led to an exciting and interesting story. I would also like to take this opportunity to thank the past members of the Westfall lab. Their expertise and the training I received were instrumental in the completion of my dissertation work. Finally, I'd like to thank the Cellular and Molecular Biology program for their support during my graduate career. Particularly, it has been wonderful to work with Drs. Jessica Schwartz, Robert Fuller and CMB administrator Cathy Mitchell for going above and beyond for CMB graduate students.

Words cannot express the gratitude I have for the unceasing love my family has given me throughout my life. I would like to thank my mother, whose un-wavering faith in me has been instrumental throughout my life. You are the picture of provided a wonderful example of strength, perseverance and dedication throughout my life. I would also like to thank my father, whose memory inspired this dissertation work. Thank you for instilling the idea that, with hard

work, I could accomplish any goal I set my mind. You are missed every day. Finally, I would like to thank the person I have been privileged to call my best friend and am now honored to call my husband. You have stood by me through it all, and a simple thank you is not enough. To my family, I love you all.

Table of Contents

LIST OF FIGURES

LIST OF TABLES

ABSTRACT

Cardiac pump performance is highly dynamic and the rhythmic contraction and relaxation during a single heart beat is produced by myofilaments composed of highly ordered thin and thick filaments arranged in sarcomeres within each cardiac myocyte. The thin filament, molecular switch protein cardiac troponin I (cTnI) toggles between actin and the Ca^{2+}-binding subunit, troponin C (cTnC) to regulate muscle contraction. Cellular signaling via the protein kinase C (PKC) pathway, modulates contractile function and phosphorylates cTnI on serines (Ser)23/24, Ser43/45, and threonine (Thr)144. While the functional effects of cTnISer23/24 phosphorylation are well characterized, the role of cTnISer43/45 remains controversial.

During cardiac dysfunction, cTnISer43/45 phosphorylation increases, but it is unclear whether this phosphorylation improves or reduces function. Gene transfer into intact cardiac myocytes is used in the present study to examine the functional role of cTnISer43/45 and reconcile divergent *in vitro* and *in vivo* responses. Phospho-null (Ala) substitution at cTnISer43/45 diminished myocyte shortening amplitude and myofilament Ca^{2+} sensitivity of tension, indicating Ala substitution is not functionally conservative at this site. However, cTnISer43/45 phospho-mimetic (Asp) substitutions produced the anticipated decrease in basal contractile function and myofilament Ca^{2+} sensitivity 2 days after gene transfer into myocytes. Moreover, cTnISer43Asp and cTnISer45Asp individually modulated function.

Interestingly, the slowed shortening and re-lengthening rates returned toward control values after more extensive sarcomeric cTnI replacement at day 4. Further studies demonstrated adaptations within myocytes, including accelerated Ca^{2+} re-uptake into the sarcoplasmic

reticulum and increased sarcomeric protein phosphorylation. Overall, these adaptations are proposed to communicate and fine-tune the modulatory effects of cTnISer43/45 phosphorylation and/or phospho-mimetic substitution. This communication was further examined with Asp substitutions at cTnI Ser23/24 and Ser43/45 (e.g. cTnIAsp$_{Quad}$). Studies with cTnIAsp$_{Quad}$ showed Ser23/24 and Ser43/45 modulate function through separate mechanisms, Ser23/24 enhances the functional response to Ser43/45, and cTnIAsp$_{Quad}$ induces a different adaptive signaling response than cTnISer43/45Asp. Overall, the present experiments identify cTnISer43/45 phosphorylation as a modulatory brake in the heart, which is fine-tuned by adaptive signaling. This modulatory brake is predicted to play an important role during sustained stress and may contribute to heart failure with the loss of adaptive signaling in cardiac myocytes.

CHAPTER 1

INTRODUCTION

Regulation of cardiac performance

The heart is a muscular organ, designed to pump blood to peripheral tissues for delivery of oxygen and nutrients and removal of waste [1] . Mammalian hearts have 4 chambers composed of 2 atria and 2 ventricles, and the ventricles are separated from the atria and large arteries by valves to maintain unidirectional blood flow [1, 2]. Blood moves through the heart via rhythmic contraction and relaxation of each chamber, with the larger ventricular chambers responsible for blood delivery to the arteries. Rhythmic pumping of the ventricles is separated into two phases known as systole (contraction) and diastole (relaxation), and individual cardiac myocytes are responsible for this rhythmic pumping action (Fig. 1.1A). A single electrical stimulus (e. g. an action potential) is sufficient to initiate cardiac depolarization and contraction of each chamber throughout the heart because myocytes are arranged as a functional syncytium to rapidly spread depolarization from cell to cell [1, 2]. Following pressure development and the ejection of blood into the vasculature, myocytes repolarize, and pressure returns to resting levels as each chamber in the heart relaxes. During this relaxation phase, valves located between the atria and ventricles open, and the ventricles fill with blood in preparation for the next cardiac cycle [1, 2].

Cardiac contraction is elegantly regulated by internal and external elements to match blood flow with the metabolic demands of peripheral organs. The amount of blood pumped from the ventricles into large arteries, such as the aorta, during a cardiac cycle is measured as stroke volume and the amount of blood pumped per minute is measured as cardiac output (CO). The load on the heart prior to contraction (preload) or the load experienced during contraction (afterload) can intrinsically regulate CO, as described by the Frank-Starling mechanism [1, 2]. External factors, including neurohormones, also work to regulate cardiac pump function over

longer periods of time [1, 2]. This neurohormonal input produces post-translational modifications of many cellular proteins including proteins located in the myofilaments, which are ultimately responsible for generating contraction and relaxation. Phosphorylation of these myofilament proteins modulates alterations in cardiac contractility and relaxation [3, 4] [5]. Under physiological conditions, the internal and external factors work seamlessly to maintain cardiac performance. However, current therapies provide palliative care and, other than transplantation, there are no treatments capable of completely restoring cardiac function in patients with heart failure. Thus, end-stage heart failure is irreversible, and both neurohormonal modulation and inherent cardiac contractility and/or relaxation are compromised in these patients [6]. In the future, development of viable heart failure therapies will require improved insights into myofilament function and its modulation.

Cellular events in the cardiac cycle

Multiple electrical and mechanical events in each cardiac myocyte and the functional syncytium between myocytes are fundamentally responsible for the cardiac cycle [7]. The first set of events in the cardiac cycle result from electrical changes in the myocyte membrane (e.g. sarcolemma) known as an action potential, which is composed of membrane depolarization and repolarization produced by Na^+, K^+ and Ca^{2+} currents. The action potential rapidly spreads from cell to cell via gap junctions present at the end to end contacts, which electrically couple rod shaped myocytes to each other [1, 2]. During the action potential, opening of voltage-gated Ca^{2+} channels located in specialized sarcolemmal invaginations, or t-tubules, initiates the amplified release of Ca^{2+} from stores located within the adjacent sarcoplasmic reticulum (SR). Ryanodine receptors located within the SR are responsible for this amplified Ca^{2+} release. Collectively, the voltage-gated and SR release of Ca^{2+} via ryanodine receptors into the cytosol is known as Ca^{2+}-

induced Ca^{2+} release or CICR [8, 9]. The resulting rise in cellular Ca^{2+} is responsible for excitation-contraction (E-C) coupling (e.g. linking electrical to mechanical events) [8]. Specifically, the elevated levels of Ca^{2+} result in binding of this cation to troponin in the myofilament, which initiates the mechanical events necessary for pressure development and the ejection of blood into large arteries by each cardiac ventricle. The myocyte sarcolemma then repolarizes, and pressure development returns to baseline levels as cytosolic Ca^{2+} is pumped back into the (SR) and/or out of the myocyte [10] [2, 7].

The contractile unit and the biophysics of contraction

Myofilaments within cardiac myocytes contain organized bundles of sarcomeres to translate the Ca^{2+} signal or transient into mechanical pressure or force (Fig.1.1B) [7, 11]. Sarcomeres are the basic functional unit of striated muscle, and each sarcomere is composed of a highly ordered and overlapping arrangement of thick and thin filaments [7]. The backbone of the thick filament is composed of parallel bundles of myosin (e.g. cross-bridge), each consisting of two myosin heavy chains (MHC) and four light chains (Fig.1.1C)[12]. An ATPase within the globular head region of the MHC hydrolyzes adenosine triphosphate (ATP) to produce adenosine diphosphate (ADP) and inorganic phosphate (P_i), which provides the energy necessary for the molecular motor function of each myosin [7, 13, 14]. Myosin light chains (MLC) modulate the stiffness of the S1 heavy chain region in myosin containing the globular head and lever arm (Fig. 1.1C) [15]. Cardiac myosin binding protein C (cMyBP-C) is also located in the thick filament and appears to play both structural and regulatory roles, although its exact function remains controversial (Fig. 1.1C) [16, 17]. Both MLC and cMyBP-C regulate MHC movement and proximity to the thin filament to prevent interactions between the thick and thin filament when Ca^{2+} levels are low [15, 18, 19].

The backbone of the thin filament is formed by an α-helical coiled coil of polymerized actin, which reversibly interacts with the myosin cross-bridge during each contraction (Fig. 1.1C) [3, 9]. The thin filament also contains regulatory proteins such as tropomyosin (Tm), which is arranged along actin in a α-helical coiled-coil (Fig. 1.1C). Tm is believed to sterically block actomyosin interactions in the absence of Ca^{2+} and rotate across the actin filament to allow the cross-bridge to attach to actin, generating force or pressure during the cellular Ca^{2+} transient [20]. Troponin (Tn) is another regulatory protein designed to coordinate Tm positioning and cross-bridge access to actin. Tn is a heterotrimeric protein consisting of cardiac troponin C (cTnC), cardiac troponin T (cTnT), and cardiac troponin I (cTnI) (Fig.1.2A). TnC binds Ca^{2+} and is the subunit responsible for initiating contraction during the Ca^{2+} transient, while cTnT links Tn to Tm and assists in Tm positioning on actin [3, 9]. The final subunit is the inhibitory protein cTnI, which acts as a molecular switch protein within the Tn complex by binding to actin in the absence of Ca^{2+} and then dissociating from actin and binding more tightly to cTnC in the presence of Ca^{2+} (Fig.1.2B). In the myocardium, cTnI also plays an important role in opening the Ca^{2+} binding domain located in an amino-terminal hydrophobic patch of cTnC (Fig.1.2A) [21]. Overall, the Ca^{2+}-induced conformational changes in Tn are critical for the generation and decay of force produced by the rhythmic interactions between actin and myosin [3, 9].

The force generated by the interaction between actin and myosin is currently explained by a 3 state model of thin filament activation, which has largely replaced the on-off mechanism described in the original Hill model (Fig. 1.2C) [22, 23]. An advantage of the 3-state model is the incorporation of both Ca^{2+}-binding to cTnC and cooperative activation by neighboring, strong-binding cross-bridges to explain force generation in the myofilament [14, 22]. In this model, Tm oscillates between 3 states, and the cellular environment determines the state most

Tm occupies at a given point in time. In the absence of Ca^{2+}, Tm primarily occupies the "blocked" position on the thin filament, and in this position, the myosin cross-bridge is unable to interact with actin (Fig.1.2C). As Ca^{2+} binds to TnC, Tm increasingly occupies an intermediate position on the actin filament known as a "closed" state, which allows weak, non-force generating cross-bridge binding to actin (Fig.1.2C) [14]. When Tm occupies the third "open" state, a cross-bridge forms strong, force-generating interactions with actin (Fig.1.2C) [14]. Currently, Tm is proposed to transition back to the intermediate "closed" state followed by the "blocked" state as the SR Ca^{2+} pump (SERCA2A) and sarcolemmal Na^{+}/Ca^{2+} exchanger reduce cytosolic Ca^{2+} levels and cause Ca^{2+} to dissociate from cTnC in the repolarized myocyte [10].

At the same time these transitions develop in the thin filament, the hydrolysis of ATP into ADP and P_i by MHC provides the energy needed for force development [14]. The release of P_i is tightly coupled to the cross-bridge power-stroke, which generates force (pressure) when length remains constant under isometric conditions or produces thin filament sliding by the cross-bridge when the sarcomere shortens under isotonic conditions. After the power-stroke, the strong, force-generating cross-bridge attachment to actin is only relieved when ADP dissociates and is replaced by ATP [14].

In addition to the individual contributions of the thick and thin filaments, there is an important allosteric component to force generation. The Tm transition from "blocked" to "closed" and "closed" to "open" states are cooperative processes whereby the transition of one functional unit, composed of 7 actins, 1 Tm and 1 Tn, increases the probability neighboring functional units will transition to the same state (Fig.1.2C) [3]. For example, strong cross-bridge binding to a thin filament functional unit in the "open" state increases the likelihood an adjacent cross-bridge will bind to actin and generate force without the need for an additional increase in

Ca^{2+} bound to cTnC (Fig.1.2C) [3, 14]. Ultimately, strong, force-generating interactions between actin and myosin are responsible for the generation of pressure and the thin filament sliding needed to eject blood from the ventricle into the large arteries during the systolic phase of each cardiac cycle.

The current model of muscle contraction outlined above demonstrates the significant progress made in understanding the molecular events responsible for force generation. However, significant gaps remain in our understanding of the conformational changes and interactions among sarcolemmal, Ca^{2+} cycling and myofilament proteins responsible for cardiac contraction and relaxation. For example, pressure development during systole depends on the rate-limiting release of Ca^{2+} from ryanodine receptors in the SR under most conditions, and yet two or more rate-limiting steps often contribute to relaxation rate [24] [8, 10]. While some components contributing to pressure decay are known, there is only a vague understanding about the precise contribution of each event over time. Currently, the initial phase of relaxation is most often attributed to Ca^{2+} dissociation from cTnC, while a second phase depends heavily on the kinetics of SR Ca^{2+} re-uptake and/or Ca^{2+} extrusion from myocytes [10]. However, recent evidence suggests cross-bridge detachment from the thin filament also influences the later phase(s) of relaxation in myocytes [24]. To gain insight into this complex, multi-phasic process, further work is necessary to define the contribution of each process over a range of physiological conditions.

Phosphorylation of cTnI and modulation of contractile function by cTnISer23/24

Post-translational modifications, such as phosphorylation, work to fine tune cardiac contraction and relaxation. A range of approaches are used to examine the role phosphorylation of individual thick and thin filament proteins plays in modulating contractile performance,

including work on cTnI. Biochemical work identified 6 kinase-targeted residues in cTnI including Ser23/24 in the cardiac-specific N-terminal domain, Ser43/45 in the HI(1) α-helix at the beginning of the IT arm, Ser78 in the I-T Arm, and Thr144 in the inhibitory peptide domain (IP) (Fig. 1.2A) [25, 26]. Additional candidate phosphorylation sites within cTnI continue to be identified using improved mass spectroscopy approaches, including recent work identifying 14 cTnI phosphorylation sites [27]. With the identification of new phosphorylation sites in cTnI, the kinases targeting each residue and the functional role modulated by phosphorylation often remain controversial. Conceptual insights into these issues are needed because alterations in phosphorylation of several sites within cTnI are associated with cardiac dysfunction and the progression to end-stage heart failure in both animal models and human patients [28, 29] [27] [30, 31].

Perhaps the most studied phosphorylation site in cTnI is Ser23/24, located in the cardiac-specific N-terminus of cTnI (Fig.1.2A). The first kinase found to phosphorylate cTnI was protein kinase A (PKA), a member of the AGC family of Ser/Thr protein kinases, which targets cTnISer23/24. Sympathetic stimulation of β_1-adrenergic receptors (β_1-AR) in cardiac myocytes activates adenylyl cyclase (AC) to increase cellular cyclic-AMP (cAMP), which in turn activates PKA [32] [5, 33, 34]. Basal cTnI Ser23/24 phosphorylation is detected in both normal human tissue and in animal models [35-37]. PKA phosphorylation at cTnISer24 occurs first, and this site is thought to be constitutively phosphorylated in cardiac myocytes [38, 39]. Additionally, phosphorylation of both Ser23 and Ser24 is required to modulate cTnI function [40, 41]. Phosphorylation of cTnISer23/24 de-sensitizes the myofilament to Ca^{2+} in both *in vitro* and cellular studies, and this desensitization results in the accelerated Ca^{2+} release from cTnC [42-46]. In agreement with this mechanism, expression of cTnI containing a phospho-null Ala

substitution at Ser23/24 in isolated rat myocytes, eliminates the accelerated relaxation response to the β-AR agonist, isoproterenol [43]. Moreover, phospho-mimetic Asp substitutions on cTnISer23/24 reduced myofilament Ca^{2+} sensitivity of tension and accelerated re-lengthening rate in intact myocytes without changing peak tension [43].

A number of genetic mouse models also have been generated to examine the modulatory role of cTnISer23/24 phosphorylation in the whole heart. Complete replacement of endogenous cTnI using a knock-out followed by knock-in of cTnI containing Ala substitutions at Ser23/24 (Ala_2^{nb}) eliminated the ability of PKA activation to decrease myofilament Ca^{2+} sensitivity (Table 1.1) [47]. In transgenic (tg) mouse models, >95% replacement of endogenous cTnI with phospho-mimetic cTnISer23/24Asp ($cTnI_{PP}$) decreased myofilament Ca^{2+}-sensitivity of tension in permeabilized cells, accelerated re-lengthening rates in intact myocytes, and increased *in vivo* cardiac relaxation rates (dP/dt_{min}) compared to non-transgenic controls (Table 1.1) [43, 48, 49]. Taken together, the *in vitro* and *in vivo* approaches uniformly demonstrated cTnISer23/24 phosphorylation reduces myofilament Ca^{2+} sensitivity and increases relaxation rate by accelerating Ca^{2+} release from cTnC [42, 43, 48]. In keeping with the observations in animal models, reduced cTnISer23/24 phosphorylation develops in end-stage heart failure and is associated with the expected increase in myofilament Ca^{2+} sensitivity and slowing of relaxation [27] [31] [29].

Influence of PKC-mediated cTnI phosphorylation on contractile function

Protein kinase C (PKC) is a second member of the AGC kinase family which phosphorylates cTnI[26] [50, 51]. Multiple neurohormones activate PKCs through G-protein coupled receptors (GPCR) including catecholamine stimulation of α-adrenergic receptors (α-AR), endothelin (ET-1) activation of ETA receptors, and angiotensin II (AngII) activation of

AT1A receptors [52] [53, 54]. Twelve PKC isoforms have been identified and divided into 3 families based on cofactors required for kinase activation [55]. Classical PKCs (α, βI, βII, and γ) require both Ca^{2+} and lipid co-factors, such as diacylglycerol (DAG), in the cell or synthetic phorbol esters, such as phorbol 12-myristate 13-acetate (PMA), for activation [50, 55]. Activation of novel class PKC isoforms (δ, ε, θ, and η) is Ca^{2+} independent but requires lipid co-factors. In contrast, atypical PKCs (ζ, ι/λ) are often activated through protein-protein interactions mediated via a Phox and/or Bem 1 domain [55]. PKCα, PKCβ, PKCδ, PKCε, and PKCζ are expressed in the adult mammalian cardiac myocytes [56-58].

Early *in vitro* work showed PKC phosphorylates 3 clusters of residues within TnI, and PKCα, PKCδ, and PKCε each phosphorylate Ser43/45 and Thr144, while PKCδ preferentially phosphorylates Ser23/24 [59-61]. Novel class PKC isoforms (δ, ε) are postulated to phosphorylate cTnI *in vivo,* based on their anticipated distribution within myocytes. However, the role PKC-mediated cTnI phosphorylation plays in modulating cardiac function remains controversial. A focal point for this controversy is the contribution of cTnISer43/45 phosphorylation, due to conflicting results obtained from *in vitro* and *in vivo* models [49, 62] [47, 51, 63, 64]. Determining the functional role modulated by cTnISer43/45 phosphorylation is critical because there is evidence linking increased PKC activity and downstream cTnI phosphorylation to contractile dysfunction [56, 65]. In agreement with this idea, phosphorylation of cTnISer43/45 is negligible in normal human and animal hearts [30, 35-37]. In contrast, PKC expression and activity increase and cTnISer43/45 phosphorylation is augmented in human end-stage heart failure [27, 29-31, 56, 65, 66].

A substantial body of *in vitro* analyses predicts PKC-dependent cTnI phosphorylation at Ser43/45 will reduce cardiac function [67] [45, 51, 63, 68]. PKC-phosphorylated cTnI

diminished myofilament Ca^{2+}-sensitivity and maximum actomyosin ATPase activity in both reconstituted thin filaments and cardiac myofibrils [45, 51, 63]. Myofibrillar ATPase activity often, but not always, predicts a similar change in loaded cross-bridge cycling rate during the ejection of blood from the ventricle. Phospho-null Ala substitutions at cTnISer43/45 or pharmacological inhibition of PKC mitigates the reduction in maximum actomyosin ATPase activity [51] [45]. Interestingly, the phosphorylation-induced decrease in myofilament Ca^{2+} sensitivity also is present after reconstitution with cTnISer43/45Ala, although investigators have repeatedly failed to comment on this phenotypic change [64] [45]. Conversely, replacement of cTnISer45, cTnISer43/45, and cTnISer43/45Thr144 with phospho-mimetic Glu reduces maximum actomyosin ATPase activity and myosin S1-binding to the thin filament in reconstituted preparations [67]. Exchange of endogenous cTnI with a recombinant cTnISer43/45Glu in permeabilized, papillary muscle bundles reduces myofilament Ca^{2+} sensitivity of tension, consistent with the results obtained using biochemical approaches [68]. In addition, this construct also reduces maximum Ca^{2+}-activated tension, maximum thin filament sliding speed and cooperative Ca^{2+}-mediated activation of sliding speed (e.g. Hill n) [68]. Although the results of one study are interpreted to indicate PKC phosphorylation of cTnIThr144 increases myofilament Ca^{2+} sensitivity, the majority of *in vitro* approaches suggest PKC-mediated cTnI phosphorylation reduces Ca^{2+} sensitivity [69] [45, 51, 63, 68]. Overall, the examination of cTnISer43/45 indicates phosphorylation of this cluster uniformly reduces MgATPase activity and myofilament Ca^{2+} sensitivity [68] [45, 51, 63, 67]. Based on chemical shift analysis by NMR, cTnISer43/45 phosphorylation is predicted to modulate myofilament Ca^{2+} sensitivity by destabilizing a C-terminal helix in cTnC [70]. More recently, Glu replacement at cTnISer45 disrupted a critical interaction between this residue and the amino (N)-

lobe of cTnC. This disruption is anticipated to decrease opening of the hydrophobic patch containing the regulatory Ca^{2+} binding site on this lobe of cTnC and also result in diminished myofilament Ca^{2+} sensitivity [71]. The separate effects of cTnISer43 and cTnISer45 on myofilament function have not been thoroughly explored using these types of *in vitro* approaches or in more complex model systems. One goal of this dissertation is to determine if cTnISer43 and cTnISer45 independently adjust contraction of individual myocytes.

As with cTnISer23/24, the development of several genetic animal models further examined the modulatory role of PKC-mediated cTnI phosphorylation in fine-tuning cardiac pump function. One mouse model utilized a knock-out/knock-in approach to replace cTnISer23/24, cTnISer43/45, and cTnIThr144 with Ala (Ala_5^{nb}) (Table 1.1) [64]. Under basal conditions, Ala replacement of all 5 PKC-targeted cTnI residues diminished myofilament Ca^{2+} sensitivity in permeabilized myocytes compared to wild-type controls, although this change was not identified or discussed in the published study [64]. As expected, treatment of heart tissue with the PKC agonists ET-1 and PMA did not change maximum actomyosin ATPase activity in myofibrils isolated from Ala_5^{nb} mice [47]. Conversely, ET-1 and PMA treatment slowed re-lengthening in intact wild-type myocytes and increased myofilament Ca^{2+} sensitivity of actomyosin ATPase activity and cellular isometric tension compared to Ala_5^{nb} myocytes [47, 64]. Based on these results, the authors concluded cTnISer43/45/Thr144 phosphorylation increases myofilament Ca^{2+}-sensitivity, which is directly opposite of the change predicted from the majority of biochemical/biophysical studies [64] [45, 68] [47]. The authors suggested the increased myofilament Ca^{2+} sensitivity and slowed re-lengthening produced by PKC activation of control myocytes may result from myosin light chain kinase (MLCK) activation and the downstream phosphorylation of myosin light chain 2 (MLC_2), also known as the regulatory light

chain (RLC) [47]. Although overall RLC phosphorylation was not different between myofilaments from wild-type and Ala_5^{nb} mice, the ability of MLCK to increase Ca^{2+} sensitivity is significantly attenuated in Ala_5^{nb} myofilaments [47]. This finding indicates adaptive changes in the Ala_5^{nb} model may confound the direct influence of phosphorylation on contractile function. In addition, the prominent reduction in myofilament Ca^{2+} sensitivity observed in Ala_5^{nb} mice suggests amino acid substitutions of cTnISer43/45 may influence the conformation of the Tn core and produce significant changes in basal cardiac function [64]. Although *in vivo* cardiac function has not been measured in the Ala_5^{nb} mouse, the development of a dilated cardiomyopathy in this model supports this idea [64].

In a separate tg model, ~50% of endogenous cTnI was replaced by cTnISer43/45Ala (Table 1.1) [72]. In cTnISer43/45Ala mice, basal cardiac function did not differ from non-tg controls, although Ca^{2+}-activated maximum actomyosin ATPase activity and isometric tension generation were significantly reduced compared to control preparations [72-74]. Interestingly, cTnISer43/45Ala expression increased overall cTnI phosphorylation and reduced cTnT phosphorylation. These results suggested adaptations could maintain overall function and/or mask functional changes induced by cTnISer43/45Ala and provided an explanation for the discrepancies between *in vitro* studies and the results observed with the Ala_5^{nb} mouse. Experiments performed in chapter 2 of this dissertation address the role of Ala substitutions at cTnISer43/45 on basal myofilament function in intact and permeabilized cardiac myocytes (Ch.2).

Animal models expressing a cTnI with phospho-mimetic replacement of the PKC-targeted clusters have also been developed to further examine the role of PKC-mediated cTnI phosphorylation in modulating cardiac pump function. In one tg mouse model, all 5 PKC-

targeted residues in cTnI are replaced with aspartic acid (Asp; $cTnI_{AllP}$) to mimic the negative charge introduced by phosphorylation (Table 1.1) [49]. Maximum Ca^{2+}-activated actomyosin ATPase activity, myofilament Ca^{2+} sensitivity, and isometric tension generation were each reduced in myofibrils and myocytes from this mouse compared to non-transgenic mice [75] [49]. These observations are consistent with the *in vitro* studies discussed earlier in this section and predict the presence of diminished cardiac function in $cTnI_{AllP}$ mice. Specifically, these mice were anticipated to show diminished peak pressure and accelerated relaxation [49]. However, hemodynamic measurements of $cTnI_{AllP}$ cardiac function revealed no change in ventricular pressure or relaxation rate (dP/dt_{min}). Instead, only the rate of pressure development (dP/dt_{max}) slowed in $cTnI_{AllP}$ mice compared to non-transgenics [49]. The inconsistency between *in vitro* and *in vivo* outcomes in this mouse model make data interpretation difficult and highlight the need for an additional model to study the functional effects of PKC-mediated cTnI phosphorylation on cardiac performance.

In another tg mouse model, ≈7% of endogenous cTnI was replaced by a cTnI with phosphomimetic Glu substitutions at cTnISer43/45 and cTnIThr144 ($cTnI_{PKC\text{-}P}$) to examine the modulatory roles of PKC-specific residues (Table 1.1) [62]. This minimal level of $cTnI_{PKC\text{-}P}$ expression unexpectedly diminished isometric force production in fibers isolated from tg mice. However, there were no changes in myofilament Ca^{2+} sensitivity in $cTnI_{PKC\text{-}P}$ fibers compared to wild-type controls. Based on these findings, diminished pressure development was anticipated in $cTnI_{PKC\text{-}P}$ hearts, and indeed, a slowed rate of contraction ($-d\sigma/dt_{max}$) and reduced peak pressure development were observed in isolated whole hearts from $cTnI_{PKC\text{-}P}$ mice [62]. However, relaxation rates also were slowed in both fiber bundles and isolated hearts [62]. Collectively, the role cTnISer43/45 phosphorylation plays in modulating function remain ambiguous based on the

inconsistencies between *in vivo* models expressing phospho-null or phospho-mimetic cTnI substitutions along with the unexpected *in vivo* phenotypes which *in vitro* studies failed to predict. Therefore, a cellular approach may be an appropriate model to evaluate the role cTnISer43/45 phosphorylation plays in fine-tuning cardiac performance. The work described in this dissertation utilizes isolated cardiac myocytes to define the functional influence of phosphorylation at one or both residues within cTnISer43/45 using phospho-mimetic Asp substitutions (Ch.3). Isolated cardiac myocytes have been shown to be a viable model to bridge earlier work in biochemical systems with more complex *in vivo* models [76] [7, 43, 77].

Isolated cardiac myocytes also could be an effective approach for addressing functional cross-talk between phosphorylated residues within cTnI, such as cTnISer23/24 and cTnISer43/45. While many of the animal models evaluating the functional impact of cTnI phosphorylation by PKC have addressed multi-residue phosphorylation, the functional relationship between cTnISer23/24 and cTnISer43/45 remain to be directly addressed in *in vitro* or *in vivo* models. The close physical proximity of these cTnI clusters and the potential ability of both clusters to reduce myofilament Ca^{2+} sensitivity provide further rationale for investigating the relationship between these PKC-targeted residues (Fig. 1.2A) [25, 26, 43, 46, 60, 68].

The relationship between cTnISer23/24 and cTnISer43/45 has been indirectly examined by comparing cardiac function in $cTnI_{AllP}$ to $cTnI_{PP}$ mice as well as comparing $cTnIAla_5^{nb}$ to $cTnIAla_2^{nb}$ mice (Table 1.1)[47, 49, 64]. For example, the ability of PKC agonists ET-1 and PMA to reduce maximum actomyosin ATPase activity and isometric tension is absent in myofilaments from Ala_5^{nb} but is more pronounced in Ala_2^{nb} mice compared to wild-type controls [47]. Conversely, reduced myofilament Ca^{2+} sensitivity of tension is observed in both $cTnI_{PP}$ and $cTnI_{AllP}$ myofilaments, and yet cardiac relaxation rate (dP/dt_{min}) is accelerated only in the $cTnI_{PP}$

mouse hearts [49]. In both sets of mice, the results are consistent with communication between cTnISer23/24 and cTnISer43/45, which influences cardiac performance. The results from the $cTnIAla_2^{nb}$ mice suggest cTnISer23/24 phosphorylation could dampen the functional influence of PKC-mediated cTnISer43/45 phosphorylation [47]. In contrast, cTnISer43/45 phosphorylation appears to suppress the actions of cTnISer23/24 based on the comparison of $cTnI_{AllP}$ to $cTnI_{PP}$ mice [49]. The functional relationship between cTnISer23/24 and cTnISer43/45 is explored in chapter 4 (Ch.4). An important goal of this work is to differentiate between direct versus potential adaptive functional influences in isolated myocytes after gene transfer of cTnI containing phospho-mimetic substitutions at these 4 residues.

Alterations in cTnI phosphorylation identified in failing hearts highlights the importance of understanding the physiological effects of each PKC-targeted cTnI residue, both alone and in combination. Moreover, divergent phosphorylation patterns at cTnISer43/45 and cTnISer23/24 are observed in many cardiac injury models, and several studies indicate PKC expression and activation are increased during periods of cardiac dysfunction [27] [56, 65] [29-31]. Phosphorylation of cTnISer23/24 is significantly reduced in tissue from end-stage heart failure patients diagnosed with either ischemic cardiomyopathy (ICM) or dilated cardiomyopathy (DCM) [27]. Conversely, diminished Ca^{2+}-activated maximum force production and increased sliding speed are linked to augmented classical PKC expression in tissue from failing hearts and could be restored to non-failing values following myofilament de-phosphorylation with protein phosphatase 2A (PP2A) [65]. The detected phosphorylation pattern of cTnISer43/45 also appears to be more complex during heart failure. Phosphorylation at cTnISer43 increases in both ICM and DCM while increased cTnISer45 phosphorylation appeared to be unique to DCM [27] . These observations are consistent with the diminished Ca^{2+}-activated force production observed

in failing human heart tissue [65]. The alterations in phosphorylation at specific cTnI residues also appear to be time and disease dependent. Phosphorylation at cTnISer23/24 increased while phosphorylation at cTnISer43 was unchanged in patients with hypertrophy and an absence of change in systolic function. In contrast, cTnISer43 phosphorylation was reduced in patients with left ventricular dilation and diminished ejection fraction [66]. Collectively, these studies provide strong evidence of an association between cTnISer43 or cTnISer45 phosphorylation and pathological alterations in cardiac contraction. Due to the complex cTnISer43/45 phosphorylation patterns detected across multiple disease states and time points, it is unclear whether PKC phosphorylation of Ser43/45 in cTnI contributes to physiological modulation of cardiac performance and/or to the progression of heart failure.

Hypothesis and aims

Work presented in this dissertation tests the hypothesis that cTnISer43/Ser45 phosphorylation decreases cardiomyocyte contractile performance. Additionally, functional cross-talk between multiple PKC-phosphorylated residues in cTnI is predicted to be present and contribute to modulatory changes in myocyte contractile performance. These hypotheses are tested in 2 separate aims. The individual versus combined modulatory role of cTnISer43 and/or cTnISer45 on myocyte contractile function is evaluated under basal conditions and in response to PKC activation in the first aim (Ch. 2 and Ch. 3). A second aim is designed to test whether phosphorylation at cTnISer23/24 impacts the effect of cTnISer43/45 on cardiomyocyte contraction and relaxation (Ch. 4). Work in this dissertation is performed on isolated myocytes expressing phospho-null (Ala) or phospho-mimetic (Asp) substitutions at one or both residues in cTnISer43/45 (e.g. cTnISer43/45Ala) (Fig. 1.3A). After verifying expression and incorporation of each construct, both direct versus indirect, adaptive influences on function are measured using

sarcomere shortening measurements, isometric tension development, and Ca^{2+} cycling in intact myocytes (Figs.1.3B-D). Primary measures of contractile function in the shortening assay include peak shortening amplitude, shortening rate and the time to peak (TTP) shortening, while relaxation is evaluated from the re-lengthening rate, times to 50% and 75% re-lengthening ($TTR_{50\%}$ and $TTR_{75\%}$, respectively), and resting length (Fig. 1.3D).Western blot also is utilized to detect changes in sarcomeric and Ca^{2+} handling protein phosphorylation following phospho-null or phospho-mimetic construct expression (Fig. 1.3A).

Experiments in chapter 2 address the influence of cTnISer43/45 on basal contractile performance and in response to PKC activation by ET-1. Under basal conditions, Ala is predicted to be a functionally conservative substitution for cTnISer43/45 since Ala replacement at cTnISer23/24 does not influence basal myocyte contractile performance [43, 78]. However, the reduced myofilament Ca^{2+}-sensitivity of isometric tension apparent in previous *in vitro* and *in vivo* studies with cTnISer43/45Ala suggest both residue size and polarity at cTnISer43/45 are critical for maintaining basal function [45, 47, 64]. Though a reduction in myofilament Ca^{2+} sensitivity could develop, most measures of cellular shortening are not expected to differ significantly from controls. Expression and sarcomere replacement with cTnISer43/45Ala also is predicted to reduce the response to ET-1 activation of PKC in intact myocytes, since cTnISer43/45Ala mitigates the response to the α-adrenergic PKC agonist phenylephrine in myofibrils from transgenic mice [73]. In the event the ET-1 response is similar between controls and cTnISer43/45Ala-expressing myocytes, the results would suggest specific agonists activate different PKC isoforms, which may target other cTnI residues and/or additional myofilament/Ca^{2+} cycling protein targets.

Studies performed in chapter 3 are designed to evaluate the influence of cTnISer43/45 phosphorylation on sarcomere shortening and isometric tension development in isolated myocytes. In these experiments, phospho-mimetic Asp is substituted for cTnISer43/45 via adenoviral gene transfer (Fig. 1.3A); this substitution is predicted to diminish peak shortening amplitude, reduce maximum isometric tension development and decrease myofilament Ca^{2+} sensitivity based on majority of previous *in vitro* and *in vivo* work (Fig 1.3D) [49, 62, 63, 52, 67, 68, 75]. However, the variable influence of cTnISer43/45 phospho-mimetic substitutions on contractile function in the literature indicates experiments are needed to differentiate between the direct versus adaptive, indirect influence on contractile function [51, 68, 79, 80]. An additional component of this chapter tests whether cTnISer43 and cTnISer45 work independently to modulate myocyte contractile function. Expression of cTnISer43Asp or cTnISer45Asp may not individually modulate sarcomere shortening and isometric tension because, like cTnISer23/24 phosphorylation, replacement at both residues may be required to produce a functional response [40]. In the event cTnISer43 and cTnISer45 function independently, work will focus on identifying whether these residues perform similar actions within the myocyte and/or they influence separate mechanisms to alter function.

The influence of functional cross-talk between cTnISer23/24 and cTnISer43/45 phosphorylation will be investigated in chapter 4. Previous work evaluating the influence of multi-site cTnI phosphorylation is limited to communication between all 5 PKC-targeted residues, cTnISer23/24 and Thr144, or cTnISer43/45 and Thr144 [47, 49, 62, 64, 75]. Work from the $cTnI_{AllP}$ mouse indirectly suggests cTnISer43/45 has a dominant influence on function over Ser23/24 [49, 75]. Therefore, a phospho-mimetic cTnI containing Asp substitutions at cTnISer23/24 and cTnISer43/45 ($cTnIAsp_{Quad}$) is introduced into isolated rat myocytes via

adenoviral-mediated gene transfer (Fig. 1.3A) and is expected to reduce myocyte contractile function and diminish myofilament Ca^{2+} sensitivity of tension (Fig. 1.3D). An acceleration of myocyte re-lengthening rate is anticipated in the event cTnISer23/24 influences function separately from cTnISer43/45 [40, 43, 45, 46, 68]. Conversely, it is possible Asp replacement at both cTnISer23/24 and cTnISer43/45 may abrogate the functional effects of each cluster and there may be no net influence on all measures of contractile function. Isolated cardiac myocytes are expected to be an effective model for evaluating the direct impact of cTnISer23/24 and cTnISer43/45 on function and determining whether these clusters influence comparable or separate steps responsible for force and/or cross-bridge cycling in the myofilament.

Mouse Model	**Replacement**	**Age/ Pathology**	**Myofilament/ Permeabilized Cell**	**Explanted Hearts/ Intact Myocytes/ Papillary Muscles**	**MRI/ *In Vivo* Hemodynamics**	**Reference**
$cTnIAla_2^{nb}$ (Ala_2^{nb})	100%; Knock-out/ Knock-in (Ser23/24)	No hypertrophy No cardiomyopathy	**MgATPase Activity:** NC **Force Production:** No **PKC Agonist:** ↓ **PKA Agonist:** NC			[47]
$cTnIAla_5^{nb}$ (Ala_5^{nb})	100%: Knock-out/ Knock-in (cTnISer23/24/43/45/Thr144)	Mild dilated Cardiomyopathy; no fibrosis; no sarcomere disarray; normal lifespan	**MgATPase Activity:** NC **ΔpC_{50}:** ↓ **PKC Agonist:** NC **PKA Agonist:** NC	**Basal shortening:** NC **Ca^{2+} Transients:** NC **PKC Agonist:** NC **PKA Agonist:** ↓		[64]
cTnI Ser43/45Ala	50%; Transgenic (cTnISer43/45)	8-40 weeks; Normal function, no hypertrophy, no histological abnormalities; TnT Phos: ↓ TnI Phos: ↑	**MgATPase Activity:**↓ **Force Production:** ↓ **ΔpC_{50}:** NC	**Wall Strain:** NC **Systolic Function:** NC **Diastolic Function:** NC **Wall Restitution:** NC	**Sarcolemma Ca^{2+} Influx**: ↓	[72-74]
$cTnI_{PP}$	100%; Transgenic (cTnISer23/24)	No hypertrophy No fibrosis No sarcomere disarray No fetal gene transcription No adaptive phosphorylation	**MgATPase Activity:** NC **ΔpC_{50}:** ↓		**Basal HR:** ↑ **Systolic Pressure**: ↑ **dP/dt_{max}:** ↑ **dP/dt_{40}:** NC **dP/dt_{min}:** ↓ **Peak Pressure:** NC **Diastolic Pressure:** NC	[49]
$cTnI_{AllP}$	100%: Transgenic (cTnISer23/24,Ser43/45,Thr144)	No fibrosis No myocyte disarray No Sarcomere disarray No fetal gene transcription No adaptive phosphorylation	**MgATPase Activity:** ↓ **ΔpC_{50}:** ↓		**Basal HR:** NC **Systolic Pressure**: NC **dP/dt_{max}:** ↓ **dP/dt_{40}:** ↓ **dP/dt_{min}:** NC **Peak Pressure:** NC **Diastolic Pressure:** NC	[49]
$cTnI_{PKC\text{-}P}$	7%: Transgenic (cTnISer43/45, Thr144)	No Hypertrophy No signs of HF No adaptive phosphorylation	**MgATPase Activity:** ↓ **ΔpC_{50}:** NC **Max. Force**: ↓	**ΔpC_{50}:** NC **Max. Force**: ↓ **dP/dt_{max}:** ↓ **dP/dt_{min}:** ↓ **Peak Pressure:** ↓		[62]

Table 1.1. *In vitro* and *in vivo* characteristics of cTnI phospho-null and phospho-mimetic mouse models. Available information concerning the mouse model, amount and location of replacement, age, pathological indicators, permeabilized preparations, intact preparations, and whole organ measurements. MRI = Magnetic Resonance Imaging. Phos = phosphorylation. ΔpCa_{50} = Change in myofilament Ca^{2+} sensitivity. **NC** = No change, ↓ = decreased, ↑ = increased.

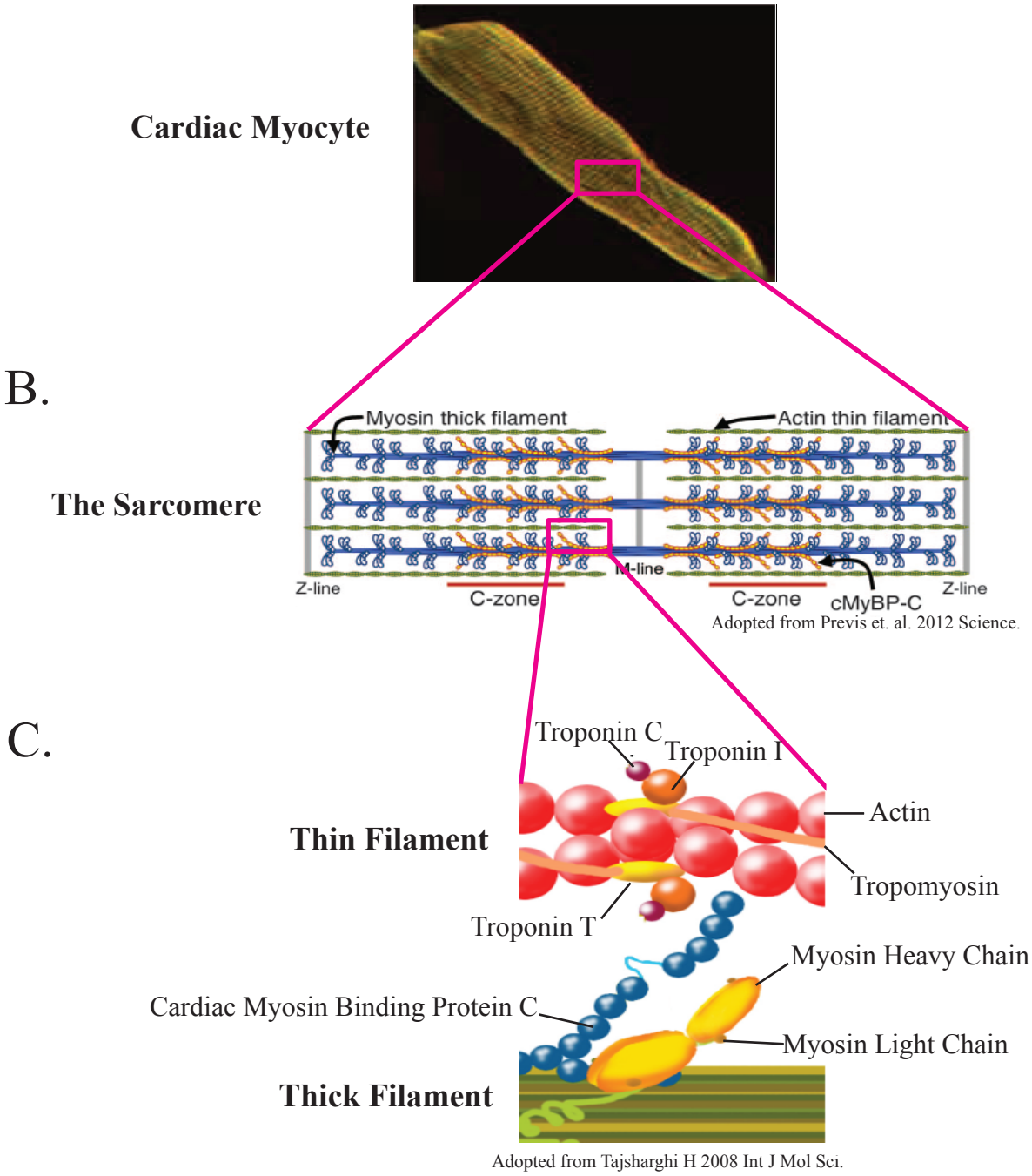

Fig. 1.1 Cellular components underlying cardiac contraction. **A.** Confocal image of an adult cardiac myocyte immunostained for troponin I (TnI; green) and FLAG (red). The striated pattern highlighted in the box is produced by the sarcomere. **B.** Illustration of a single sarcomere containing overlapping arrays of thick and thin filaments. A sarcomere is defined as the region between 2 z-lines. Thin filaments are absent in the bare area formed around the central region (M-line), and cardiac myosin binding protein C (cMyBP-C) is distributed within the C-zone of each sarcomere. **C.** Illustration of a magnified section of the sarcomere highlighted in B. Individual proteins within the thin and thick filaments are shown in this illustration. The thick filament is composed of myosin, myosin light chain 1 (e.g. essential light chain; ELC) and 2 (regulatory light chain; RLC) plus cMyBP-C. Actin forms the coiled-coil backbone of the thin filament. Tropomyosin (Tm) and heterotrimeric troponin (troponin C, troponin I, and troponin T) are regulatory proteins distributed along the thin filament, as described in more detail in the text.

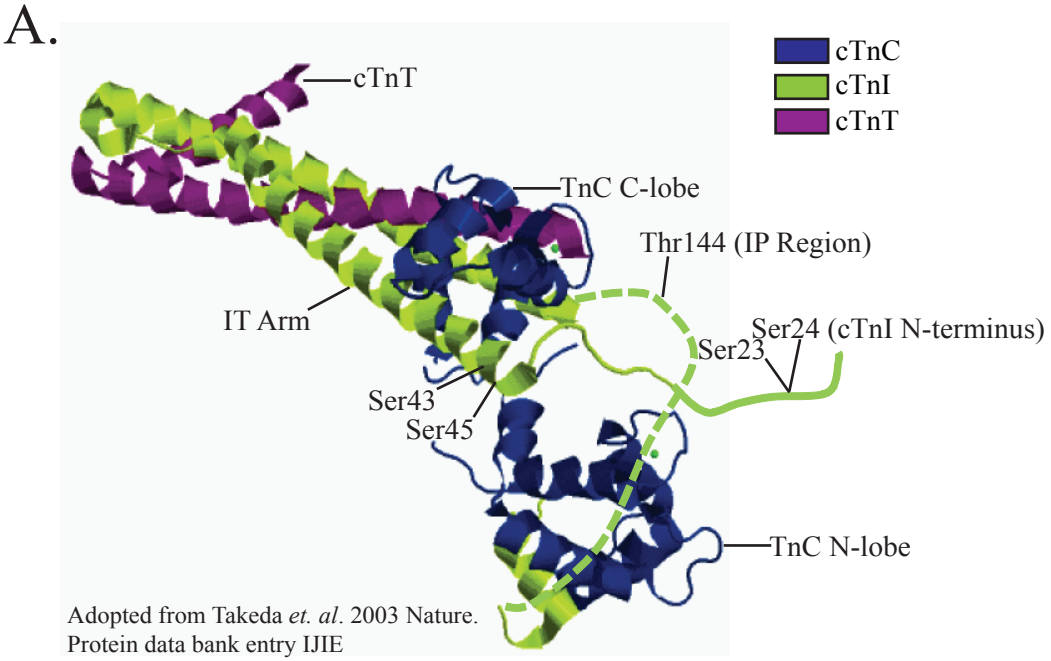

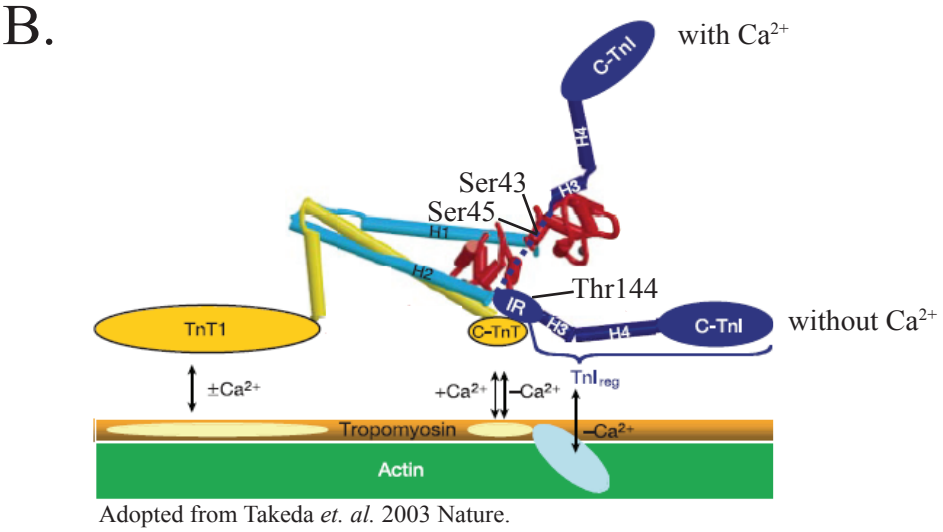

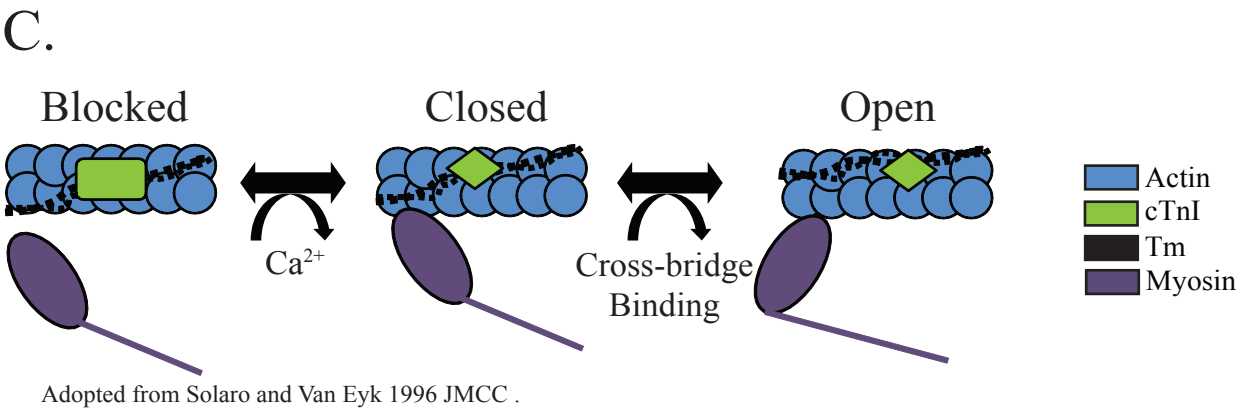

Fig. 1.2. Cardiac troponin I in the myofilament. A. Structural model of the Tn core containing cTnI (green), cTnC (blue), and cTnT (magenta). The locations of the 5 PKC-targeted phosphorylation sites within cTnI are noted. Important points of interaction between cTnI and the additional Tn subunits are also highlighted. **B.** A cartoon illustrating the conformation change that occurs within cTnI in the presence or absence of Ca^{2+} **C.** Cartoon depiction of the 3 state model. The transition from "blocked" to "closed" is mediated by Ca^{2+} binding to troponin. The myofilament further transitions to an open, force generating state following the interactions with strongly-bound cross-bridges.

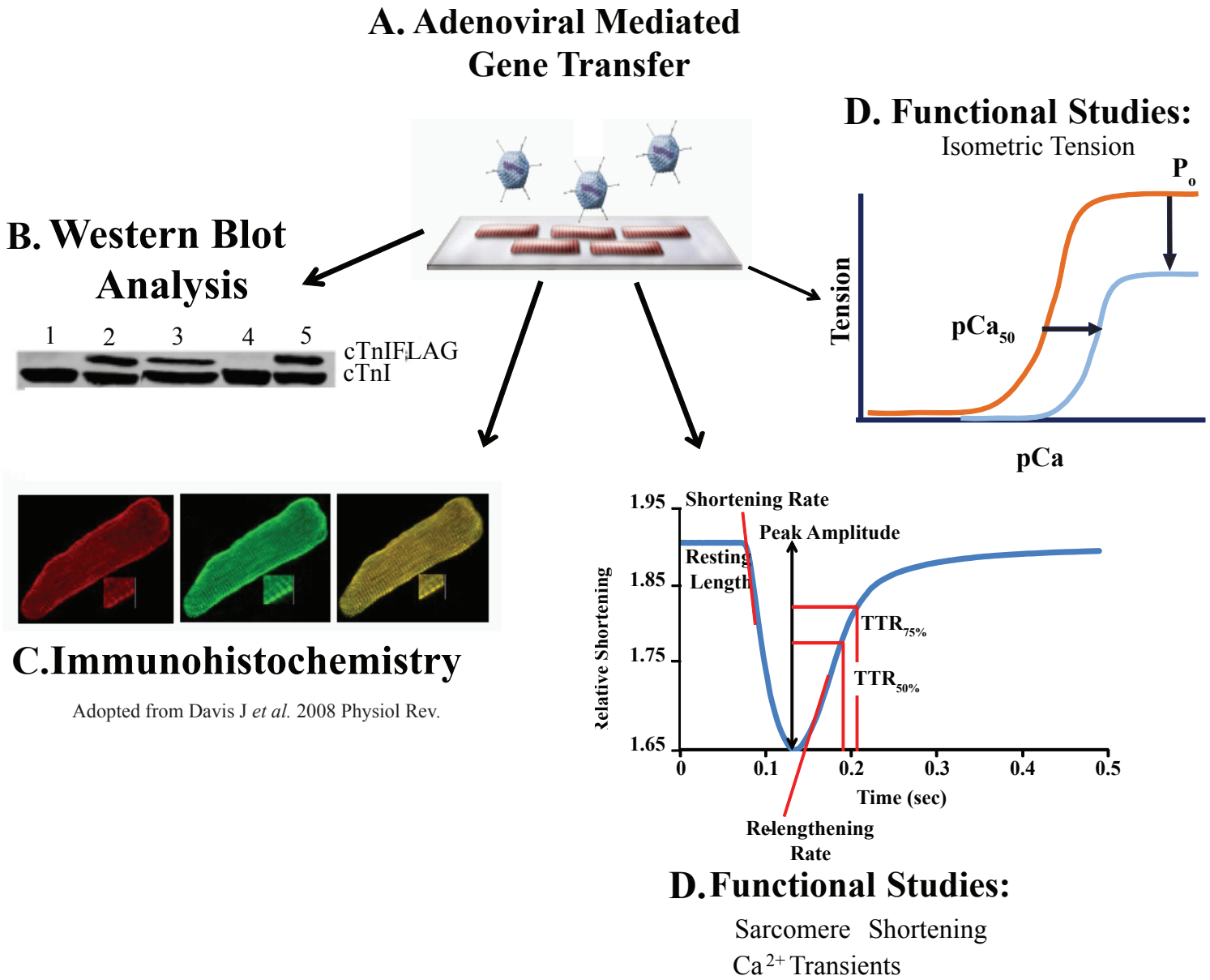

Fig. 1.3 Approaches to evaluate expression and contractile function in myocytes expressing cTnI with phospho-null or phospho-mimetic substitutions in PKC-targeted residues. A. The cTnI constructs with substitutions are introduced into isolated adult rat cardiac myocytes via recombinant adenoviral-mediated gene transfer. **B.** Expression and replacement of endogenous cTnI with the cTnI constructs and phosphorylation of specific residues within myofilament proteins are detected by Western blot analysis. **C.** Sarcomeric localization of the individual constructs is detected using dual immunohistochemical labeling for cTnI and FLAG-tagged cTnI. **D.** Contractile function responses are determined by measuring isometric tension (upper panel) in detergent-permeabilized myocytes over a range of Ca^{2+} concentrations (pCa = -log [Ca^{2+}]). The Ca^{2+}-activated tension curves are analyzed to determine maximum tension (P_o) and myofilament Ca^{2+} sensitivity (pCa_{50}= Ca^{2+} required for 50% tension generation). The arrows in this illustration indicate decreases in P_o and in pCa_{50} values for myocytes shown in the blue curve versus the orange curve. In a second approach, sarcomere shortening is measured in intact cardiac myocytes (lower panel). A representative trace demonstrates the contractile function measurements analyzed using this approach, including resting length, peak shortening amplitude, the rates of shortening and re-lengthening, time to peak (TTP; not labeled), and the times to 50% and 75% re-lengthening ($TTR_{50\%}$ and $TTR_{75\%}$, respectively). For measurements of the cellular Ca^{2+} transient, the same approach is utilized to measure shortening except myocytes are loaded with cell permeable Fura-2AM dye and Ca^{2+} transients are measured at the same time contractile function is measured in myocytes.

CHAPTER 2

MYOFILAMENT INCORPORATION AND CONTRACTILE FUNCTION AFTER GENE TRANSFER OF CARDIAC TROPONIN I SER43/45ALA

License Number: 3286690235710

License Date: 12/12/13

License Publisher: Elsiever

License Content Publication: Archives of Biochemistry and Biophysics

ABSTRACT

Phosphorylation of cardiac troponin I serines 43/45 (cTnISer43/45) by protein kinase C (PKC) is associated with cardiac dysfunction and yet there is disagreement about the role this cluster plays in modulating contractile performance. The present study evaluates the impact of phospho-null Ala substitutions at cTnISer43/45 (cTnISer43/45Ala) on contractile performance in intact myocytes. Viral-based gene transfer of cardiac troponin I (cTnI) or cTnISer43/45Ala resulted in time-dependent increases in expression, with 70-80% of endogenous cTnI replaced within 4 days. Western analysis of intact and permeabilized myocytes along with immunohistochemistry showed each exogenous cTnI was incorporated into the sarcomere of myocytes. In contractile function studies, there were no differences in shortening and re-lengthening for cTnI and cTnISer43/45Ala-expressing myocytes 2 days after gene transfer. However, more extensive replacement with cTnISer43/45Ala after 4 days diminished peak shortening amplitude and accelerated re-lengthening measured as the time to 50% re-lengthening ($TTR_{50\%}$). A decrease in myofilament Ca^{2+} sensitivity of tension also was observed in permeabilized myocytes expressing cTnISer43/45Ala and was consistent with accelerated re-lengthening observed in intact myocytes under basal conditions. Phosphorylation of cTnISer23/24 and the Ca^{2+} transient were not changed in these myocytes. These results demonstrate extensive sarcomere expression of cTnISer43/45Ala directly modulated myofilament function under basal conditions. In further work, the accelerated re-lengthening observed in control or cTnI-expressing myocytes treated with the PKC agonist, endothelin-1 (ET, 10nM), was slowed in myocytes expressing cTnISer43/45Ala. This outcome may indicate cTnISer43/45 is targeted for phosphorylation by ET-activated PKC and/or influences transduction of this agonist-activated response.

INTRODUCTION

Thin filament cardiac troponin (cTn) interacts with tropomyosin and actin to regulate actomyosin interactions in response to changes in calcium during cardiac systole and diastole [7, 20]. Cardiac troponin I (cTnI) acts as a molecular rheostat within the Tn complex by strongly interacting with actin in the absence of Ca^{2+} and then toggling to interact with troponin C (cTnC) as Ca^{2+} levels increase [2]. Multiple kinases phosphorylate TnI and often modulate myofilament Ca^{2+} sensitivity. In biochemical studies, protein kinase C (PKC), a serine/threonine kinase, phosphorylated the cardiac isoform of troponin I (cTnI) at three residue clusters: serines 23/24 (Ser23/24), serines 43/45 (Ser43/45), and threonine 144 (Thr144), based on the rat sequence [26]. Phosphorylation of cTnISer43/45 is of interest because heart failure is associated with increased phosphorylation of the analogous Ser41 and Ser43 residues in human cTnI [27] [65]. Increased cTnISer43 and/or cTnISer45 phosphorylation in myocardium also develops with cardiac dysfunction caused by pressure overload in rats [29, 30]. In addition, transient increases in cTnI Ser43 phosphorylation are observed in a mouse model of myocardial infarction [31].

Experimental work with PKC-phosphorylated cTnI indicates phosphorylation at these residues decreases myofilament Ca^{2+} sensitivity and peak contractile function. Biochemical studies indicate moderate TnI phosphorylation by PKCδ decreases myofilament Ca^{2+} sensitivity and peak actomyosin ATPase [45, 51, 60]. Further phosphorylation by this isozyme significantly reduces maximum ATPase activity and dampens the Hill coefficient (n_H). Extraction and replacement with cTnI containing phospho-mimetic Glu at cTnISer43/45 produces a similar decrease in Ca^{2+} sensitivity and peak isometric force as well as peak sliding velocity [68, 81]. In a transgenic (tg) mouse model, replacement of wild-type cTnI with phospho-mimetic Asp

residues at all 3 PKC-targeted clusters produced a similar shift in peak actomyosin ATPase activity[49]. These changes are consistent with the slowed rate of contraction measured *in vivo*.

In contrast to this work, studies with phospho-null cTnISer43/45Ala substitutions have generated different ideas about the role played by this cluster in modulating myofilament function. In keeping with phosphorylation and phospho-mimetic studies, replacement of wild-type cTnI with phospho-null Ala substitutions at Ser43/45 blunted the Ca^{2+} sensitivity shift of actomyosin ATPase activity during moderate cTnI-specific phosphorylation by PKCδ [61]. However, cTnISer43/45Ala also appeared to decrease maximum ATPase and Ca^{2+} sensitivity compared to cTnI under basal conditions.

The myofilament functional response associated with cTnISer43/45Ala expression could significantly influence organ-level function. However, cardiac performance is not detectably different between wild-type littermates and a transgenic (tg) mouse model expressing about 50% of total cTnI as cTnISer43/45Ala [82]. Further analysis of cellular function in this model indicated there are changes in myofilament function compared to controls [72] [73]. Myofilament Ca^{2+} sensitivity also appeared to decrease relative to wild-type cTnI in a separate knock-in mouse expressing cTnI with Ala substitutions in all 3 PKC-targeted clusters [64]. Other indices of contractile shortening and the Ca^{2+} transient remained similar to controls.

Results from these earlier studies in mouse models indicate this construct may significantly impact myofilament function, although it is unclear whether the functional response is caused by a direct or adaptive change with cTnISer43/45Ala expression. While Ala substitutions for Ser are favored as a phospho-null substitution due to similarities between these residues, it remains unclear whether Ser43/45Ala is a functionally conservative substitution in cTnI. In the present study, recombinant adenoviral-mediated gene transfer of cTnISer43/45Ala is used to evaluate the

impact of this substitution mutant on contractile function in isolated myocytes. Experiments also tested whether a PKC agonist targets cTnISer43/45 using this substitution mutant.

METHODS

Mutagenesis strategy and adenoviral constructs

Full-length wild-type rat cTnI cDNA [83] was used to substitute serines 43 and 45 with alanines and produce a phospho-null cTnISer43/45Ala using the QuikChange site-directed mutagenesis kit (Invitrogen) [78]. The mutagenesis primers were 5'-gtctaagatc**g**ccgcc**g**ccagaaaacttcag-3' (sense; mutated residues are shown in bold/underlined) and 5'ctgaagttttctgg**c**ggcgg**c**gatcttagac-3' (anti-sense), which removed a BglII site from cTnI. The cDNA for cTnISer43/45Ala with and without a carboxy-terminal FLAG-tag were then sub-cloned into the pDC315 shuttle vector [84]. Recombinant adenoviral vectors for each cDNA were created by homologous recombination of the shuttle vector with pBHGloxΔE1,3Cre in HEK293 cells. High titer, recombinant adenovirus was generated and the titer was determined by plaque assay [85].

Myocyte isolation and gene transfer

Myocytes were isolated from adult, female Sprague-Dawley rats (200g) as previously described in detail [85]. All animal procedures were approved and performed following the guidelines outlined by the University Committee on the Use and Care of Animals at the University of Michigan. Briefly, hearts removed from heparinized rats were perfused on a Baker perfusion apparatus and digested with collagenase and hyaluronidase. Isolated, Ca^{2+}-tolerant myocytes were plated onto laminin-coated coverslips and cultured in DMEM supplemented with 5% FBS, penicillin (50 U/ml), and streptomycin (50μg/ml: P/S) at 37°C in a 5% CO_2 incubator for 2 hrs. Recombinant adenovirus containing cTnI (±FLAG) or cTnISer43/45Ala (±FLAG) was diluted in serum-free media and added to myocytes. One hr later, additional serum-free M199 media supplemented with P/S was added to each well. Media was changed the next day, and then

every other day thereafter for non-paced myocytes. Other coverslips were transferred into a stimulation chamber and paced at 0.2Hz with media changed every 12 hours.

Western blot analysis

The levels of expression and myofilament replacement for each cTnI substitution mutant, myofilament stoichiometry, and cTnI phosphorylation of Ser23/24 were determined via Western blot. Sarcomeric proteins were separated by SDS-PAGE on a 12% acrylamide gel then transferred onto PVDF membranes [86]. Membranes were blocked with 5% milk or albumin and then probed with primary antibody (Ab), followed by conjugated secondary antibodies (Abs). Primary Abs included an anti-troponin I monoclonal Ab (mAb; 1:4000, MAB1691, Millipore), anti-phospho-cTnI Ser23/24 polyclonal Ab (pAb; 1:1000, Cell Signaling), and anti-troponin T mAb (1:500, Fitzgerald). Secondary Abs included Alexa-Fluor 680-conjugated goat anti-mouse (GAM; 1:25,000, Invitrogen), horseradish peroxidase (HRP)-conjugated GAM (1:2000, GAM-HRP, Cell Signaling), and HRP-conjugated goat anti-rabbit (GAR) (1:2000, GAR-HRP, Cell Signaling) Abs. Alexa Fluor-conjugated Ab was detected using an Odyssey infrared imaging system, while a BioRad imaging system detected HRP-conjugated Ab using enhanced chemiluminescence (ECL, Pierce). Quantity One software (BioRad) was used for quantitative analysis of expression. Expression of cTnI, Tm or cTnT were normalized to a silver (Ag)-stained band on the gel or Sypro-stained band on the blot (cTnI only), and phosphorylation of Ser23/24 was normalized to cTnI.

Immunofluorescence

Cellular localization was determined with cTnIFLAG and cTnISer43/45AlaFLAG using indirect immunohistochemistry, as previously described [85]. Localization of each construct was compared to non-treated controls or cTnIFLAG-expressing myocytes. Briefly, myocytes were

fixed in paraformaldehyde, treated with NH_4Cl_4 to minimize excess aldehydes, and then blocked in phosphate buffered saline (PBS) containing 20% normal goat serum (NGS) plus 0.5% Triton X-100. TnI immunostaining was performed with the anti-troponin I mAb described in the Western protocol (1:500), washed and blocked again prior to incubation in secondary GAM Ab conjugated to Texas Red (TR) (1:500, Sigma). After blocking with GAM IgG overnight and GAM IgG Fab fragments for 1 hr, FLAG-tagged cTnI was detected using anti-FLAG mAb (1:500, Invitrogen) and secondary GAM Ab conjugated to fluorescein isothiocyanate (FITC; 1:500, Invitrogen). Cells were imaged with a Fluoview 500 laser scanning confocal microscope (Olympus) and images were de-convoluted with Autoquant X (Media Cybernetics).

Phosphorylation detected by radiolabeling in intact myocytes

Myofilament proteins in intact myocytes were labeled with [^{32}P]orthophosphate in M199 media containing calyculin A (Cal A; 10 nM), as described previously [78]. Radiolabeled proteins were separated with 12% SDS-PAGE. Then, gels were exposed to a phosphorimage cassette to detect myofilament protein phosphorylation.

Sarcomere shortening and calcium transient measurements

Myocytes were paced at 0.2 Hz starting 24 hrs after isolation and then paced for up to 4 days after gene transfer. Resting sarcomere length, peak shortening amplitude (% baseline), time to peak (TTP) shortening, and times to 25%, 50%, and 75% re-lengthening ($TTR_{25\%}$, $TTR_{50\%}$, and $TTR_{75\%}$) were measured on signal-averaged traces collected with a CCD-camera (Ionoptix). Coverslips with myocytes were perfused in a 37ºC chamber. For some experiments, signal-averaged Ca^{2+}-transient and sarcomere shortening measurements were recorded in myocytes loaded with Fura-2AM, as described in detail earlier [86]. Resting and peak Ca^{2+} ratios, the rate of Ca^{2+} rise and decay within the myocyte, and the times to 25%, 50% and 75%

Ca^{2+}-transient decay ($TTD_{25\%}$, $TTD_{50\%}$, $TTD_{75\%}$) were measured 4 days after gene-transfer for these studies.

Isometric force measurements

Isometric force was measured in myocytes 4 days after gene transfer, as described earlier [87, 88]. Briefly, one end of a myocyte was mounted to a motor (Model 315C, Aurora Scientific) and the other end to a force transducer (model 403A, Aurora Scientific) with a resonance frequency of 1.1MHz on the stage of a Nikon TS-*i* Eclipse microscope. Myocytes attached to the force transducer and length controller were incubated in ice-cold high relaxing solution (HR; pH 7.0) composed of pCa (-log [Ca^{2+}]) 9.0, 10 mM EGTA, 20 mM Imidazole, 1 mM free Mg^{2+}, 4 mM free ATP, 14.5 mM creatine phosphate and sufficient KCl to bring the ionic strength to 180 mM at 15^{o}C. Myocytes were permeabilized in HR containing 0.1% Triton X-100 and sarcomere length was set to 2.0 μm. Active isometric tension at each pCa was determined using the slack method, with pCa concentrations ranging from 9.0 to 4.5 [87]. Ion concentrations for each pCa were calculated using MATLAB, as described earlier [89]. Tension was measured in low EGTA-containing relaxing (pCa 9.0) and activating (pCa 4.5) solutions after every two measurements in sub-maximal calcium solutions [87]. Each pCa solution was buffered to pH 7.0 at 15^{o}C and contained Ca^{2+} ranging from 10^{-9} to $10^{-4.5}$ M, 20 mM Imidizole, 7 mM EGTA, 1 mM free Mg^{2+}, 4 mM free ATP, 14.5 mM creatine phosphate along with sufficient KCl to bring the ionic strength to 180 mM. The tension-pCa curve for each group was fitted using the Marquardt-Levenburg nonlinear, least squares algorithm for the Hill equation, where P is the fractional tension, K is the midpoint or –log [Ca^{2+}] producing 50% peak tension (pCa_{50}) and n_H is the Hill coefficient for the equation: $P = [Ca^{2+}]^{nH}/(K^{nH} + [Ca^{2+}]^{nH}$.

Statistical analysis

Results are expressed as mean ± SEM. Myocyte contractile function was analyzed using an unpaired Student's t-test for data collected 2 days after gene transfer. Protein expression and contractile function measured 4 days after gene was analyzed using a one-way analysis of variance (ANOVA) and post-hoc Newman-Keuls tests. Statistical significance was set at $p < 0.05$ (*) for all comparisons.

RESULTS

The initial experiments evaluated sarcomere expression and endogenous cTnI replacement with FLAG-tagged versions of cTnI and cTnISer43/45Ala 2 and 4 days after gene transfer. Sarcomere incorporation of cTnISer43/45AlaFLAG and cTnIFLAG was comparable over this time interval. A second important component of this study evaluated whether Ala acts as a neutral amino acid substitution for cTnISer43/45, meaning Ala is functionally conservative and has no impact on contractile function in myocytes. The results show this substitution produces direct, functional changes in contractile performance following extensive cTnISer43/45Ala replacement without generating adaptive responses within the myocyte.

Expression and sarcomeric replacement with cTnI substitution mutants.

The initial work focused on analyzing expression and sarcomere replacement of endogenous cTnI with cTnISer43/45Ala. Western analysis showed both cTnIFLAG and cTnISer43/45AlaFLAG replaced endogenous cTnI over time, with 35-45% replacement after 2 days and 70-80% by day 4 (Figs. 2.1A-C). In myocytes expressing cTnI and cTnISer43/45Ala, protein expression was normalized to a band on the silver-stained gel or Sypro-stained blot, which indicated replacement with either cTnI construct did not change total cTnI expression (Fig. 2.1D). The expression level of other thin filament proteins such as tropomyosin (Tm, Fig. 2.1B) and troponin T (TnT; results not shown) also showed preservation of stoichiometry in myocytes expressing FLAG-tagged cTnI and cTnISer43/45Ala. These results are consistent with sarcomeric cTnI replacement and maintenance of thin filament stoichiometry reported in earlier studies [43, 49, 90, 91].

Biochemical studies and indirect immunohistochemistry indicated both constructs are incorporated into the sarcomere. Similar levels of non- and FLAG-tagged cTnI and

cTnISer43/45Ala expression were detected by Western analysis in intact and detergent permeabilized myocytes (Fig. 2.2A). Confocal image analysis of immunostained myocytes provided further proof these exogenous cTnIs were incorporated into sarcomeres (Fig. 2.2B). The striated staining observed with anti-FLAG Ab overlapped with the sarcomere pattern detected with anti-TnI Ab in myocytes expressing cTnIFLAG or cTnISer43/45AlaFLAG (Fig. 2.2B).

Influence of cTnISer43/45Ala on basal contractile performance.

In the next set of studies, sarcomere shortening and re-lengthening in intact myocytes was measured to evaluate the impact of cTnISer43/45Ala expression on contractile function. There were no significant differences in the mechanics and kinetics of shortening and re-lengthening between myocytes expressing cTnI versus cTnISer43/45Ala 2 days after gene transfer (Fig. 2.3A). Resting sarcomere length, shortening and re-lengthening rate, and time to peak shortening (TTP) also were similar in myocytes expressing cTnI or cTnISer43/45Ala compared to non-treated controls 4 days after gene transfer (Fig. 2.3B). However, peak shortening amplitude was significantly decreased in myocytes expressing cTnISer43/45Ala compared to controls (Fig. 2.3B). In addition, the time to 50% re-lengthening ($TTR_{50\%}$) was significantly accelerated in cTnISer43/45Ala-expressing myocytes compared to myocytes expressing cTnI. These results indicate more extensive replacement of endogenous cTnI with cTnISer43/45Ala diminished shortening amplitude and accelerated re-lengthening 4 days after gene transfer.

Isometric tension measurements were performed to determine whether cTnISer43/45Ala directly influences myocyte contractile function. Analysis of the pCa_{50} derived from the tension/pCa relationship indicated cTnISer43/45Ala produced a significant decrease in myofilament Ca^{2+} sensitivity of tension (Fig. 2.3C). However, similar peak tension values were

observed in control, cTnI- and cTnISer43/45Ala-expressing myocytes (controls: 3.48mN±0.51, n=10; cTnI: 5.00mN±0.54, n =11; cTnISer43/45Ala: 3.20mN±0.67, n=6). The accelerated re-lengthening in intact myocytes and rightward shift in Ca^{2+}-activated tension indicate cTnISer43/45Ala decreases myofilament Ca^{2+} sensitivity. However, the reduction in shortening amplitude without peak tension changes may result from adaptive changes within the myocyte.

Compensatory adaptations in cardiac myocytes expressing cTnISer43/45Ala.

The cellular Ca^{2+} transient was measured in Fura-2AM-loaded myocytes to determine whether direct or adaptive changes contributed to the diminished shortening amplitude in myocytes. In agreement with the earlier results, shortening amplitude in Fura-2AM-loaded myocytes remained significantly lower and $TTR_{50\%}$ was accelerated in cTnISer43/45Ala-expressing myocytes relative to cTnI-expressing myocytes (Fig. 2.3; results not shown). Basal and peak Ca^{2+} ratios were not significantly different between myocytes expressing cTnI versus cTnISer43/45Ala (Fig. 2.4). There was a trend toward accelerated TTD values in Fura-loaded myocytes expressing cTnISer43/45Ala, although this change was not statistically different from controls (Fig. 2.4).

The potential for myofilament adaptations to differentially impact peak shortening versus tension was evaluated in the next group of studies. There were no detected differences in ^{32}P incorporation into proteins when comparing radiolabeled control and cTnISer43/45Ala-expressing myocytes (Fig. 2.5A). Additional work with a cTnISer23/24 specific phospho-Ab showed phospho-cTnISer23/24/total cTnI ratios tended to increase in cTnISer43/45Ala-expressing myocytes but were not significantly different from controls (Fig. 2.5B-C). The absence of change in the Ca^{2+} transient and myofilament phosphorylation suggest this cTnI substitution mutant directly influences cross-bridge cycling rate, but not peak tension.

The effects of cTnISer43/45Ala on the contractile response to endothelin-1.

Introduction of a phospho-null cTnI into the myofilament, such as cTnISer43/45Ala, is often used to determine whether specific residue(s) are targeted by kinases such as PKC. Thus, the ability of the endogenous PKC-activating neurohormone, endothelin-1 (ET), to modulate contractile function was compared in cTnI- and cTnISer43/45Ala-expressing myocytes. In earlier work, cTnI phosphorylation by ET preserved re-lengthening rate [78]. Studies with a cTnISer23/24Ala phospho-null indicated this cluster contributed to re-lengthening rate after 60 min of ET (10 nM) treatment but had little influence during an acute 15 min treatment with ET. In the present studies, ET increased shortening amplitude and accelerated the shortening rate in all 3 groups of myocytes, in keeping with the earlier work (Fig. 2.6). There was a trend for re-lengthening rate to be slower in cTnISer43/45Ala-expressing myocytes compared to myocytes expressing cTnI or cTnIFLAG, although this difference was not statistically significant (Fig. 2.6). However, myocytes expressing cTnISer43/45Ala developed a significant increase in the time to 75% re-lengthening ($TTR_{75\%}$) compared to control or cTnIFLAG-expressing myocytes. This slowed re-lengthening also was matched by a trend toward an accelerated time to peak shortening (TTP) with cTnISer43/45Ala, although the ET-induced change in TTP was not statistically different from controls. Taken together, these results suggest the cTnISer43/45 cluster helps to preserve re-lengthening rate during the ET response. ET activation of PKC presumably phosphorylates this cluster to maintain re-lengthening rate, which is absent from myocytes expressing cTnISer43/45Ala.

DISCUSSION

The goals of the present study were to determine whether cTnISer43/45Ala is a functionally conservative substitution and to identify whether this residue cluster contributes to functional responses to the PKC agonist, ET. Ala substitution for Ser at 43/45 in cTnI is expected to be functionally conservative and not diminish the myocyte contractile function response to PKC. This substitution mutant has no detectable influence on intact myocyte shortening when it replaced less than 50% of endogenous cTnI 2 days after gene transfer (Figs. 2.1, 2.3). However, more extensive sarcomere incorporation of cTnISer43/45Ala by day 4 decreased myofilament Ca^{2+} sensitivity and accelerated re-lengthening, in addition to reducing myocyte shortening amplitude under basal conditions (Figs. 2.1-2.3). Collectively, this work demonstrates Ser residues at cTnI43/45 contribute to basal contractile function in the myofilament. In addition, high cTnISer43/45Ala levels slowed re-lengthening in response to the PKC agonist ET compared to controls (Fig. 2.6). These later results are consistent with Ala substitutions at cTnISer43/45 acting as phospho-null residues during the agonist response and support the idea this cluster contributes to PKC agonist-induced modulation of contractile function.

The functional changes caused by extensive replacement with cTnISer43/45Ala may be due to the polar attributes of Ser compared to Ala. In the x-ray crystal structures for the Tn core domain, both cTnISer43 and cTnISer45 reside in an α-helical region at the start of the I-T arm and are in close proximity to the N-lobe of cardiac troponin C (cTnC) [25]. Kobayashi and colleagues suggested cTnISer45 interacts with Glu10 in cTnC and cTnISer45 phosphorylation would disrupt this interaction [71]. Introduction of a less polar Ala at this site and at cTnISer43 also could modify interactions between cTnI and cTnC and lead to the decreased Ca^{2+} sensitivity predicted to result from phosphorylation. The shift in myofilament Ca^{2+} sensitivity of tension

and the accelerated $TTR_{50\%}$ in intact myocytes (Fig. 2.3B) are consistent with this interpretation. My findings also indicate cTnISer43/45Ala may be a useful tool to investigate cTnI residues leading into the amino-terminus of the I-T arm (aa 33-45). This region has the potential to interact with multiple domains within cTnI and cTnC, as it traverses the region between the amino- and carboxyl- globular TnC domains.

The results showing a reduction in myofilament Ca^{2+} sensitivity with cTnISer43/45Ala expression are predicted to accelerate relaxation in intact myocytes. Indeed re-lengthening was accelerated in myocytes, although this acceleration was detected midway through re-lengthening (Fig. 2.3B). Diminished myofilament Ca^{2+} sensitivity also was evident in a $cTnIAla_5^{nb}$ mouse model expressing cTnI with Ala substitutions at Ser23/24, Ser43/45 and Thr144 [47, 64]. In addition, there was a trend toward reduced myofilament Ca^{2+} sensitivity in a transgenic mouse expressing cTnISer43/45Ala, although the change was not statistically significant [74]. While cTnISer43/45Ala replaced about 50% of endogenous cTnI in the transgenic model, expression of $cTnI\text{-}Ala^5$ on a null background left no endogenous cTnI in these hearts. Changes in re-lengthening and Ca^{2+} sensitivity were detected with more extensive cTnISer43/45Ala replacement at day 4 in this study (Fig. 2.3B). These results, together with findings in mouse models suggest extensive cTnISer43/45Ala replacement is required to shift myofilament Ca^{2+} sensitivity.

Based on earlier work, it was unclear whether peak isometric tension would change in myocytes expressing cTnISer43/45Ala compared to controls. No changes in peak tension are observed in the current work, although decreased peak tension is observed in fiber bundles from transgenic hearts expressing cTnISer43/45Ala compared to non-transgenic controls [82]. This difference is not likely explained by the level of cTnISer43/45Ala expression, as 70-80%

replacement is achieved in the present study, which exceeds the ~50% replacement in tg myocytes (Fig. 2.1) [82]. Instead, the dissimilar outcomes may be explained by elevated cTnI and troponin T (TnT) phosphorylation in the transgenic fiber bundles [72, 74]. There are no detectable changes in myofilament phosphorylation compared to control levels in the present study (Fig. 2.5). The reductions in peak tension and sliding velocity observed with a phospho-mimetic cTnISer43/45Glu during i*n vitro* studies also are consistent with diminished peak tension caused by adaptive Tn phosphorylation in the transgenic mouse model [68] [82]. In addition, the lack of change in peak tension and myofilament phosphorylation detected in myocytes from the $cTnIAla_5^{nb}$ mouse are similar to results in the present study (Figs. 2.3, 2.5) [47, 64].

In contrast to peak tension, extensive replacement with cTnISer43/45Ala is associated with diminished shortening amplitude in myocytes in the present study (Fig. 2.3). Changes in the amplitude and re-lengthening rate are not observed in myocytes from the $cTnIAla_5^{nb}$ mouse [47, 64]. The divergent outcomes between the current work and the $cTnIAla_5^{nb}$ may be due to different experimental conditions, such as pacing frequency, temperature and/or animal model. Alternatively, there may be other adaptive differences between the 2 studies, such as changes in the Ca^{2+} transient. Similar Ca^{2+} transients are observed in cTnISer43/45Ala and cTnI-expressing myocytes for the current study, and it is unclear whether myocytes expressing $cTnIAla_5^{nb}$ develop differences in the basal Ca^{2+} transient (Fig. 2.4)[47, 64]. However, cTnISer43/45Ala also reduced unloaded peak actomyosin ATPase activity by 50% in biochemical studies [45]. The later results suggest the Ala substitution may significantly impact unloaded or lightly-loaded myofilament cross-bridge cycling.

A final component of this study compared the contractile response to the PKC agonist, ET in cTnISer43/45Ala and controls. As anticipated, ET enhanced peak shortening in myocytes expressing cTnI or cTnISer43/45Ala (Fig. 2.6). Earlier work established cellular alkalosis produces this enhanced peak shortening response to ET [86, 92]. In contrast, ET accelerated re-lengthening in controls, as measured by $TTR_{75\%}$, while cTnISer43/45Ala slowed this re-lengthening response (Fig. 2.6) [86]. This result is consistent with cTnISer43/45Ala acting as a phospho-null for Ser43/45 during the ET response, although there are alternative explanations for these results. For example, cTnISer43/45Ala-induced decrease in myofilament Ca^{2+} sensitivity under basal conditions may prevent a further shift in Ca^{2+} sensitivity during the ET response and/or modify the troponin conformation such that it is unable to respond to phosphorylation of other target residues. The current work, along with results obtained in several earlier studies, is not able to distinguish between these possibilities [64, 73, 74]. However, more extensive myofilament phosphorylation appeared to be required to decrease the actomyosin ATPase Ca^{2+} sensitivity in response to PKC in at least one study, which provides some support for these alternative possibilities [61].

In conclusion, results from the present study show sarcomeric incorporation of cTnISer43/45Ala in myocytes decreases myofilament Ca^{2+} sensitivity of tension and peak shortening amplitude without triggering adaptive changes in the Ca^{2+} transient or Ser23/24 phosphorylation within cTnI. The slowed re-lengthening produced by cTnISer43/45Ala during the ET response is consistent with this construct acting as a phospho-null substitution during the response to this PKC agonist.

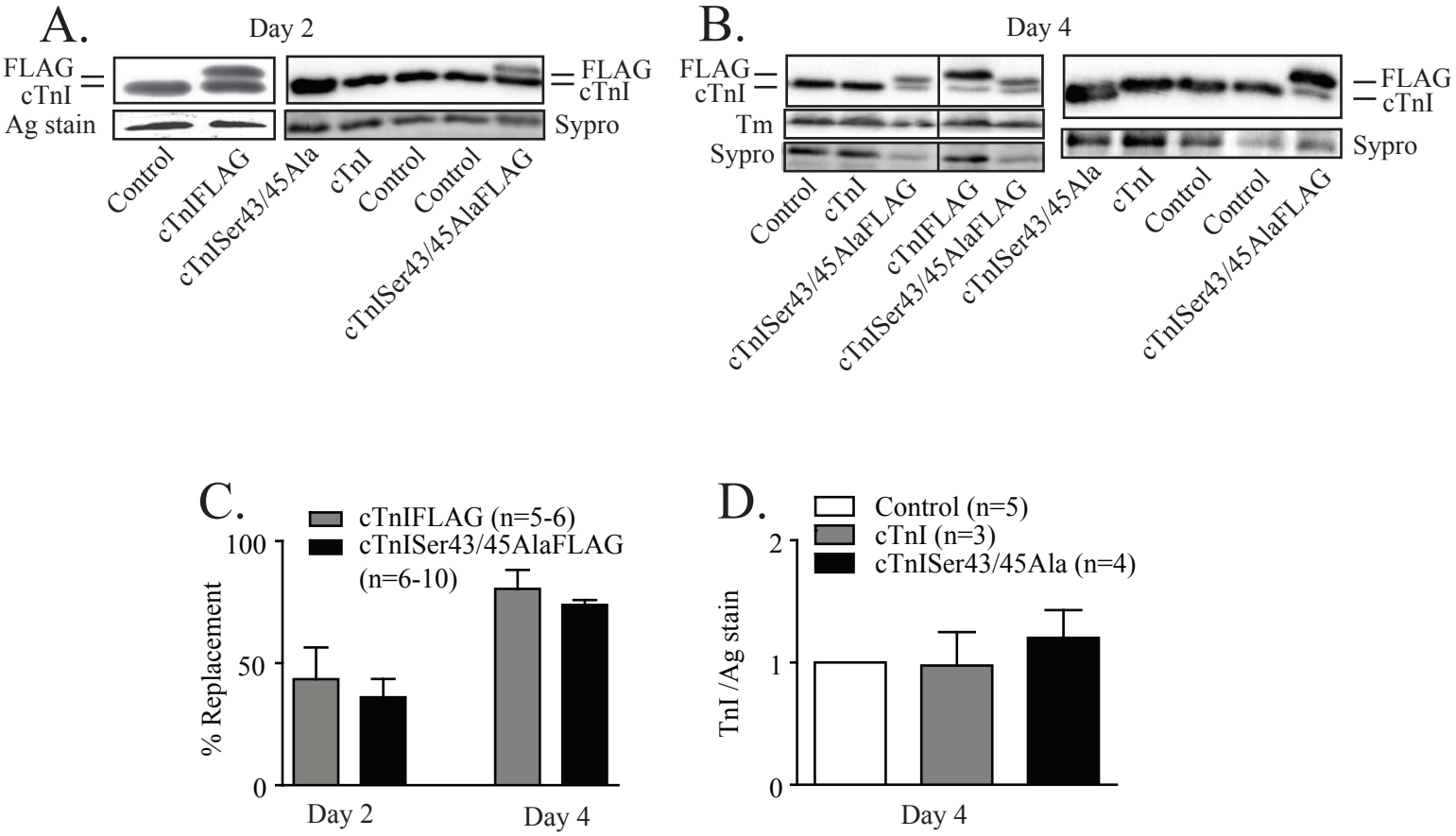

Fig. 2.1 Expression of cTnI and cTnISer43/45Ala with and without FLAG 2 and 4 days after gene transfer. A. Representative Western blot illustrating cTnI expression in myocytes 2 and 4 days after adenoviral-mediated gene transfer of cTnI, cTnIFLAG, cTnISer43/45Ala, and cTnISer43/45AlaFLAG into adult rat myocytes. **B.** Representative Western showing cTnI expression 4 days after gene transfer of the same recombinant viral constructs listed in A. A representative example of tropomyosin (Tm) also is shown in the left panel of B to demonstrate maintenance of thin filament stoichiometry. A silver (Ag)-stained portion of the gel is included in A (right panel) and B to indicate protein loading. Samples show in the left panel of B were separated on the same gel, and the black line between samples indicates separation by additional samples. **C.** Quantitative comparison of endogenous cTnI replacement by cTnIFLAG and cTnISer43/45AlaFLAG 2 and 4 days after gene transfer. Results are expressed as FLAG expression as a percentage of total TnI expression. **D.** Quantitative analysis of cTnI stoichiometry in myocytes 4 days after gene transfer of cTnI or cTnISer43/45Ala. TnI expression is normalized to expression in control myocytes. A one-way ANOVA indicated there were no significant differences (*$p>0.05$) in cTnI expression compared to controls in panel D.

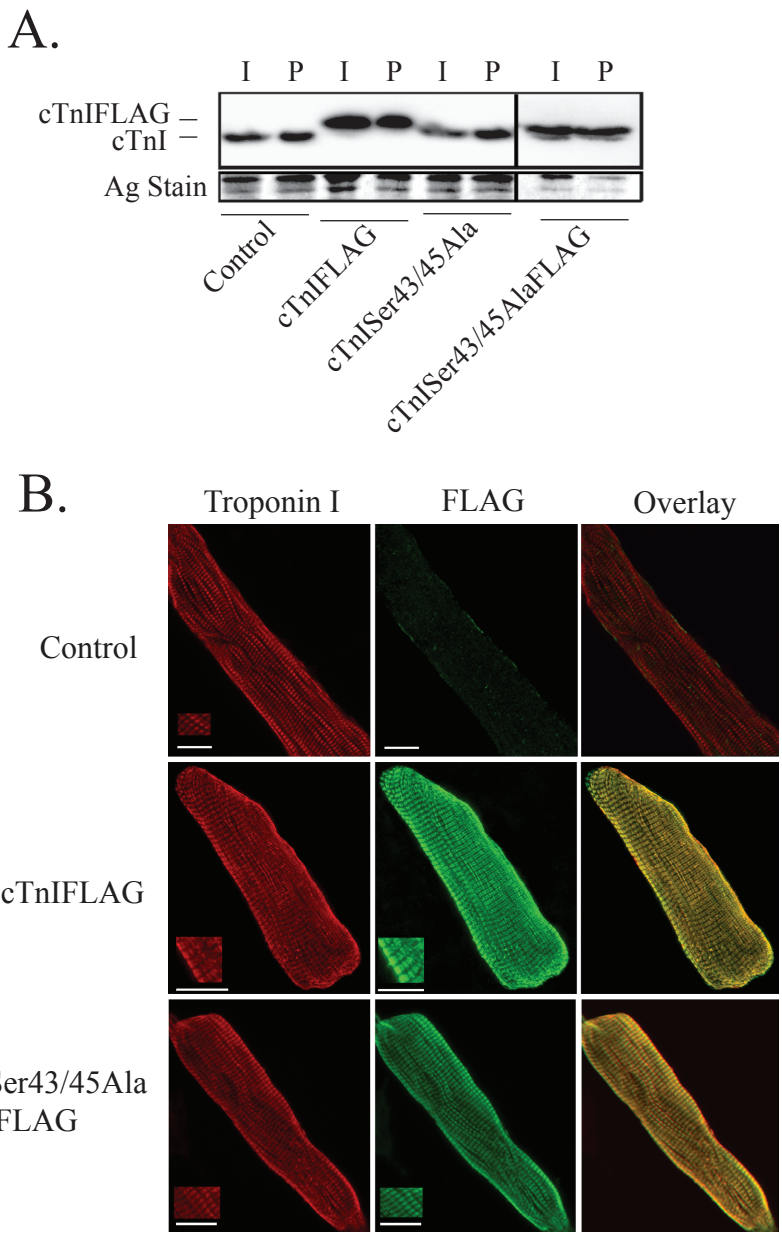

Fig. 2.2 Analysis of sarcomere incorporation of cTnI and cTnISer43/45Ala with and without FLAG tags. A. A representative Western comparing cTnIFLAG, cTnISer43/45Ala, and cTnISer43/45AlaFLAG expression in intact (I) and detergent-permeabilized (P) myocytes 4 days after gene transfer. Samples shown were separated on the same gel and the black line between samples indicates separation by additional samples. A silver (Ag)-stained portion of the gel is shown to indicate protein loading in each lane. There were no detectable differences in the expression detected in intact and permeabilized myocytes, which provides evidence of sarcomere incorporation for each construct. **B.** Projection confocal images showing cTnI (left panel) and FLAG (middle panel) immunostaining along with the overlay (right panel) for control myocytes (top panels) and myocytes expressing cTnIFLAG (middle panels) and cTnISer43/45AlaFLAG (lower panel). Dual immunostaining for cTnI and FLAG were detected with TR and FITC, respectively, as described in the Methods section. Insets for each myocyte are shown to demonstrate a higher resolution striated pattern of immunostaining. These results show sarcomere localization of cTnIFLAG and cTnISer43/45AlaFLAG in the myofilament.

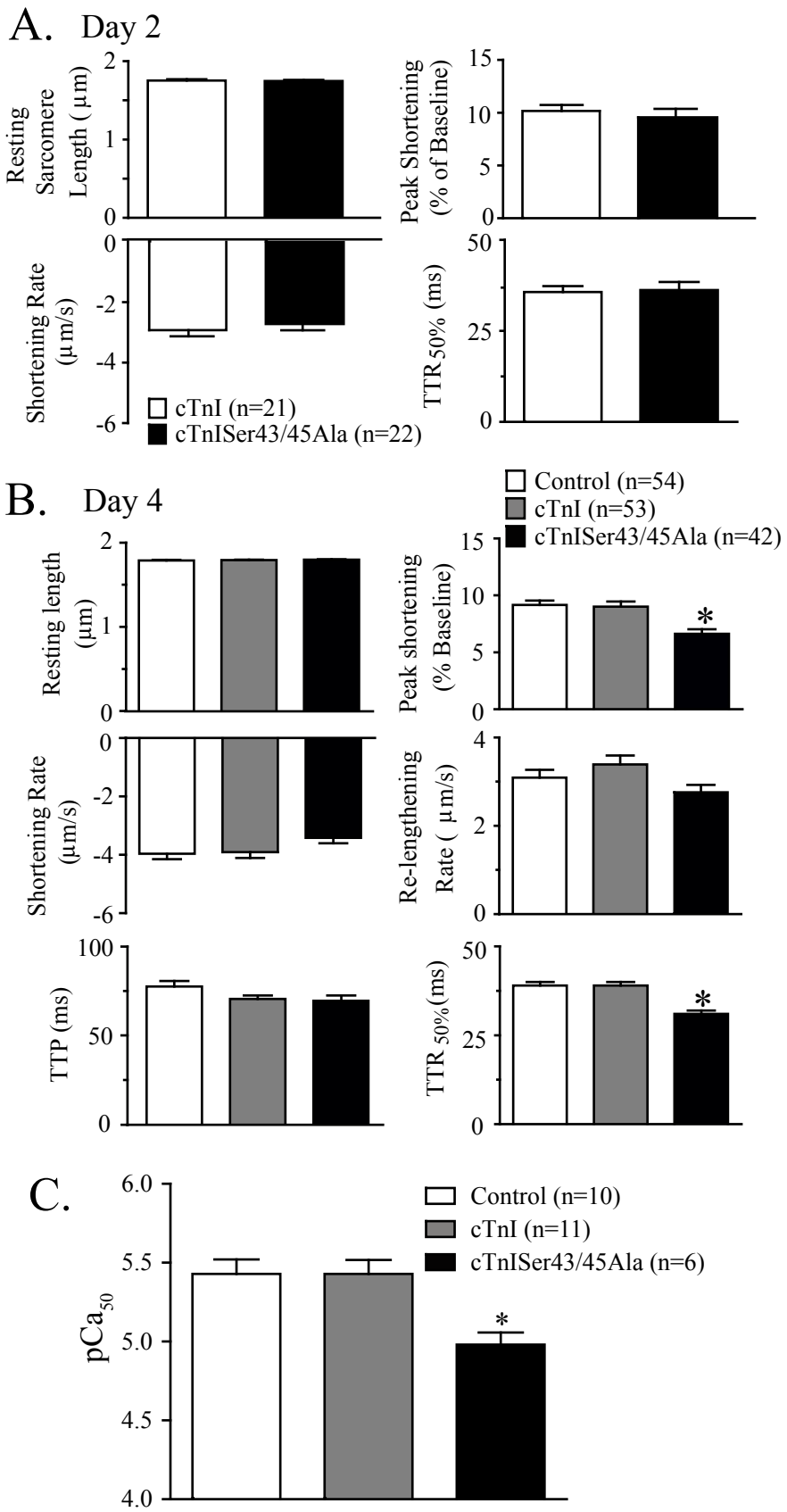

Fig. 2.3. Cardiac myocyte contractile function 2 and 4 days after gene transfer of cTnI constructs. A. Comparison of sarcomere shortening and re-lengthening measurements in control myocytes and myocytes expressing cTnISer43/45Ala 2 days after gene transfer. An unpaired Student's t-test indicated there were no significant differences between myocyte groups.

Fig 2.3 (cont.) In addition to these measurements, the time to peak (TTP), re-lengthening rate, and times to 25% and 75% re-lengthening also were not different between these 2 groups. **B.** Comparison of cardiac myocyte shortening and re-lengthening 4 days after gene transfer of cTnI and cTnISer43/45Ala. Results were compared using a one-way ANOVA and Newman-Keuls post-hoc test with $p<0.05$ (*) considered statistically significant from control values. Resting sarcomere length, shortening and re-lengthening rates and TTP were not different in controls and myocytes expressing cTnIFLAG or cTnISer43/45Ala. The shortening amplitude decreased and there was an acceleration midway through re-lengthening ($TTR_{50\%}$) detected in myocytes expressing cTnISer43/45Ala. **C.** Quantification of pCa_{50} in control myocytes 4 days after gene transfer. Myofilament Ca^{2+} sensitivity was significantly reduced in cTnISer43/45Ala-expressing myocytes versus controls (Control 5.43±0.091, n=10, cTnI 5.43±0.088, n=11 and cTnISer43/45Ala-expressing myocytes 4.98±0.077, n=6). Statistical differences between the pCa_{50} values were identified using one-way ANOVA and Newman-Keuls post-hoc test with (*$p<0.05$) considered statistically significant.

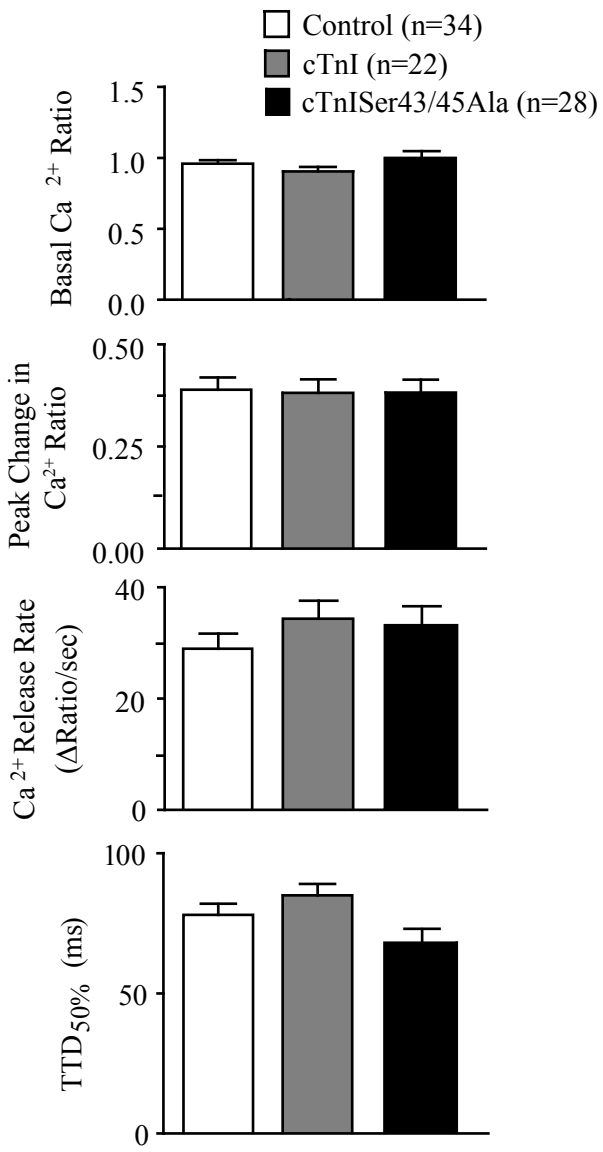

Fig. 2.4 Comparison of Ca^{2+}-transients in Fura-2AM-loaded myocytes 4 days after gene transfer. Basal and peak Ca^{2+} levels were similar in control, cTnI-, and cTnISer43/45Ala-expressing myocytes. The rates of Ca^{2+} release and decay also were similar among the 3 groups. There was a trend toward acceleration of Ca^{2+} decay, as indicated in the $TTD_{50\%}$, although a one-way ANOVA indicated there was no statistically significant difference from control values ($p>0.05$).

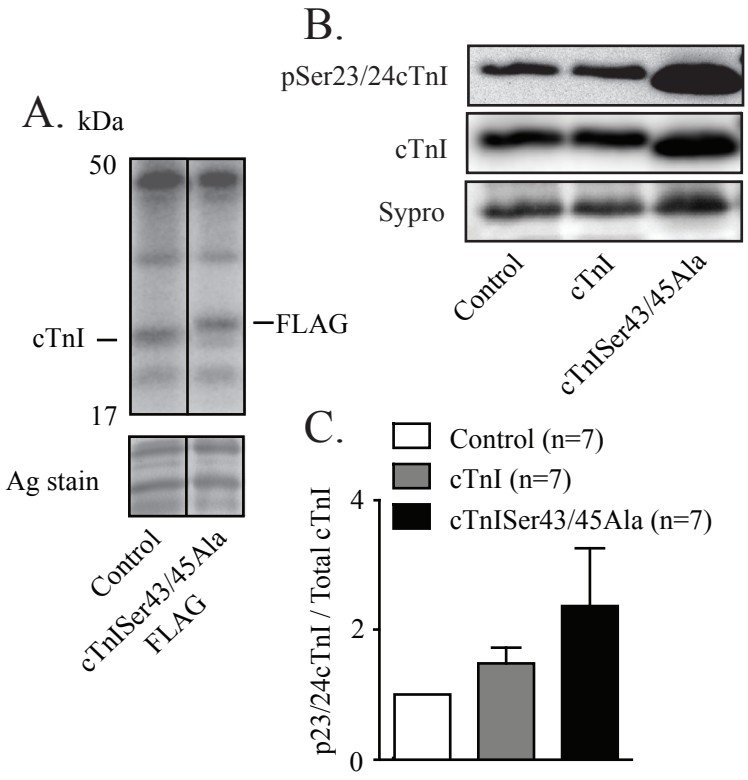

Fig. 2.5 Myofilament phosphorylation 4 days after gene transfer. A. Radiolabeling of proteins observed after 32P incorporation into control and cTnISer43/45Ala-expressing myocytes. **B.** Representative Western blot showing cTnISer23/24 phosphorylation (top panel), cTnI expression (middle panel) and a band on the Sypro-stained blot (lower panel). **C.** Quantitative comparison of cTnISer23/24 phosphorylation in myocytes expressing cTnI. Total cTnI was normalized to a quantified band on Sypro-stained blots. A one-way ANOVA and Newman-Keuls post-hoc tests showed there was no significant elevation in cTnISer23/24 phosphorylation in cTnISer43/45Ala-expressing myocytes.

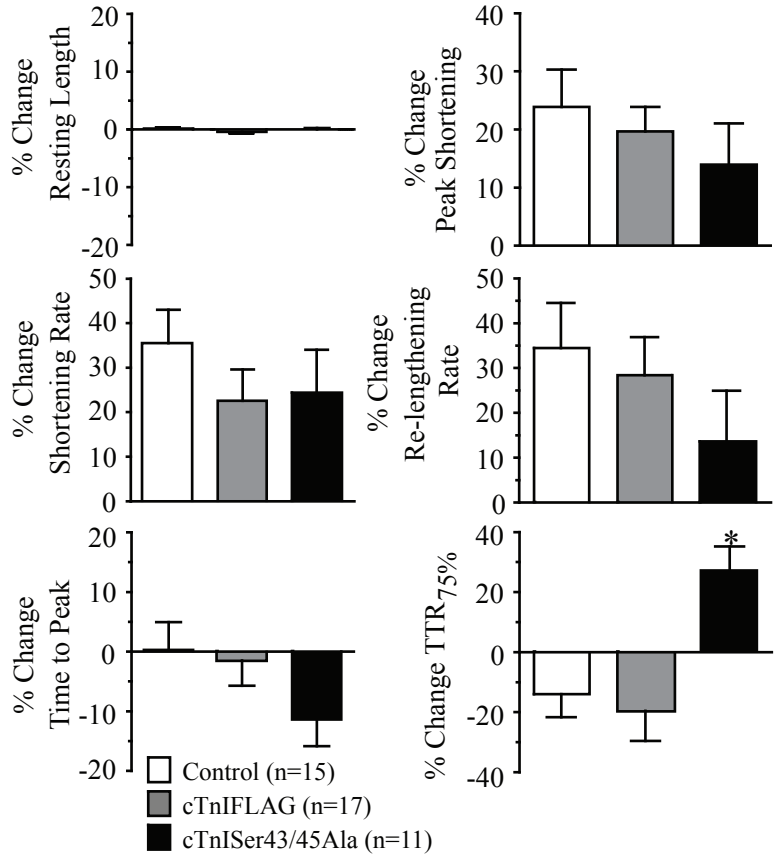

Fig. 2.6 Sarcomere shortening and re-lengthening in response to the PKC agonist, endothelin-1 (ET, 10 nM). Experiments were performed using control myocytes and myocytes expressing cTnIFLAG or cTnISer43/45Ala 4 days after gene transfer. Results are expressed as a % change from basal during 15 minutes of ET. A one-way ANOVA analysis and post-hoc Neuman-Keuls tests (*$p<0.05$) showed significant increases in $TTR_{75\%}$ for cTnISer43/45Ala-expressing myocytes compared to controls. This increase indicates a slowing of relaxation in myocytes expressing cTnISer43/45Ala and suggests cTnISer43/45 phosphorylation may preserve relaxation rate during the ET response. Measurements of times to 25% and 50% re-lengthening were not significantly different between the 3 groups.

CHAPTER 3

PHOSPHO-MIMETIC SUBSTITUTION OF CARDIAC TROPONIN I SER43 AND SER45 GENERATES COMPENSATORY ADAPTATIONS

ABSTRACT

Protein kinase C (PKC)-mediated phosphorylation of cardiac troponin I (cTnI) is predicted to modulate contractile function in the heart. PKC targets multiple residues on cTnI including serines 43/45 (cTnISer43/45), although the specific modulatory role played by cTnISer43/45 phosphorylation is controversial. The goals of the present study are to bridge differences between *in vitro* and *in vivo* studies by determining the functional impact of cTnISer43/45 phosphorylation on intact myocyte function. Specifically, contractile function in intact cardiac myocytes is analyzed after viral-based gene transfer to replace endogenous cTnI with phospho-mimetic cTnISer43Asp and/or cTnISer45Asp. Partial replacement with cTnISer43Asp or cTnISer45Asp reduced peak shortening amplitude, while cTnISer45Asp also slowed shortening and re-lengthening rates 2 days after gene transfer. Increased replacement of cTnISer43Asp and cTnISer45Asp over 4 days, along with cTnISer43/45Asp, continued to reduce peak shortening amplitude. Diminished myofilament Ca^{2+} sensitivity of tension also is observed at the same time point in permeabilized myocytes expressing cTnISer45Asp. Taken together, these results demonstrate cTnISer43 and cTnISer45 independently modulate contractile function. Results from intact cells also show the cTnISer43/45 substitutions produce a different functional phenotype than cTnISer23/24 phosphorylation, in agreement with *in vivo* measurements in genetic animal models. In addition, the later phase of shortening and re-lengthening are accelerated in myocytes with cTnISer43 and cTnISer45 substitutions at day 4 compared to day 2. This finding indicates the onset of an adaptive signaling response. Indeed, significant changes in cellular Ca^{2+} re-uptake and myofilament protein phosphorylation are detected and are consistent with the adaptive functional response, which is predicted to help fine tune the influence of PKC-

mediated cTnISer43/45 phosphorylation on contractile performance in myocytes and the intact heart.

INTRODUCTION

Dynamic regulation of myofilament proteins is essential for coordinating cardiac pump performance during both systole and diastole. Calcium binding to the thin filament during systole initiates the transition of the myofilament to a pressure generating state. The function of this pump is modulated by post-translational phosphorylation of many sarcomeric proteins, such as the thin-filament protein cardiac troponin I (cTnI) [3, 4]. Many kinases target cTnI, including the Ser/Thr kinase PKC, which phosphorylates 3 cTnI clusters of residues, including Ser23/24 in the cardiac-specific N-terminal domain, Ser43/45 in the H1(I) α helix, and Thr144 in the inhibitory peptide (IP) region [60] [25, 26]. PKC expression and activation increases and cTnI phosphorylation patterns are altered in both human and animal models of cardiac dysfunction [27] [28-31, 56, 65]. Thus, understanding the precise functional role of each PKC-targeted cluster in cTnI will provide insight into their contribution and/or role during cardiac dysfunction and the progression to end-stage heart failure.

Extensive work has focused on the functional impact of cTnISer23/24 phosphorylation. In addition to PKC, this cluster is targeted by other kinases in the AGC family, including protein kinase A (PKA), protein kinase G (PKG), as well as a member of the Ca^{2+}/calmodulin-dependent kinase superfamily, protein kinase D (PKD) [93] [34] [33] [94] [95] [96]. Phosphorylation at cTnISer23/24 enhances the Ca^{2+} dissociation rate from the regulatory site on troponin C (TnC), which reduces myofilament Ca^{2+} sensitivity of tension and actomyosin ATPase activity [42]. In the heart, this shift augments cardiac relaxation rate in both *in vitro* and *in vivo* systems [49] [43, 45, 46, 60]. Accelerated relaxation rate helps to preserve diastolic filling time, which is particularly important in response to sympathetic stimulation of PKA during the "fight or flight" response. A consistent reduction in cTnISer23/24 phosphorylation also develops in both animal

and human models of end-stage heart failure, which is postulated to contribute to diastolic dysfunction during end-stage heart failure [27] [28-31].

In contrast, the modulatory role of cTnISer43/45 phosphorylation remains controversial. Several earlier studies showed PKC-mediated phosphorylation of cTnI reduced Ca^{2+} sensitivity and maximum MgATPase activity in reconstituted myofilaments , while PKC phosphorylation of the myofilament was associated with increased Ca^{2+} sensitivity in other studies [68] [47, 64, 69] [97, 98]. More recent studies examined the impact of cTnI with phospho-null Ala or negatively charged Asp/Glu phospho-mimetic substitutions on cTnISer43/45 to determine whether this cluster produces and increased or decreased myofilament Ca^{2+} sensitivity. Substitution of cTnISer43/45 with phospho-mimetic Asp reduced myofilament Ca^{2+} sensitivity and maximum actomyosin ATPase activity while non-phosphorylatable alanine (Ala) attenuated these changes [67] [51, 60, 63]. Exchange of endogenous cTnI with a phospho-mimetic cTnISer43/45Glu also reduced Ca^{2+}-sensitivity and maximum isometric tension in a permeabilized, multi-cellular papillary preparation. Moreover, exchange with cTnISer43/45Glu reduced maximum thin filament sliding speed and cooperativity (reduced Hill coefficient [nH]) without altering the Ca^{2+} sensitivity of sliding in motility assays [68]. Based on these *in vitro* analyses, PKC-mediated cTnISer43/45 phosphorylation appears to reduce contractile function, although the changes responsible for the divergent PKC-mediated functional responses are not completely understood.

Further work examined the role of cTnISer43/45 and the other 2 clusters in transgenic (tg) mouse models to better understand the role of PKC-mediated cTnI phosphorylation in modulating whole heart function. Full replacement of endogenous cTnI with cTnI containing phospho-mimetic Asp substitutions in all 5 PKC-targeted residues ($cTnI_{AllP}$ mouse) reduced myofilament Ca^{2+} sensitivity and maximum values for tension and actomyosin MgATPase

activity [49, 75]. These changes are predicted to reduce peak pressure or perhaps accelerate relaxation rates. However, *in vivo* cardiac function measurements indicated only pressure development is slowed in the $cTnI_{AllP}$ mouse heart, without significant changes in peak pressure or relaxation rate (dP/dt_{min}) compared to non-transgenic controls [49]. Replacement of cTnISer43/45 and cTnIThr144 with phospho-mimetic Glu ($cTnI_{PKC-P}$) in approximately 10% of the cTnI produced a much different phenotype in a second animal model. Peak tension development decreased in papillary muscles isolated from these mice, without a significant change in myofilament Ca^{2+} sensitivity and/or in peak actomyosin MgATPase activity [62]. These myofilament alterations were associated with a reduction in peak pressure and slowing of relaxation in isolated, perfused hearts [62]. Slowing of cardiac pressure development is the one shared component in both $cTnI_{AllP}$ and $cTnI_{PKC-P}$ mice, and yet the difference in the cTnISer23/24 substitution between these models is unable to explain the other phenotypic differences between these mice. Other explanations for these discrepancies, including the contribution of and/or role for adaptive response(s), have not been explored. Additionally, the divergent functional outcomes observed using *in vitro* versus *in vivo* approaches in a mouse model such as the $cTnI_{AllP}$ mouse make it difficult to determine the direct functional role of cTnISer43/45. Based on the current state of understanding, a cellular model combining the simplicity of reconstituted myofilaments with the intact cellular environment is expected to provide insight into the functional impact of cTnISer43/45 phosphorylation on contractile function.

In addition, it remains unclear whether cTnISer43 or cTnISer45 independently modulate contractile function. Phosphorylation at both cTnISer23 and cTnISer24 is required to reduce myofilament Ca^{2+} sensitivity of force and accelerate muscle relaxation [41] [40, 46]. A single *in*

vitro study examined the role of cTnISer45 alone using a Glu substitution in reconstituted actomyosin complexes. This substitution compromised the ability of Ca^{2+} to bind to the actomyosin complex and diminished Ca^{2+}-activated MgATPase by stabilizing the "inactive" or "blocked" state of actin (Fig. 1.2C) [67]. There are no published studies comparing the individual impact of cTnISer43 and cTnISer45 on contractile function.

Experiments in the present study are designed to determine the impact of cTnISer43/45 phosphorylation on isolated cardiac myocyte contractile function using viral-based gene transfer and replacement of endogenous cTnI with cTnI containing phospho-mimetic substitutions at one or both of the Ser43/45 residues. This work demonstrates the direct functional response produced by cTnISer43/45 substitutions and also allows for testing the hypothesis cTnISer43 and cTnISer45 individually influence myofilament function. Overall, the results are in agreement with both earlier *in vitro* and *in vivo* work, and thus bridge the gap emerging from studies in less versus more complex models. The outcome of this work also demonstrates the rapid adaptive response developed with expression of cTnI containing Ser43/45 phospho-mimetic substitutions. Finally, preliminary work is shown to determine whether the increased sarcomeric protein phosphorylation results from increased kinase and reduced phosphatase targeting to myofilament proteins.

METHODS

Gene transfer and cardiac myocyte isolation

Site-directed mutagenesis (QuikChange, Invitrogen) was used to substitute aspartic acid (Asp) for cTnISer43 and/or cTnISer45 in full-length, wild-type cTnI cDNA (rat), as described previously [83, 85, 99]. The cTnI phospho-mimetic substitutions generated include: cTnISer43Asp, cTnISer45Asp, and cTnISer43/45Asp with and without a FLAG tag [99]. The primers for site-directed mutagenesis at cTnISer43 were 5'-atgccaagaaaaagtctaa**gat**cgatgcctccagaaaacttcagttgaag-3' (sense: mutagenized residues are underlined/bolded) and 5'-cttcaactgaagttttctggaggc**atc**gatcctagacttttttcttggcat-3' (anti-sense), which introduced a Hind III site. For cTnISer45Asp, a Cla I site was introduced with a sense primer of 5'-gatctccgcc**ga**cagaaa**g**cttcagttgaag-3' and anti-sense primer of 5'-cttcaactgaag**c**tttctg**tc**ggcggagatc-3'. Phospho-mimetic substitutions were introduced at both residues using the sense primer 5'-gccaagaaaaagtctaagatc**gat**gcc**ga**cagaaaacttcag-3' and the anti-sense primer 5'-ctgaagttttctg**tc**ggc**atc**gatcttagacttttttcttggc-3', which also introduced a ClaI site. Recombinant adenoviruses were constructed by homologous recombination of the pDC315 shuttle vector and pBHGLoxΔE1,3Cre (Microbix) in HEK293 cells for each cDNA [85, 100].

Myocytes were isolated from adult Sprague Dawley rats (200g; female) as approved by and in accordance with the guidelines of the University Committee on the Use and Care of Animals at the University of Michigan (UCUCA). The generation of Ca^{2+}-tolerant myocytes was described in detail in Ch.2 [85] [99]. After plating the myocytes on laminin-coated coverslips, vector-based gene transfer was used to express wild-type cTnI, cTnISer43Asp, cTnISer45Asp, or cTnISer43/45Asp with and without a FLAG-tag [99]. For gene transfer into myocytes, recombinant adenovirus was diluted in serum-free DMEM containing penicillin (50U/ml) and

streptomycin (50μg/ml; P/S) was added to myocytes for 1 hr [99] [85]. Then, M199 media supplemented with P/S was added to cells, and media was changed again 24hr later. Thereafter, media was replaced every other day in quiescent myocytes maintained in 6-well plates. Media was replaced every 12 hrs in a subset of electrically paced cells stimulated at 0.2 Hz.

Expression analysis: Westerns and immunohistochemistry

Replacement of endogenous cTnI with FLAG-tagged wild-type cTnI or phospho-mimetic substitutions, maintenance of myofilament stoichiometry, and changes in myofilament phosphorylation were monitored by Western blot, as described earlier (Ch.2) [99]. Both replacement and sarcomere stoichiometry were analyzed 2 and 4 days post-gene transfer. Studies to assess changes in myofilament phosphorylation were performed 4 days after gene transfer. For Western analysis, PVDF membranes were probed with the primary and secondary antibody pairs shown in Table 3.1, and then proteins were quantified and normalized as previously described (Ch.2)[99].

Primary Antibodies	Secondary Antibodies
Total troponin I (mAb, 1:4000, MAB1691, Millipore)	GAM-HRP (1:2000)
Tropomyosin (mAb, 1:1000, Sigma Aldrich)	GAM-HRP (1:2000)
Phospho-cTnI Ser23/24 (pAb, 1:1000)	GAR-HRP (1:2000)
Total cMyBP-C (pAb, 1:1000, Santa Cruz Biotechnology)	GAR-HRP (1:2000)
Phospho-cMyBP-C Ser273 (pAb, 1:2500)*	GAR-HRP (1:2000)
Phospho-cMyBP-C Ser282 (pAb, 1:2500)*	GAR-HRP (1:2000)
Phospho-cMyBP-C Ser302 (pAb, 1:5000)*	GAR-HRP (1:2000)
Total Phospholamban (pAb: 1:1000, Sigma Aldrich)	GAR-HRP (1:2000)
Phospho-phospholamban Ser16 (pAb, 1:1000, Upstate Biologicals)	GAR-HRP (1:2000)
Phospho-phospholamban Thr17 (mAb, 1:5000, Badrilla)	GAM-HRP (1:2000)

Table 3.1. Antibodies used for Western blot analysis. The left column lists the primary antibody and the corresponding HRP-tagged secondary antibody is listed in the right column. Goat-anti-mouse (GAM), goat-anti-rabbit(GAR), horseradish-peroxidase (HRP). Unless otherwise noted, antibodies were obtained from Cell Signaling Technology. *Site-specific phospho-cMyBP-C antibodies were a kind gift of Dr. Sadayappan [101].

Myofilament incorporation of FLAG-tagged wild-type and substituted cTnI were visualized via indirect immunofluorescence using dual primary antibodies, as described in detail

earlier (Ch.2) [85, 99]. Non-treated and cTnIFLAG-expressing cardiac myocytes served as negative and positive controls, respectively. Immunostaining with an anti-cardiac troponin I antibody (mAb, 1:500, MAB1691, Millipore) and goat-anti-mouse (GAM)-conjugated fluorescein isothiocyanate secondary antibody (1:500, FITC, Sigma) was used to immunostain and localize cTnI. Expression and sarcomere incorporation of exogenous cTnI was examined using a primary antibody directed to the FLAG-tag (mAb; 1:500, Invitrogen) followed by a GAM secondary antibody conjugated to Texas Red (1:500, TR, Invitrogen). Projection images of immunostained myocytes were captured on a Fluoview 500 laser scanning confocal microscope (Olympus), and de-convoluted using Autoquant X software (Media Cybernetics).

Cellular function: sarcomere shortening, Ca^{2+} transient and isometric tension

Two and 4 days after gene transfer, sarcomere shortening was measured in 0.2Hz-paced intact myocytes expressing cTnISer43Asp, cTnISer45Asp, or cTnISer43/45Asp and compared to control myocytes and myocytes expressing wild-type cTnI (Ch.2) [86, 99, 102]. Signal-averaged traces collected using a CCD camera system (Ionoptix) were analyzed for changes in resting sarcomere length, peak amplitude (% baseline), time to peak (TTP), shortening and re-lengthening rates, time to re-lengthening$_{25\%}$ ($TTR_{25\%}$), time to re-lengthening$_{50\%}$ ($TTR_{50\%}$), and time to re-lengthening ($TTR_{75\%}$). In separate studies, the Ca^{2+}-transient and sarcomere shortening were recorded in a subset of chronically paced myocytes loaded with Fura-2AM 2 and 4 days after gene transfer [86] [99, 103]. In these myocytes, resting and peak Ca^{2+}-ratios, rates of Ca^{2+} rise and decay, and the time to decay$_{25\%,\ 50\%,\ 75\%}$ ($TTD_{25\%,}$ $TTD_{50\%,\ and}$ $TTD_{75\%}$, respectively) were determined from signal-averaged traces as described earlier (Ch.2) [99] [86].

Isometric tension was measured in myocytes 4 days after gene transfer to evaluate the effects of cTnISer43/45 phospho-mimetic substitution on myofilament Ca^{2+} sensitivity and peak

tension. Individual myocytes were mounted to a piezoelectric motor (Model 315C, Aurora Scientific) on one end and a force transducer (Model 403A, 600Hz resonance frequency, Aurora Scientific) on the other end, and then sarcomere length was set to either 2.0 μm or 2.3μm in high relaxing (HR; pH 7.0) solution [87, 99]. Cells were permeabilized in (HR) solution containing 0.1% Triton X-100 (Ch. 2), and active tension was measured over Ca^{2+} (pCa = -log [Ca^{2+}]) ranging from pCa 9.0 to 4.5 using the slack test approach (20% of original length [L_o]) (Ch.2) [87-89, 99]. Resting (pCa 9.0) and maximum tension (pCa 4.5) were recorded after each pair of sub-maximal pCa solutions to determine total and resting tension, respectively (Ch. 2). Tension-pCa curves were generated for control, wild-type cTnI, and cTnISer45Asp-expressing myocytes and fitted using the Marquardt-Levenburg non-linear, least squares algorithm for the Hill equation (SigmaPlot). For this algorithm, *P* equals the fractional tension, *K* is equal to the pCa_{50}, and n_H is the Hill coefficient in the following equation: $P = [Ca^{2+}]^{nH}/(K^{nH}+[Ca^{2+}]^{nH})$

Phosphorylation assays

Myocytes cultured for 4 days after gene transfer were treated with kinase and phosphatase inhibitors using the agonists/inhibitors shown in Table 3.2. Inhibitors were diluted in M199 media and applied to cells for 10min-2hr. Cells were incubated in a 37°C water-jacketed incubator. A second set of cells was treated with DMSO (1%) diluted in media or M199 alone to serve as a control for the assay conditions. After inhibitor treatment, Myocytes were collected into ice-cold sample buffer and stored at -80ºC immediately after the incubation with inhibitors/agonists was completed. Myofilament proteins were separated by SDS-PAGE and detected by Western blotting.

Agonist/Inhibitor	Kinase/Phosphatase Targeted	Concentration	Dilution Method	Supplier
H89	Protein Kinase A	1 μM	dH_20	Sigma-Aldrich
kb-NB-142-70	Protein Kinase D	10μM	DMSO	Tocris
Calyculin A	Protein Phosphatases	10nM	Ethanol	CalBiochem

Table 3.2. Kinase and phosphatase inhibitor utilized for phosphorylation assays. Table lists the agonist or inhibitor used, its target, the concentration used, and the vehicle used for dilution.

Data analysis and statistics

Data are presented as the mean ± SEM. Each data set is analyzed by one-way analysis of variance (ANOVA) followed by a Newman-Keuls post-hoc test unless otherwise noted. Results are considered statistically significant when $p \leq 0.05$ (*).

RESULTS

Myofilament expression of cTnISer43/45 phospho-mimetic substitutions

Gene transfer of FLAG-tagged wild-type cTnI, cTnISer43Asp, cTnISer45Asp and cTnISer43/45Asp increasingly replaced endogenous cTnI over time (Fig. 3.1A,B). Each construct replaced 35-45% of endogenous cTnI by day 2, and replacement increased to 65-85% by day 4, in agreement with earlier work (Fig. 3.1B) [78, 86, 99]. Total cTnI protein expression levels remained comparable to controls for each of the constructs (Fig. 3.1C). Western analysis and quantitation of tropomyosin (Tm) expression also indicated thin filament stoichiometry remained unchanged in myocytes expressing each of the cTnI phospho-mimetic substitutions (Fig. 3.1C). Immunohistochemical staining with cTnI and FLAG primary mAbs in myocytes expressing either FLAG-tagged wild-type cTnI or cTnISer43/45 phospho-mimetic substitutions show co-staining of these antibodies in a pattern consistent with sarcomere localization (Fig. 3.2) [99].

Influence of cTnISer43/45 substitutions on myofilament function

Sarcomere shortening and re-lengthening measurements in intact myocytes determined phospho-mimetic cTnISer43 or cTnISer45 replacement significantly diminished peak shortening amplitude 2 days after gene transfer without changing resting sarcomere length (Fig. 3.3). Peak shortening amplitude tended to decrease in cTnISer43/45Asp-expressing myocytes, but this change was not yet statistically different at this time point. Partial replacement of endogenous cTnI with cTnISer45Asp slowed the shortening rate and re-lengthening rate. Both cTnISer43Asp and cTnISer43/45Asp also tended to slow myocyte shortening and re-lengthening, but the reduction produced by either construct was not significantly different from controls at day 2 (Fig. 3.3). All other indices of sarcomeric shortening and re-lengthening also

remained unchanged from controls (Fig. 3.3). These results demonstrate partial myofilament replacement with cTnISer43Asp or cTnISer45Asp independently modulates contractile performance. The relatively enhanced ability of phospho-mimetic replacement at cTnISer45 to modulate shortening and re-lengthening rates also suggests this residue dominantly modulates contractile function. However, the preserved peak shortening amplitude in myocytes expressing cTnISer43/45Asp suggests the individual residues modulate myofilament contractile performance through separate mechanisms.

Four days after gene transfer, cTnISer43Asp, cTnISer45Asp, and cTnISer43/45Asp each diminished peak shortening amplitude to a similar degree as the individual cTnISer45Asp substitutions at day 2 (Figs. 3.3, 3.4A). The reduced peak shortening amplitude was not accompanied by a change in resting sarcomere length for any of the cTnISer43/45 phospho-mimetic constructs. In contrast to day 2, the shortening rate in myocytes expressing cTnISer45Asp returned to control levels while cTnISer43Asp reduced shortening rate (Fig. 3.3 vs. Fig.3.4). Moreover, the time to peak (TTP) shortening is significantly reduced in myocytes expressing cTnISer43Asp or cTnISer45Asp compared to controls 4 days after gene transfer (Fig. 3.4A). An accelerated TTP is consistent with the return of shortening rate toward control values in myocytes expressing cTnISer45Asp but is incongruent with the continued slowing of shortening produced by cTnISer43Asp expression (Fig 3.4A). The re-lengthening rate in cTnISer45Asp-expressing myocytes also returned toward to control values, though the time to re-lengthening 50% ($TTR_{50\%}$) did not differ from controls (Fig. 3.4A). The functional results obtained 4 days after gene transfer support the conclusion cTnISer43 and cTnISer45 independently modulate contractile function. In addition, an acceleration of TTP in the presence of a slowed shortening rate, observed in myocytes expressing cTnISer43Asp, provides evidence

adaptations develop in isolated myocytes with increased cTnISer43/45 phospho-mimetic replacement. The restoration of shortening and re-lengthening rate in myocytes expressing cTnISer45Asp supports this hypothesis.

Based on work in animal models expressing cTnI with phospho-mimetic replacements at cTnISer43/45, the shortening/re-lengthening responses observed in the present study are expected if cTnISer43/45 substitutions reduce myofilament Ca^{2+} sensitivity of tension (pCa_{50}) (Fig. 3.4B) [49, 62]. Therefore, the impact of the cTnISer45Asp substitution on isometric tension generation in permeabilized myocytes was measured over a range of Ca^{2+} concentrations (pCa) 4-5 days after gene transfer. The cTnISer45Asp construct was selected for analysis because it exerted the greatest impact on peak shortening amplitude 2 days post-gene transfer (Fig. 3.3). The tension-pCa relationship remained comparable among control, wild-type cTnI, and cTnISer45Asp-expressing myocytes at a sarcomere length of 2.0 μm (Fig. 3.4B). In earlier work, cTnISer43/45Glu exchanged into permeabilized papillary muscles reduced pCa_{50} and peak tension, but measurements were performed at a sarcomere length of 2.3μm [68]. Thus, tension measurements were repeated at the same sarcomere length, and a reduction in pCa_{50} is observed at this longer length in myocytes expressing cTnISer45Asp compared to controls or myocytes expressing wild-type cTnI (Fig. 3.4B). In contrast to the earlier findings, peak tension remained comparable to controls in myocytes expressing cTnISer45Asp at either sarcomere length. Based on these findings, the reduction in maximum tension observed with cTnISer43/45Glu is either mediated via cTnISer43 and/or could depend on other differences in the experimental approach. However, the observed reduction in myofilament Ca^{2+} sensitivity in myocytes expressing cTnISer45Asp agrees with previous work and may contribute to the restored re-lengthening observed with increased cTnISer45Asp expression 4 days post-gene transfer (Fig. 3.4).

Adaptations in Ca^{2+} cycling and myofilament phosphorylation with cTnISer43/45 substitutions

The restored shortening rate, restored re-lengthening rate, and accelerated TTP observed at day 4 indicates the onset of adaptive responses as cTnISer43/45 phospho-mimetic substitutions increasingly replace endogenous cTnI. One cellular adaptation that can modulate cardiomyocyte shortening and re-lengthening is altered Ca^{2+} cycling. Thus, Ca^{2+} transients were measured in Fura-2AM-loaded myocytes 2 and 4 days post-gene transfer (Figs. 3.5, 3.6). There were no significant changes to the basal Ca^{2+} transient measured in myocytes expressing any of the cTnI phospho-mimetics at day 2 compared to control levels (Fig. 3.5). Additionally, the contractile response was comparable to non-Fura-treated myocytes 2 days after gene transfer (Fig. 3.3 vs. Fig. 3.5). In contrast, adaptations in the Ca^{2+} transient are detected 4 days after gene transfer of the cTnI phospho-mimetic substitutions (Fig. 3.6). In these cells, the $TTR_{50\%}$ was significantly faster than controls after extensive cTnISer45Asp replacement and was accompanied by a faster $TTD_{50\%}$ for Ca^{2+} in all myocytes, including wild-type cTnI (Fig. 3.6). Additionally, basal Ca^{2+} levels increased in both wild-type cTnI and cTnISer43/45Asp-expressing myocytes 4 days after gene transfer. However, this increase did not impair peak Ca^{2+} levels in these myocytes. In contrast, cTnI phospho-mimetic substitutions on one or both cTnISer43/45 residues reduced peak shortening, although the Ca^{2+} transient amplitude remained comparable to controls. No other alterations to Ca^{2+} handling were noted in these studies. Overall, cTnISer43Asp or cTnISer45Asp appear to directly modulate contractile function 2 days after gene transfer. The alterations in baseline Ca^{2+} and $TTD_{50\%}$ observed after 4 days are consistent with a modest adaptive response in the Ca^{2+} cycling pathway.

While altered Ca^{2+} handling could restore or maintain re-lengthening rate in myocytes expressing cTnISer43/45 phospho-mimetic substitutions, the adaptations contributing to the

restored shortening rate are unclear. Basal shortening measurements indicate adaptive changes in the regulation of thin filament function could also contribute to the differences in myocyte contraction observed at 2 versus 4 days. Thus, representative sarcomeric proteins likely to contribute to the adaptive response were examined by comparing the phospho-to-total protein ratios detected using Western analysis in controls and myocytes expressing each of the phospho-mimetic cTnI substitutions. Additional phosphorylation sites within cTnI, cMyBP-C, and PLB were examined to assess adaptive signaling.

Altered phosphorylation in the un-modified, PKC-targeted Ser23/24 cTnI residues was determined using site-specific phospho-antibodies (Fig 3.7). In previous studies, cardiac specific expression of cTnISer23/24Asp reduces myofilament Ca^{2+} sensitivity of tension and accelerates *in vivo* dP/dt_{min} [43]. Indeed, elevated phosphorylation of cTnISer23/24 develops in myocytes expressing cTnISer43Asp or cTnISer45Asp 4 days after gene transfer compared to controls (Fig 3.7A). Phosphorylation also tended to increase with cTnISer43/45Asp expression but did not reach statistical significance (Fig.3.7A). Expression of all 3 cTnISer43/45 phospho-mimetic substitutions also increased phosphorylation of cTnIThr144, but adaptive phosphorylation of this residue was not significantly increased in myocytes studied here (Fig. 3.7B). The cTnIThr144 phospho-mimetic cTnIThr144Glu reduces the Ca^{2+} sensitivity of cross-bridge cycling in *in vitro* motility assays but did not alter tension generation [68]. Interestingly, cTnISer43Asp alone elevated cTnIThr144 phosphorylation to the greatest extent while the effects of cTnISer45Asp or cTnISer43/45Asp expression were not as pronounced (Fig. 3.7B). These results demonstrate phospho-mimetic substitutions at Ser43 and Ser45 clearly enhance phosphorylation of other cTnI sites, although the communication is dependent on the substitution site. The adaptive cTnISer23/24 phosphorylation produced by increased cTnISer43/45 phospho-mimetic

replacement likely aids in maintaining myocyte re-lengthening rate but is not expected to modulate cellular shortening rates.

Additional sarcomeric modifications could also play a role in the adaptive response. Because of its ability to increase cross-bridge cycling rates in response to an altered phosphorylation state, cMyBP-C phosphorylation was examined using site-specific phospho-antibodies individually directed to 3 well-characterized target residues within its cardiac-specific m-motif: pSer273, pSer282, and pSer302 (Fig. 3.8) [16, 101]. Interestingly, only phosphorylation at cMyBP-CpSer282 was significantly increased by expression of the 3 phospho-mimetic cTnI substitutions compared to controls. Phosphorylation of cMyBP-CpSer273 was highly variable in these same myocytes, but not statistically different from controls. There was less variable phosphorylation at the cMyBP-CSer302 residue, and the phosphorylation state did not differ from controls in myocytes expressing cTnISer43Asp and/or cTnISer45Asp. The present results show the augmented cMyBP-CSer282 phosphorylation is consistent with the restored/maintained shortening in myocytes expressing phospho-mimetic cTnISer43/45 substitutions.

The influences of cTnI phospho-mimetics on contractile protein phosphorylation cannot account for the accelerated Ca^{2+} decay (Fig. 3.6). Thus, studies also examined phospholamban (PLB) phosphorylation, which modulates sarcoplasmic reticulum (SR) Ca^{2+} uptake by the SERCA2A pump. PLB is targeted by multiple kinases including protein kinase A (PKA) at Ser16 and Ca^{2+}/Calmodulin-dependent protein kinase C (CaMKII) at Thr17 [104] . Phosphorylated PLB accelerates removal of Ca^{2+} from the cytosol into the SR, which could produce the accelerated $TTD_{50\%}$ (Fig. 3.6). PLB phosphorylation at the PKA-targeted residue Ser16 tended to increase in myocytes with >50% replacement by cTnISer43/45 phospho-mimetic substitutions, though this increase did not reach statistical significance (Fig. 3.9). However,

expression of these cTnI substitutions did not generate significant alterations in PLBThr17 phosphorylation (Fig. 3.9). Based on these findings, increased replacement with cTnISer43/45 phospho-mimetics enhances Ser16 phosphorylation on PLB, which could produce the accelerated Ca^{2+} $TTD_{50\%}$. Overall, enhanced phosphorylation both within cTnI as well as additional myofilament and Ca^{2+}-handling proteins result from the presence of negative charges at cTnISer43/45. These adaptive changes modulate cross-bridge cycling and Ca^{2+} cycling and likely contribute to the return of shortening and re-lengthening rates toward controls values in myocytes expressing the cTnISer43/45 substitutions.

DISCUSSION

The present experiments demonstrate cTnISer43 and cTnISer45 independently modulate contractile function (Fig. 3.3-3.6). My studies also provide evidence the two residues may work against each other within the same cTnI to prevent changes in function, at least at low levels of expression (Fig. 3.3). In addition, the differences in function observed 2 and 4 days after gene transfer of cTnI with phospho-mimetic substitutions at Ser43 and/or Ser45 led me to examine the development of signaling adaptations mediated via post-translational modifications of myofilament and Ca^{2+} cycling proteins (Figs.3.7-3.9). Finally, the present set of experiments demonstrate the cellular analysis of cTnISer43/45 serves as a bridge for understanding both *in vitro* and *in vivo* studies on cTnISer43/45 phosphorylation.

Prior to these studies, it remained unclear whether the cTnISer43/45 cluster was similar to cTnISer23/24 phosphorylation, which requires phosphorylation of both residues to produce a functional response [40, 41]. These results show partial replacement of endogenous cTnI with either cTnISer43Asp or cTnISer45Asp is sufficient to diminish peak shortening amplitude (Figs. 3.1-3.3). The inability of low level cTnISer43/45Asp expression to change cell shortening suggests these individual residues may work to counter the actions of the other residue (Fig. 3.3). However, the potential for one residue to counteract the other is expression-level dependent, as more extensive cTnISer43/45Asp expression is capable of reducing peak shortening amplitude (Fig. 3.4A).

The independent mechanisms employed by cTnISer43 and cTnISer45 in cTnI to modify function may result from their positioning on different faces of the H1(I) α helix in the IT arm of cTnI, which may lead to different interactions with residues in cTnC and cTnI and/or overall positioning of the H1 α-helix (Fig. 1.2A). Specifically, cTnISer45 is predicted to make critical

contacts with both the Ca^{2+} binding N-lobe and the structural C-lobe of TnC. My results indicate cTnISer45 exerts the most dramatic influence on shortening amplitude and the rates of shortening and re-lengthening, which may be due to interactions with both lobes of cTnC (Figs.1.2A, 3.3, 3.4A)[70] [71] [25]. In contrast, the positioning of cTnISer43 at the very beginning of the H1 α-helix may influence up- or down-stream cTnI residues and have less direct impact on the cTnC N- or C-lobes [25]. If one or more of these predictions are correct, one of these Ser residues could counteract and/or attenuate the conformational change(s) necessary for the other residue to change contractile function when combined in the same cTnI (e.g. cTnISer43/45Asp).

Multiple mechanisms are proposed to contribute to the reduction in peak shortening produced by phospho-mimetic substitutions at cTnISer43/45. The rightward shift in myofilament Ca^{2+} sensitivity produced by cTnISer23/24 phosphorylation translates into an acceleration of cardiac relaxation in the intact myocyte or heart [43, 46] [49] [42]. While cTnISer43/45 phosphorylation could produce the same effect, it is not observed in the current studies (Figs. 3.3, 3.4). Recently, separate mutations within TnC differentially affected the on rate (e.g. affinity) and off rate (e.g. dissociation) of TnC binding to Ca^{2+}, with a similar impact on myofilament Ca^{2+} sensitivity [105]. This idea clearly applies to the influence of cTnISer23/24 and cTnISer43/45 phosphorylation on function. The slowed shortening rate observed in myocytes expressing cTnISer43/45Asp substitutions, and the amplified influence of cTnISer43/45Asp substitutions on both shortening rate and peak shortening in the presence of Ca^{2+}-buffering Fura-2AM support the idea these functional changes result from slowed Ca^{2+} binding to TnC (Figs. 3.3-3.6). The slowing of loaded shortening velocity in permeabilized preparations, and the significant slowing of *in vivo* pressure development observed in hearts from

both $cTnI_{AllP}$ and $cTnI_{PKC\text{-}P}$ mouse models provide further support for this mechanism [75] [49] [62]. Moreover, reductions in the Ca^{2+} association constant (K_a) and actomyosin ATPase activity are observed in biochemical studies using cTnISer45Glu, which is predicted to result from the a reduced interaction with Glu10 in the N-lobe of TnC [67, 71]. Overall, the lack of change in maximum tension is consistent with the observed ability of cTnISer45Glu to slow Ca^{2+} binding kinetics to cTnC, without this cluster causing cTnI to interfere with maximal steady state Ca^{2+} binding to cTnC [67].

Morimoto *et al.* proposed another possibile mechanism by suggesting cTnISer43/45 phosphorylation destabilizes the interaction between cTnI and the C-lobe of TnC to diminish myofilament activation [106]. This group predicted destabilization limits the ability to shift tropomyosin (Tm) away from the cross-bridge binding site on actin [68, 106]. A NMR analysis of cTnC-cTnI after cTnISer43/45 phosphorylation also indicated destabilization of the C-lobe of TnC [70]. However, the results indicate this possibility is unlikely to be a mechanism contributing to the functional response in the intact myofilament, as destabilization also should reduce maximum isometric tension production, which is not observed with cTnISer45Asp (Figs. 3.4B). Phosphorylation or phospho-mimetic substitutions at cTnISer43/45 have variously reduced or had no impact on maximum isometric tension production (Figs. 3.4B) [68] [62, 79, 80]. Collectively, this differential impact of phospho-mimetic residues suggests the residue selected (i.e. Glu versus Asp) may affect the functional phenotype. Alternatively, the preparation utilized for the experiment (papillary fibers vs. myocytes) may contribute to a differential impact on maximal tension [62, 68] [49] [79] [80]. However, in either case, it is unclear how cTnISer43/45-induced destabilization of the C-lobe could explain the observed functional changes.

The reduced Ca^{2+} association to TnC also cannot easily explain the slowed re-lengthening rate observed in myocytes expressing cTnISer43/45 phospho-mimetics (Figs 3.3, 3.5,3.6). Instead, a slowing of cross-bridge detachment from the thin filament is proposed as an alternative mechanism, which would contribute to the diminished peak shortening and slowing of re-lengthening rate observed in the present study (Figs. 3.3-3.4) [68]. The reduced binding affinity of S-1 myosin observed with cTnI phosphorylated at cTnISer43/45, decreases in thin filament sliding (V_{max}) and Ca^{2+} senstivity of sliding produced by cTnISer43/45Glu, and slowed actomyosin ATPase activity over a range of tension in PKC-treated cardiac fiber bundles are each consistent with prolonged cross-bridge displacement [45] [68] [74]. Hearts isolated from $cTnI_{PKC\text{-}P}$ mice develop slowed ventricular relaxation, although slowed relaxation is not evidence in PKC_{AllP} mouse hearts [62] [49]. The exact mechanism responsible for slowing cross-bridge detachment is not known, but presumably could be mediated via changes in the stiffness of the cTn I-T arm (Figure 1.2A). Previous work also established unloaded shortening velocity is not dependent on cross-bridge binding, and therefore, this mechanism is not expected to contribute to the slowed rate of shortening (Figs. 3.3, 3.4) [107] [68] [108] . Thus, the results are consistent with a dual role for cTnISer43/45 to reduce Ca^{2+} binding affinity to cTnC and slow cross-bridge detachment rate.

In addition to the direct influence of cTnISer43/45 phosphomimetic expression, adaptive signaling in intact myocytes was examined in this set of experiments. Previously, replacement of endogenous cTnI with cTnISer43/45Ala in a tg mouse model increased cTnISer23/24 phosphorylation, indicating load-dependent adaptive signaling may occur in the heart [72]. Compensatory signaling has not been detected in mouse models expressing cTnI with phospho-mimetic substitutions [62] [49]. However, my results demonstrate several adaptations are

detected in both Ca^{2+} cycling and sarcomeric protein phosphorylation, which are expected to preserve myocyte contractile function (Figs. 3.7-3.9). Specifically, the faster cytosolic Ca^{2+} decay and increased PLBSer16 phosphorylation are consistent with the return of re-lengthening rate in myocytes expressing cTnISer45Asp toward control values on day 4 (Fig. 3.4, 3.9). In addition, the heightened cTnISer23/24 phosphorylation observed with Asp substitutions at cTnISer43 and cTnISer 45 is expected to increase Ca^{2+} dissociation from cTnC and work to restore cTnISer43/45Asp-induced slowing of re-lengthening rates back toward control values (Fig. 3.7) [42] [43] [40]. The present results also show augmented cMyBP-CSer282 phosphorylation at day 4 in myocytes expressing all 3 phospho-mimetic substitutions, which is expected to accelerate cross-bridge cycling [16, 109, 110]. This adaptation could help restore the slowed shortening rate, as observed at day 4 in the current studies (Fig. 3.4).

In preliminary work, the mechanism for the adaptive increase in cTnISer23/24 phosphorylation is examined and this data is consistent with a contribution of the stress-activated kinase PKD, but not PKA (Figs. 3.10A-B). However, further work is necessary to prove this point, as there was inadequate power for the statistical comparison. Additional work also is needed to determine if other stress-activated kinases, such as PKC or PKG, contribute to this adaptive signaling response [93, 94] [111] [112] [26, 33, 45, 95, 96, 113]. The present studies demonstrated phosphatase inhibition may be another contributor to the adaptive signaling response. The change in phosphorylation at cTnISer23/24 (Δ phospho-ratio) was greater in control and cTnI-expressing myocytes following phosphatase inhibition with Cal A, suggesting phosphatase activity is already reduced by cTnISer43/45 substitution (Fig. 3.10C). As with the PKD study, more work is needed to achieve adequate power for statistical comparisons. There is a growing recognition destabilization of the balance between kinase and phosphatase activity may

play a key role in the transition to cardiac dysfunction [102, 114, 115]. An important remaining question is whether this adaptive signaling is maintained over time and/or continues to be present under pathophysiological conditions associated with heart failure.

The adaptive changes here also could contribute to the cardiac phenotype in intact animal models expressing cTnI with phospho-mimetic substitutions at cTnISer43/45. Both the Ca^{2+} cycling and cTnISer23/24 phosphorylation adaptations are expected to preserve diastolic function in the intact heart. While adaptive signaling in the $cTnI_{AllP}$ mouse model was not detectable, these adaptations could account for the comparable relaxation rates (dP/dt_{min}) observed in $cTnI_{AllP}$ mouse hearts compared to non-transgenic controls [49]. Alternatively, the response in isolated myocytes measured over several days may be absent and/or different from the adaptations detected in hemodynamic measurements made in the $cTnI_{AllP}$ mice [49]. The depressed relaxation rate and lack of adaptations in Ca^{2+} handling and protein phosphorylation suggests adaptations may not develop with low-level expression, such as the $cTnI_{PKC\text{-}P}$ mouse model expressing cTnISer43/45GluThr144Glu [62].

In summary, the results provide insight into the modulatory role of cTnISer43/45 phosphorylation on cardiac myocyte contractile performance. In contrast to cTnISer23/24, cTnISer43 and cTnISer45 independently modulate contraction. Importantly, these studies, together with earlier work, also demonstrate cTnISer43/45 acts via a separate mechanism than cTnISer23/24. Overall, cTnISer43/45 acts as a molecular brake on cardiac contraction in intact myocytes, in keeping with the *in vitro* ability of this cluster to slow Ca^{2+} binding to TnC and cross-bridge dissociation from the myofilament. The adaptive Ca^{2+} cycling and sarcomeric protein phosphorylation observed here also indicates mechanisms are in place to further fine tune

the brake. Finally, results from the present study also effectively bridge the gap between *in vitro* and *in vivo* models by helping to reconcile divergent results from different approaches.

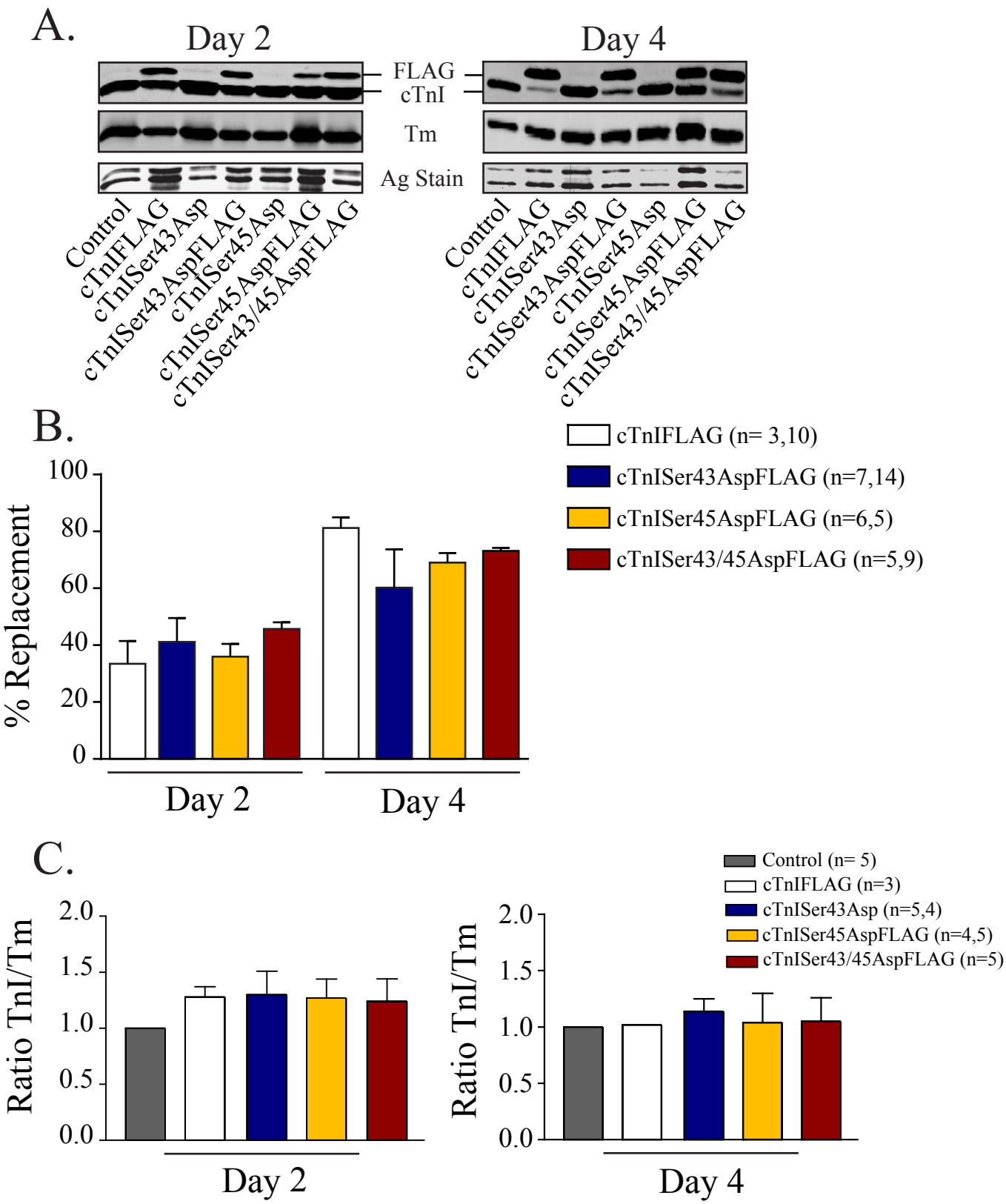

Fig. 3.1 Expression of cTnISer43/45 phospho-mimetic substitutions with and without FLAG 2 and 4 days after gene transfer. A. Representative Western blot showing expression of cTnI (±FLAG), cTnISer43Asp(±FLAG), cTnISer45Asp(±FLAG), or cTnISer43/45Asp (±FLAG) 2 (left column) and 4 (right column) days after gene transfer. Blots probed for total cTnI (top panel) and total Tm (middle panel) show maintenance of thin filament stoichiometry. A section of silver (Ag) -stained gel illustrates protein loading in each lane (bottom panel).

Fig. 3.1 Expression of cTnISer43/45 phospho-mimetic substitutions with and without FLAG 2 and 4 days after gene transfer (cont.). B. Quantitative analysis of percent replacement (%) for each cTnI phospho-mimetic substitution at 2 (left section) and 4 (right section) days after gene transfer. Replacement is calculated from the ratio of cTnIFLAG /total cTnI x100 for each cTnI construct. **C.** Quantitative analysis of thin filament stoichiometry 2 and 4 days after adenoviral-mediated gene transfer. Stoichiometry was calculated from the ratio of total cTnI/Tropomyosin (Tm) protein expression for each cTnI substitution and normalized to the control ratio. Results were analyzed via one-way ANOVA with $p<0.05$* considered statistically significant compared to the control.

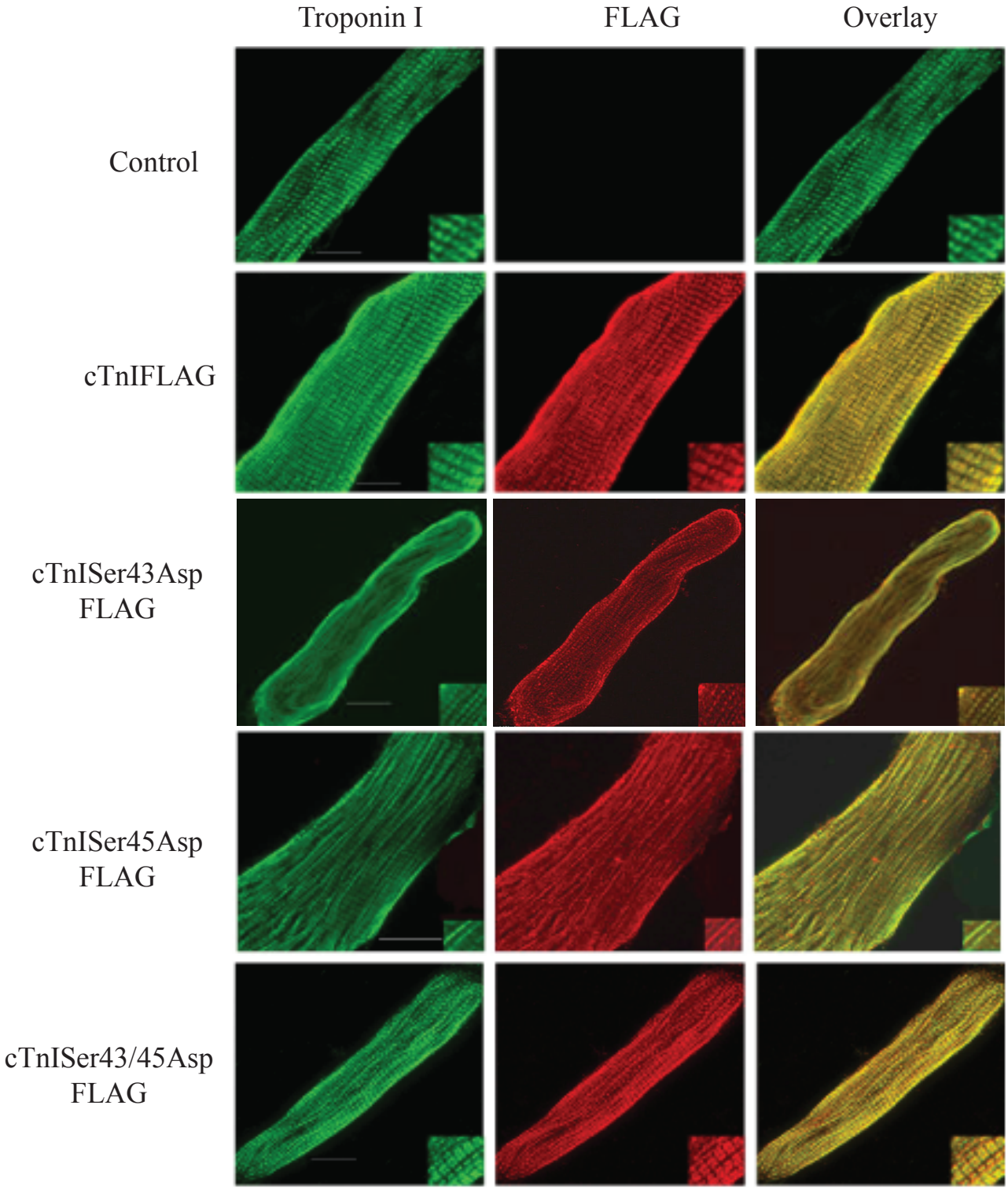

Fig. 3.2 Sarcomeric localization of cTnI and cTnISer43/45 phospho-mimetic substitutions. Dual immunostaining with monoclonal antibodies determined myofilament incorporation of FLAG-tagged phospho-mimetic substitutions. Staining with a troponin (Tn)-specific antibody was detected with a secondary antibody conjugated to fluorescein isothiocyanate (FITC; left panels). A second primary antibody directed to FLAG was detected with a secondary antibody conjugated to Texas Red (TR; center panels). Overlays of the projection confocal images are included to show co-localization of FLAG-tagged cTnI phospho-mimetic substitutions and endogenous troponin I (TnI) (yellow; right panels). An insert is provided for controls, cTnIFLAG, and each FLAG-tagged cTnI phospho-mimetic substitution shows a magnified section of the myocyte to demonstrate the striated pattern of phospho-mimetic expression in the myofilament. Bars in each panel represent 10μm, except for the bar in the cTnISer45Asp panel which represents 25μm.

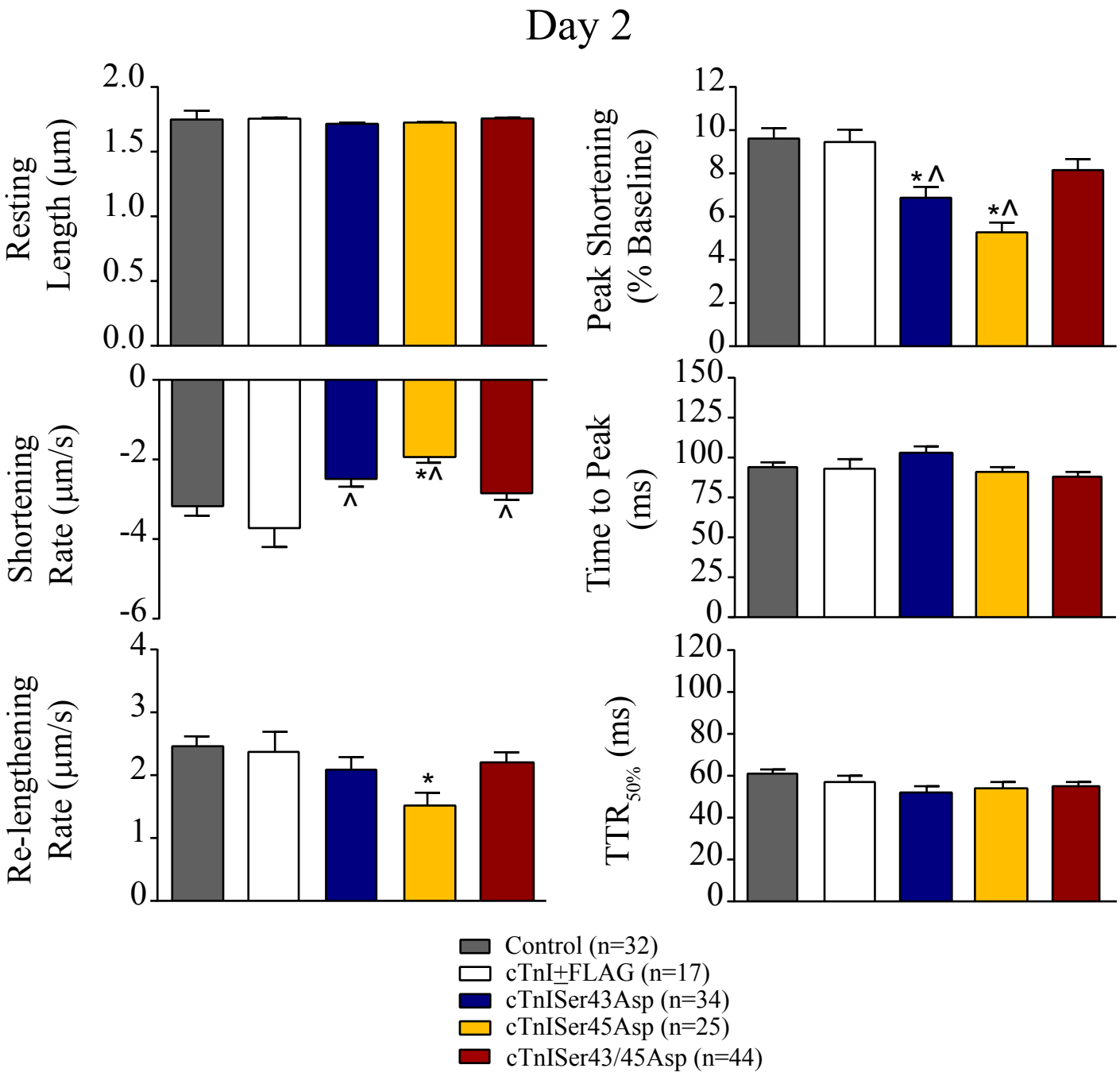

Fig. 3.3. Basal cardiac shortening and re-lengthening 2 days after gene transfer.
Sarcomeric shortening was measured in control myocytes and myocytes expressing wild-type cTnI, cTnIFLAG, cTnISer43Asp, cTnISer45Asp, and cTnISer43/45Asp. For these studies, measurements from myocytes expressing wild-type cTnI and cTnIFLAG were not significantly different and were pooled into a single group designated as "cTnI±FLAG". Contractile function was evaluated using measurements of resting sarcomere length, peak shortening amplitude (% basal), shortening and re-lengthening rates, TTP, and $TTR_{50\%}$. A $p<0.05$(*) was considered significantly different from control. $p<0.05$(^) was statistically different from cTnI±FLAG.

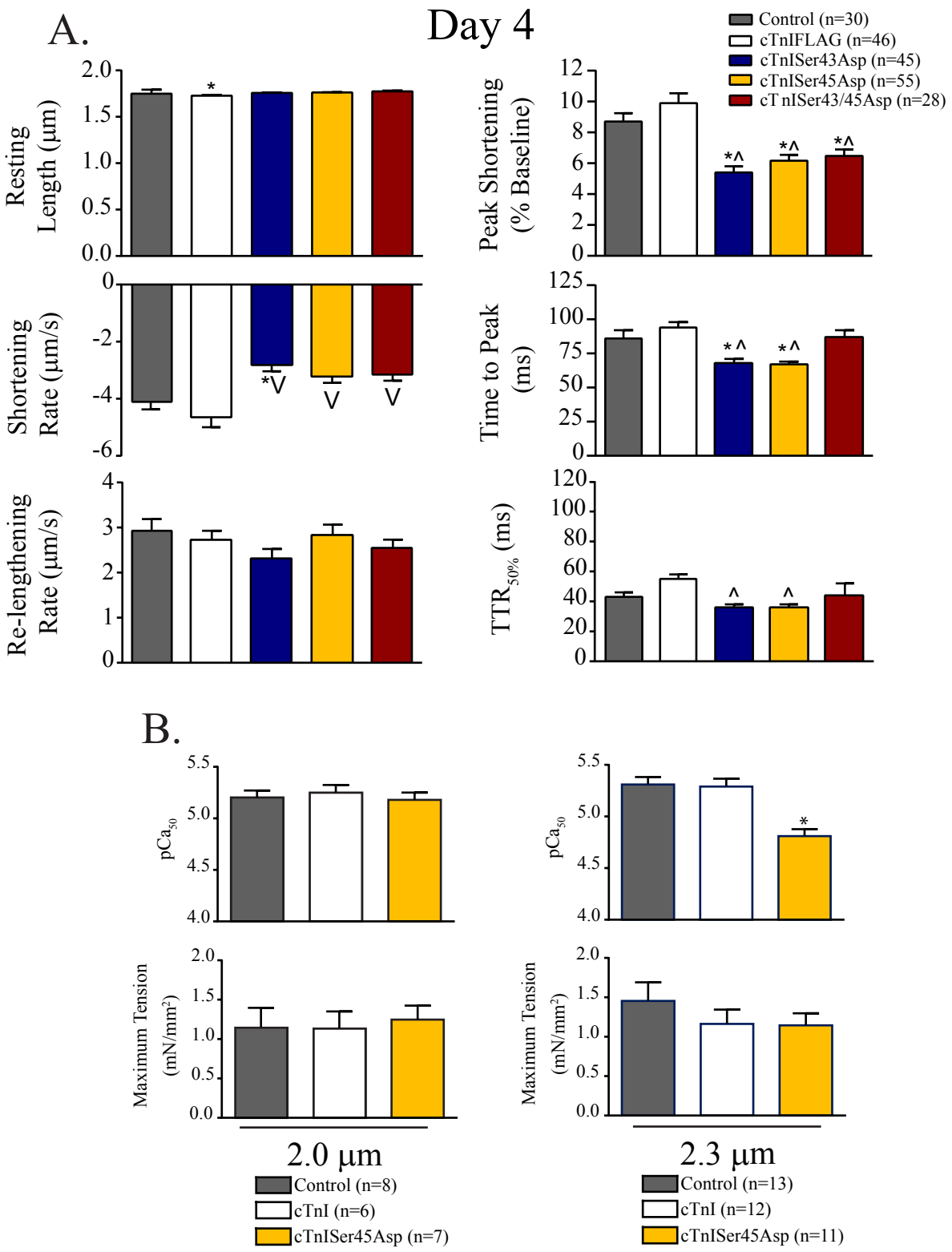

Fig. 3.4. Sarcomeric shortening 4 days after gene transfer of cTnISer43/45 phospho-mimetic substitutions. A. Basal sarcomeric shortening measurements after increased replacement of endogenous cTnI by cTnISer43/45Asp phosphomimetics. Resting sarcomere length, peak shortening amplitude (% basal), shortening and re-lengthening rates, TTP, and $TTR_{50\%}$ were quantified for controls and wild-type cTnI-expressing myocytes and compared to myocytes expressing cTnISer43Asp, cTnISer45Asp, and cTnISer43/45Asp. Data was analyzed with a 1-way ANOVA and post-hoc tests, as described in the Methods section, with * indicating $p<0.05$ versus control and ^ for $p<0.05$ compared to the cTnI±FLAG group.

Fig. 3.4 Sarcomeric shortening 4 days after gene transfer of cTnISer43/45 phospho-mimetic substitutions (cont.). B. Calculated pCa_{50} and maximum tension measured at a sarcomere length of 2.0μm (left) and 2.3μm (right) in controls (2.0μm: 5.20±0.068, n=8; 2.3μm 5.31±0.072, n=12) and myocytes expressing either wild-type cTnI (2.0μm: 5.25±0.074, n=6; 2.3μm: 5.31±0.071, n=5) or cTnISer45Asp (2.0μm: 5.18±0.071, n=7; 2.3μm: 4.86±0.063, n=9) 4-5 days after gene transfer. Isometric force was measured over a range of Ca^{2+} as described in the Methods section. The * indicates statistical significance ($p<0.05$) compared to controls.

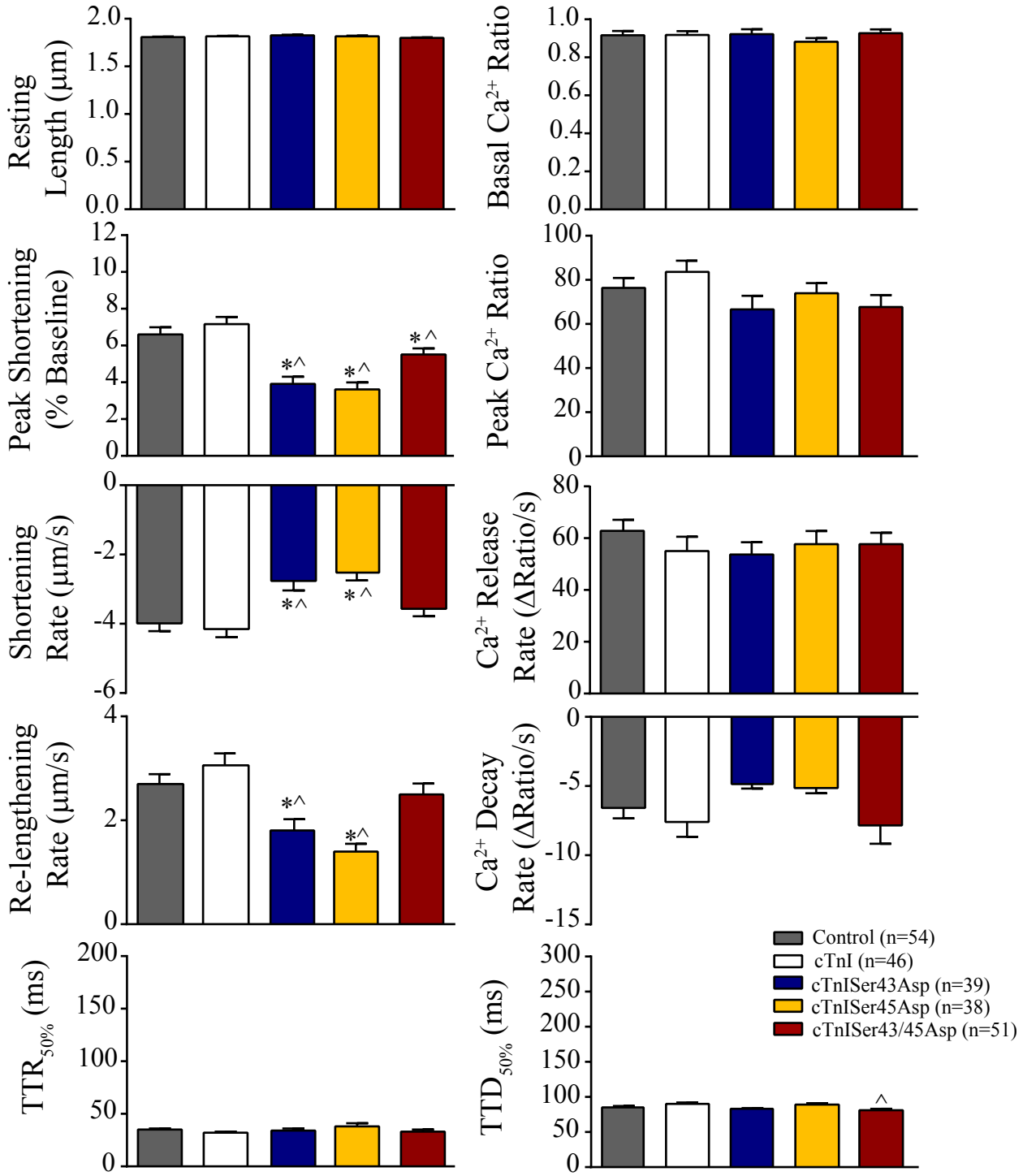

Fig. 3.5 Analysis of myocyte contractile function and Ca^{2+} handling in cTnISer43/45 phosphomimetic expressing myocytes 2 days after gene transfer. Basal shortening measurements including resting sarcomere length, peak shortening amplitude, shortening and re-lengthening rate, and the time to 50% re-lengthening ($TTR_{50\%}$) were measured and analyzed in Fura-2AM- loaded myocytes as described in chapter 1 (Figure 1.3D). Ca^{2+} transients also were simultaneously measured in these myocytes to determine whether there were changes in baseline Ca^{2+} ratio, peak change of the Ca^{2+} transient (% baseline), the rates of Ca^{2+} release and re-uptake, and the time to 50% decay ($TTD_{50\%}$). Panels with statistically significant responses ($p<0.05$) compared to controls (*) and (^) cTnI are shown.

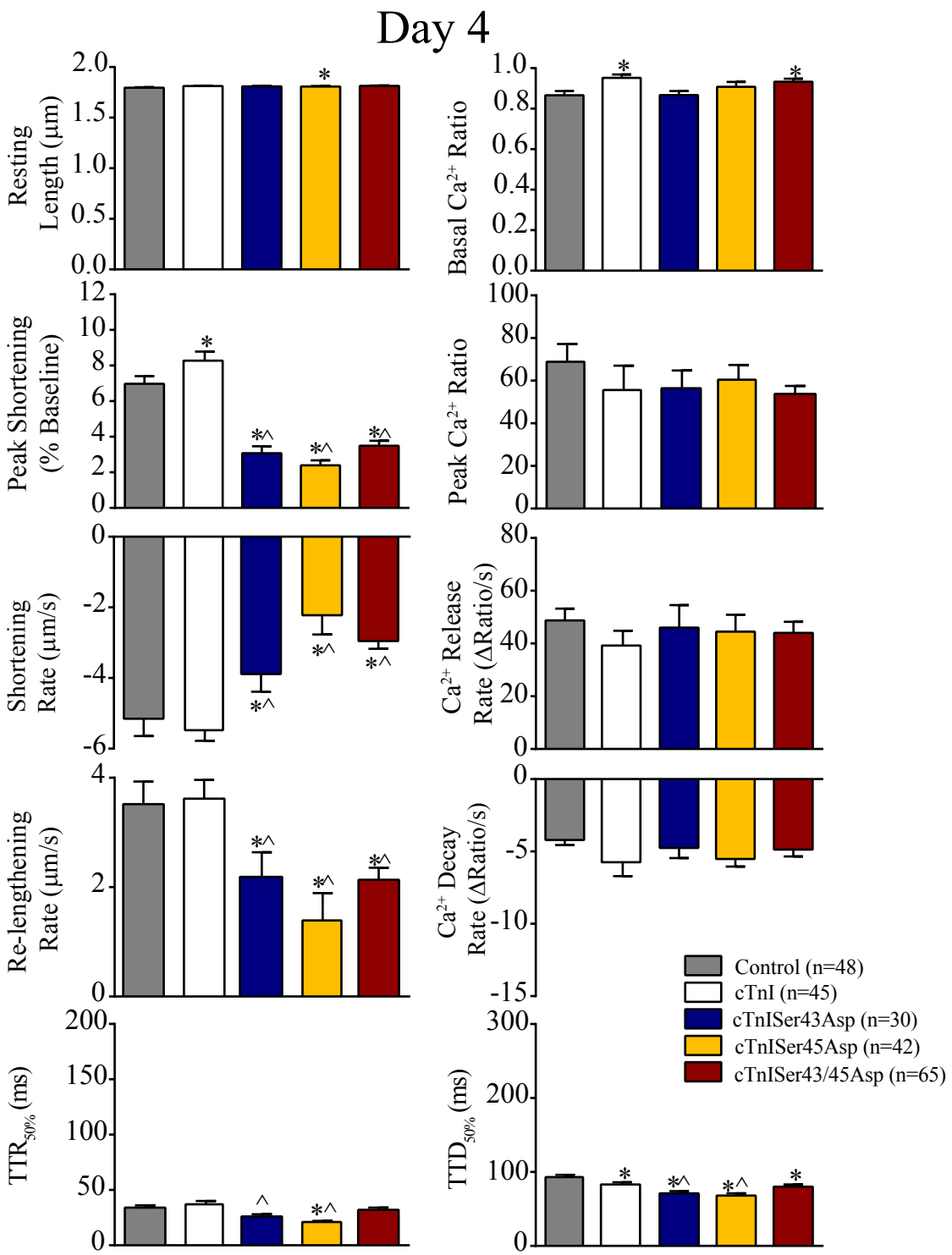

Fig. 3.6 Increased cTnISer43/45 phosphomimetic replacement accelerates Ca^{2+} decay. Basal shortening and Ca^{2+} transients were simultaneously measured in Fura-loaded myocytes 4 days post-gene transfer in control, wild-type cTnI, and cTnISer43/45 phospho-mimetic-expressing myocytes. Measurements included resting sarcomere length and baseline Ca^{2+} ratio, peak shortening amplitude and peak Ca^{2+} ratio, shortening and Ca^{2+} release rates, re-lengthening and Ca^{2+} reuptake rates, and the time to 50% re-lengthening ($TTR_{50\%}$) and the time to 50% Ca^{2+} decay ($TTD_{50\%}$). Statistical significance compared to controls (*$p<0.05$) and cTnI (^$p<0.05$) are shown.

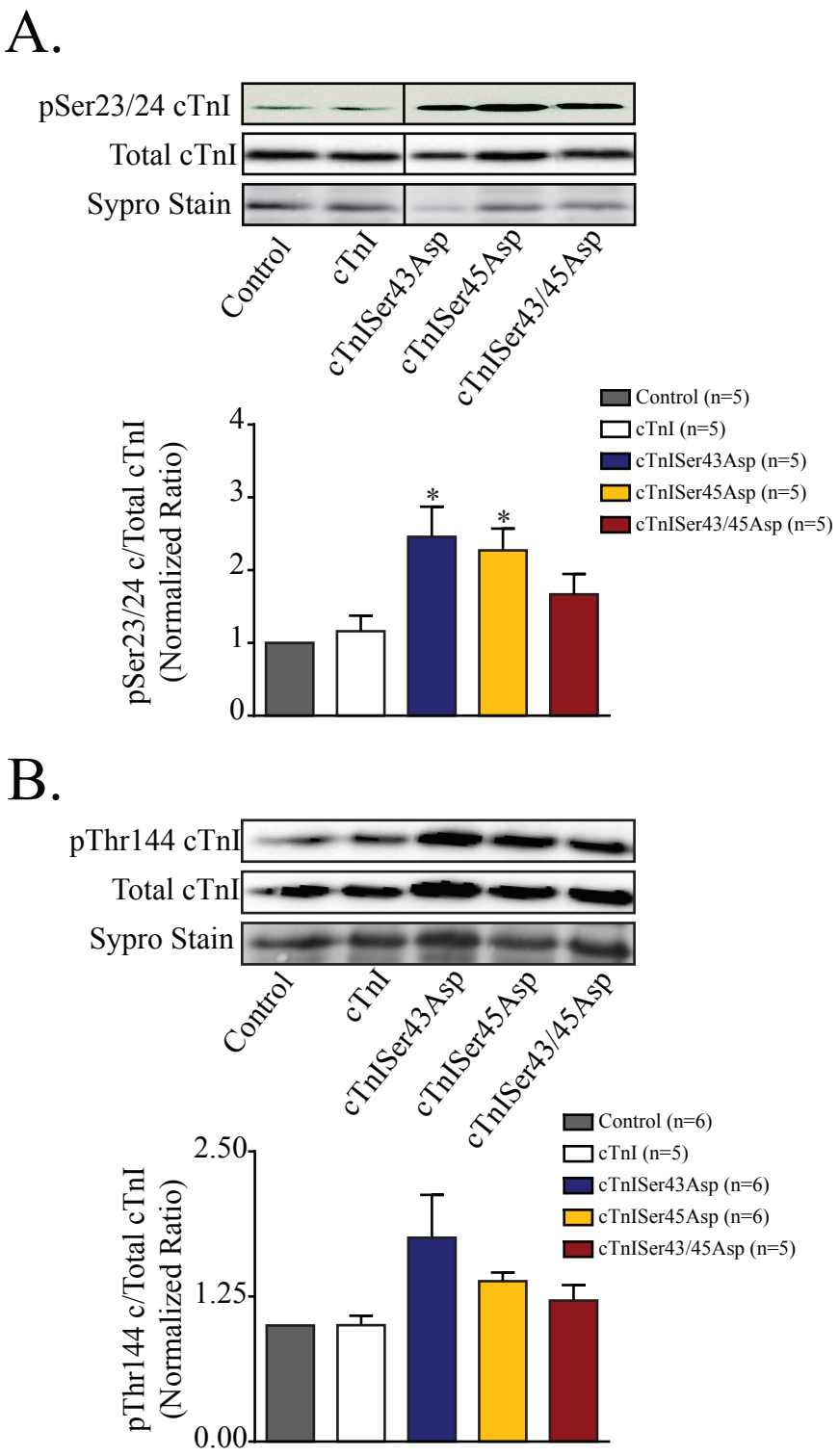

Fig. 3.7 Adaptive cTnI phosphorylation increases with extensive phosphomimetic replacement at cTnISer43/45. A. Representative immunoblot showing cTnISer23/24 phosphorylation (top panel), total cTnI expression (middle panel), and sypro-stained band at 40 kDa for each blot (bottom panel) to determine total protein in each lane. The black line separating bands indicates additional lanes were removed between samples on the same gel. The quantitative comparison of phospho-cTnI/total cTnI ratios for each cTnI construct is shown in the lower panel (mean±SEM; n=5). A 1-way ANOVA and post-hoc analysis (see Methods) demonstrated significantly elevated phosphorylation at cTnISer23/24 in myocytes expressing cTnISer43Asp and cTnISer45Asp (*$p<0.05$ versus control). **B.** Representative Western blot analysis of phospho-cTnIThr14 (top panel), total cTnI protein (middle panel), and protein band on sypro-stained blot (bottom panel). The quantitative analysis of phospho-cTnI/total cTnI ratios for each control and phosphomimetic sample is shown in the lower panel (mean±SEM, n=5-6). Results are considered significantly different from controls at $p<0.05$*.

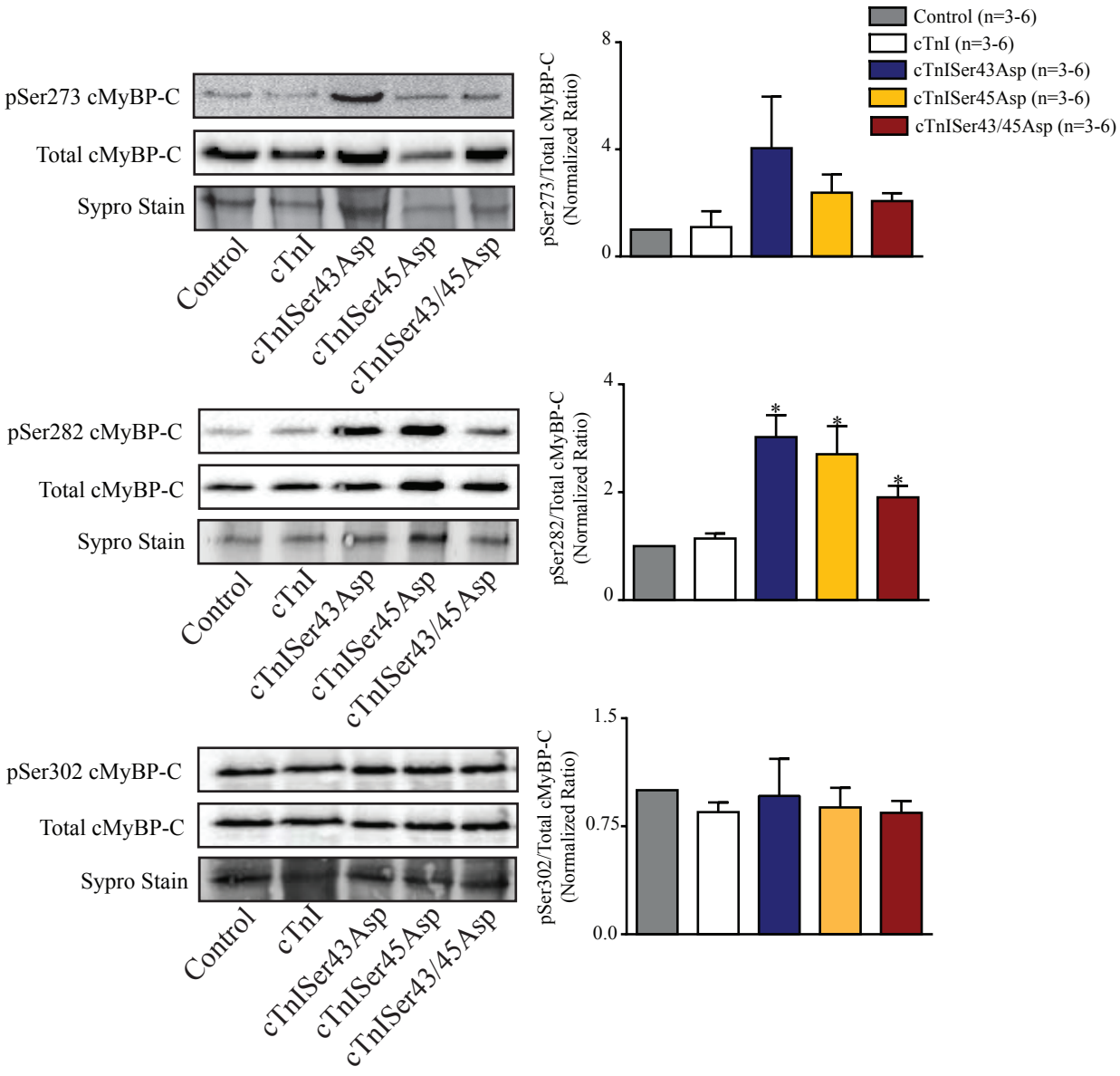

Fig. 3.8 Phospho-mimetic replacement at cTnISer43/45 increases adaptive phosphorylation in cMyBP-C. Representative Western blot analysis evaluating phosphorylation at 3 well characterized residues within cMyBP-C: pSer273 (top panel), pSer282 (middle panel), and pSer302 (bottom panel). Site-specific phospho-antibodies were used to detect phosphorylation at cTnISer273, cMyBP-CSer282, and cMyBPCSer302 (top panels). Blots were re-probed for total cMyBP-C protein (middle panels), and a sypro-stained portion of the blot (bottom panels) is shown to demonstrate protein loading in each lane (150 KDa band). Quantitative analysis of the phospho-cMyBP-C/total cMyBP-C ratio for each construct is shown in the panels located to the right of each representative blot (mean±SEM; n=3-6). Statistically different detection compared to control values is indicated by the *($p<0.05$).

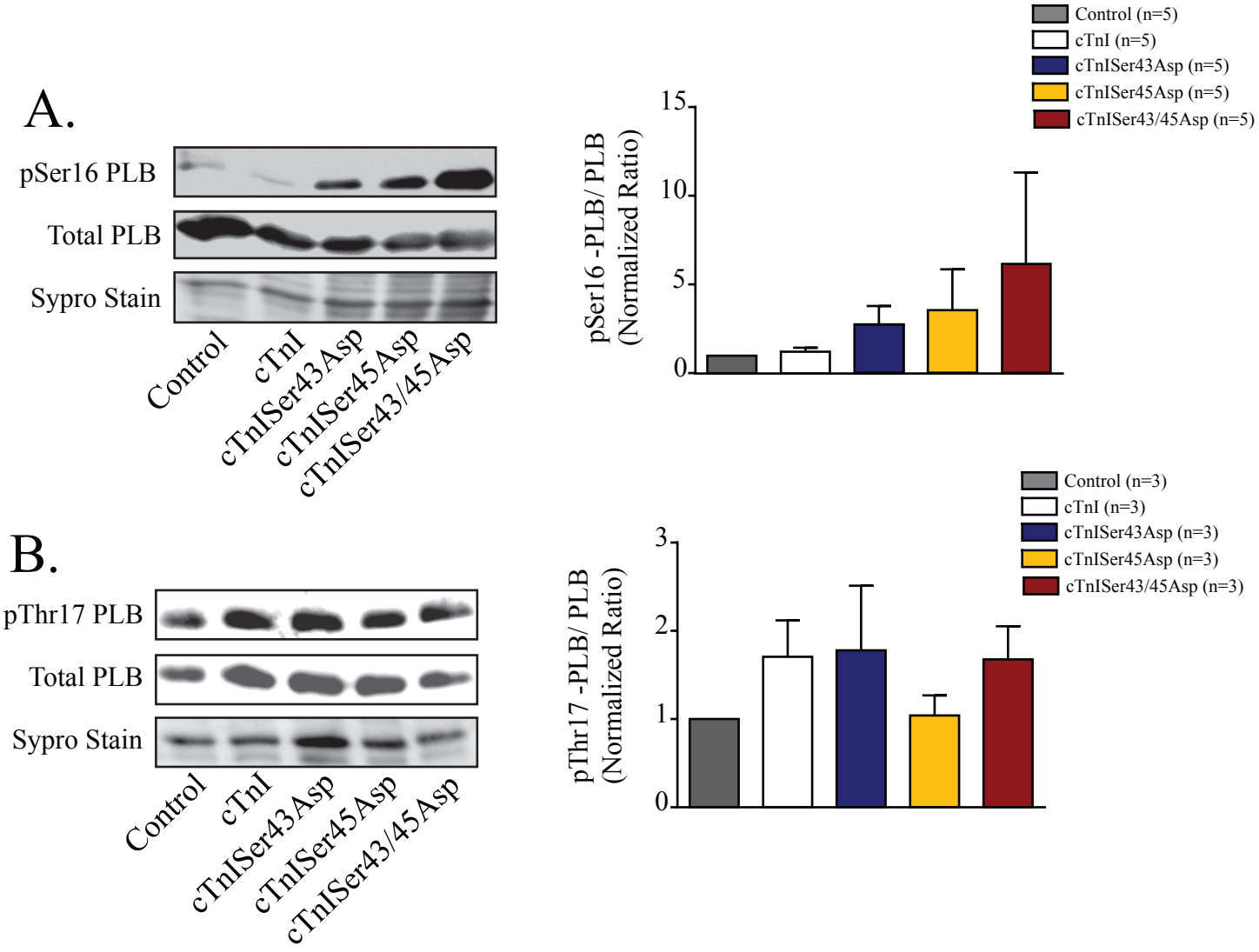

Fig. 3.9 Phospho-mimetic replacement at cTnISer43/45 increases PLB phosphorylation 4 days after gene transfer. A. Representative Western blot (left panel) illustrating changes in phosphorylation at pSer16 PLB (top panel), total PLB (middle panel), and a band on the sypro-stained blot (40KDa band; bottom panel). Quantitative analysis of phospho-Ser16-PLB/total PLB ratio normalized to the control ratio (1.0) are shown in the right panel (mean+SEM; n=3). **B.** Representative Western blot (left panel) probed with a site-specific phospho-antibody for phospho-Ser17 PLB (top panel). Blots were stripped and re-probed for total PLB protein expression (middle panel) and a sypro-stained band is shown to indicate protein loading (bottom panel). The phospho-Ser17-PLB/total PLB ratio normalized to control values (1.0) is shown (mean+SEM; n= 3) for controls and cells expressing wild-type cTnI, cTnISer43Asp, cTnISer45Asp, or cTnISer43/45Asp (bar graph; right).

A.

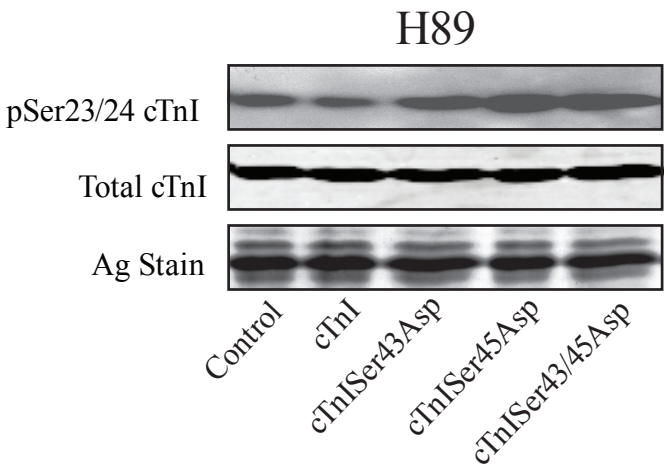
H89
pSer23/24 cTnI
Total cTnI
Ag Stain
Control
cTnI
cTnISer43Asp
cTnISer45Asp
cTnISer43/45Asp

B.

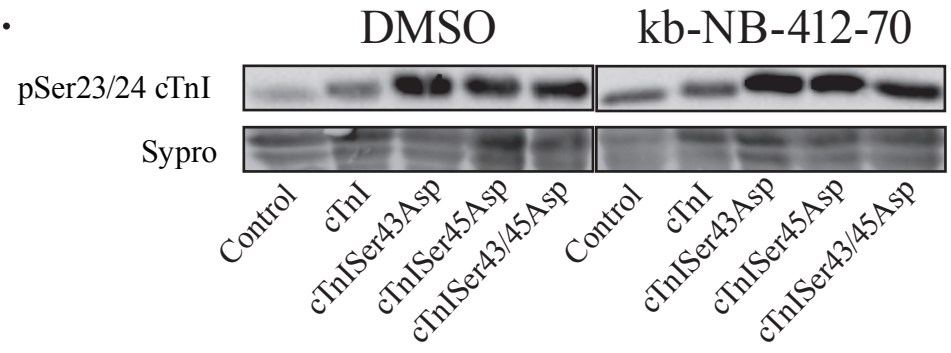
DMSO
kb-NB-412-70
pSer23/24 cTnI
Sypro
Control
cTnI
cTnISer43Asp
cTnISer45Asp
cTnISer43/45Asp
Control
cTnI
cTnISer43Asp
cTnISer45Asp
cTnISer43/45Asp

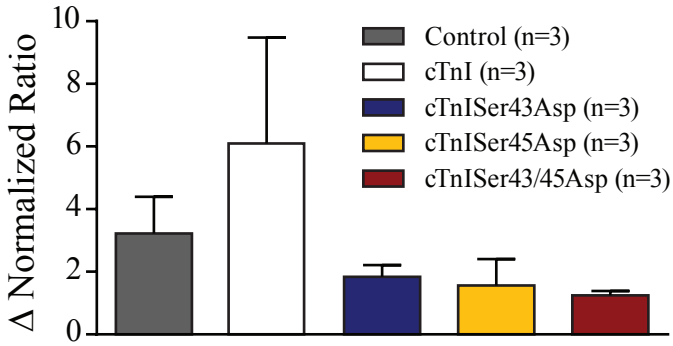
Δ Normalized Ratio
0
2
4
6
8
10
Control (n=3)
cTnI (n=3)
cTnISer43Asp (n=3)
cTnISer45Asp (n=3)
cTnISer43/45Asp (n=3)

C.

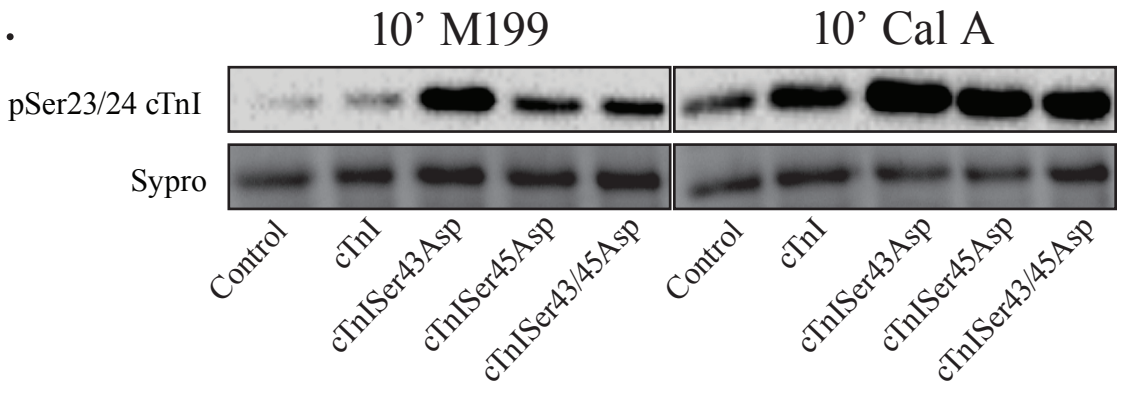
10’ M199
10’ Cal A
pSer23/24 cTnI
Sypro
Control
cTnI
cTnISer43Asp
cTnISer45Asp
cTnISer43/45Asp
Control
cTnI
cTnISer43Asp
cTnISer45Asp
cTnISer43/45Asp

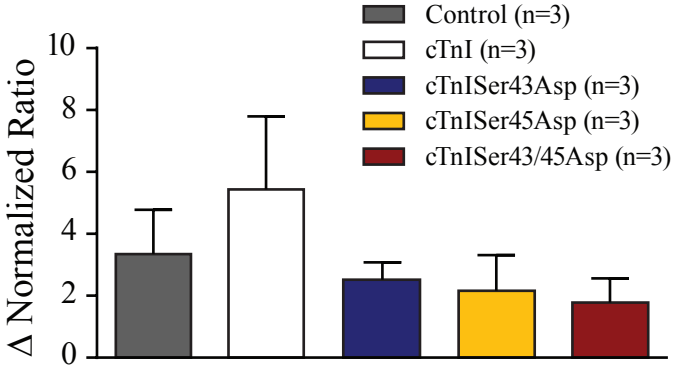
Δ Normalized Ratio
0
2
4
6
8
10
Control (n=3)
cTnI (n=3)
cTnISer43Asp (n=3)
cTnISer45Asp (n=3)
cTnISer43/45Asp (n=3)

Fig. 3.10 Preliminary studies of adaptive sarcomeric protein phosphorylation in the presence of a PKD and a phosphatase inhibitor. A. Western blot illustrating pSer23/24 cTnI phosphorylation (top panel) in phospho-mimetic-expressing myocytes 4 days post-gene transfer. Blots were re-probed for total cTnI to determine total cTnI protein levels (middle panel). A section of silver (Ag)-stained gel was included to demonstrate protein loading in each lane (bottom panel). **B.** Representative Western blot of cTnISer23/24 phosphorylation (top panels) in control, wild-type cTnI-, and phospho-mimetic-expressing myocytes treated with DMSO alone (left panels) or the PKD-inhibitor kb-NB-142-70 (10μm; right panels). A band of the sypro-stained blot is included to indicate protein loading between lanes (bottom panels). The ratio of phospho-cTnI to total protein was calculated for each sample then normalized to the DMSO-treated control. Initial quantitative analysis of the change in the phospho-cTnI/total protein ratio before and after inhibitor treatment (Δ Normalized Ratio; mean$\pm$SEM, n=3; lower panel) was determined in controls, and myocytes expressing wild-type or the phospho-mimetic constructs detected on the same membrane. Statistical analysis indicated there are no significant differences compared to control values ($p>0.05$). **C.** Representative Western blot showing phospho-cTnISer23/24 (upper panels) and total protein (lower panels) before (M199; left panels) and after treatment with a PP1/PP2A inhibitor (10 nM Cal A; right panels) for controls and myocytes expressing wild-type cTnI, cTnISer43Asp, cTnISer45Asp, or cTnISer43/45Asp 4 days after gene transfer. Initial quantitative analysis of preliminary data is shown in the lowest panel. The change in phosphorylation is expressed as the difference (Δ) between phospho-cTnISer23/24/Total protein before and after Cal A treatment. Statistical analysis indicated there are currently no significant changes from control ratios ($p>0.05$).

CHAPTER 4

FUNCTIONAL CROSS-TALK BETWEEN PKC-TARGETED CARDIAC TROPONIN I PHOSPHORYLATION SITES

ABSTRACT

Altered phosphorylation of PKC-targeted cTnISer23/24 and cTnISer43/45 residues is associated with cardiac dysfunction. In earlier work, expression of cTnISer43/45Asp augmented cTnISer23/24 phosphorylation, which suggests cross-talk between these clusters may contribute to differences reported in the earlier work. The cross-talk idea is now further explored by functionally comparing viral-mediated gene transfer of cTnISer43/45Asp versus cTnI with Ser23/24 and Ser43/45 phospho-mimetic substitutions ($cTnIAsp_{Quad}$). Epitope-tagged $cTnIAsp_{Quad}$ progressively replaced endogenous cTnI over time, in agreement with earlier cTnI gene transfer studies. Two days after gene transfer, partial replacement with $cTnIAsp_{Quad}$ diminished peak shortening amplitude and slowed shortening and re-lengthening rates, while faster time to peak (TTP) and time to 50% re-lengthening ($TTR_{50\%}$) intervals developed compared to cTnI-expressing controls. In contrast, there were no significant changes in function with comparable cTnISer43/45Asp expression. By 4 days post-gene transfer, >80% replacement with $cTnIAsp_{Quad}$ or cTnISer43/45Asp each reduced shortening amplitude, while $TTR_{50\%}$ continued to be faster in myocytes expressing $cTnIAsp_{Quad}$. However, TTP, shortening and re-lengthening rates no longer differed between controls and $cTnIAsp_{Quad}$-expressing myocytes. These results indicate cTnISer43/45 exerts a dominant influence to reduce peak shortening and slow shortening and re-lengthening rates. The cTnISer23/24 cluster appears to enhance the impact of cTnISer43/45 on peak shortening, and likely contributes to the faster $TTR_{50\%}$. The restoration of TTP and shortening rates observed by day 4 suggest compensatory adaptations contribute to the functional response with $cTnIAsp_{Quad}$. Indeed, adaptive increases in the phosphorylation of cTnI and other myofilament proteins are observed with $cTnIAsp_{Quad}$ expression. Collectively, these results support the idea cTnISer43/45 phosphorylation directly

and adaptively modulate contractile function, with the direct influence working as a brake to reduce cardiac performance and/or contributing dysfunction.

INTRODUCTION

Human heart failure is characterized by diminished pressure generation, slowed rates of pressure development and/or decay, and increased myofilament Ca^{2+} sensitivity of tension or pressure. Increased protein kinase C (PKC) expression and activation are linked to these functional deficits in human and animal models end-stage heart failure [30, 56, 65]. In addition, cardiac troponin I (cTnI) is a significant myofilament protein target for PKC phosphorylation [26, 59, 60]. PKC can target both cTnISer23/24 and cTnISer43/45 for phosphorylation, and both clusters modulate cardiac contractile function [43, 46, 51, 68].

However, the functional influence of cTnISer43/45 alone and in combination with cTnISer23/24 remains controversial [47, 49]. Evidence from biophysical studies indicates phospho-mimetic substitutions at cTnISer43/45 and another PKC target, cTnIThr144, are necessary to maximally reduce myofilament tension and sliding speed [116] [67, 68]. These studies did not address the combinatorial effects of cTnISer23/24 and cTnISer43/45 phosphorylation. In contrast, *in vivo* analysis using phospho-mimetic substitutions in cTnISer23/24 alone and in combination with cTnISer43/45 and cTnIThr144 indicated the Ser43/45 and/or Thr144 sites exert a dominant influence on function, which obscures the influence of cTnISer23/24 on cardiac pump performance[49] [62]. However, the dominant cluster responsible for modulating cardiac function remains unclear [47] [49]. The different outcomes observed using reconstituted myofilaments compared to *in vivo* cardiac function measurements in animal models indicate experiments are needed to define the functional consequences of cTnISer23/24 and cTnISer43/45 phosphorylation in a cellular model to bridge the gap between the earlier *in vivo* and *in vitro* studies.

Alterations in the phosphorylation state of cTnISer23/24 and cTnISer43/45 are also linked to cardiac dysfunction, with reduced cTnI Ser23/24 and enhanced Ser43/45 phosphorylation reported during end-stage heart failure [27] [28-31, 65]. In contrast, phosphorylation of both clusters is enhanced in a rodent model of spontaneous hypertension [30]. The association between elevated cTnISer43/45 phosphorylation and heart failure led to the idea Ser43/45 phosphorylation may contribute to cardiac dysfunction [30]. Earlier work also indicated cTnISer43/45 influences cTnISer23/24 phosphorylation state (Ch. 3). Thus, the reduction in cTnISer23/24 phosphorylation during heart failure may indicate cross-talk between these 2 clusters is compromised under pathophysiological conditions and/or could further contribute to cardiac dysfunction. Experiments are needed to evaluate the contributions of cTnI Ser43/45 alone and in combination with Ser23/24 as a first step toward understanding the role these clusters play in the development of cardiac dysfunction. A longer term goal of this work is to determine whether these changes in cTnI phosphorylation are a key contributor to dysfunction and the progressive transition towards end-stage heart failure [27].

The present study tests the hypothesis cTnI Ser43/45 has a dominant influence on modulating contractile function by reducing function alone and in combination with Ser23/24. This idea is tested by comparing the functional impact of cTnISer43/45Asp to a cTnI containing Asp substitutions at Ser23/24 and Ser43/45 ($cTnIAsp_{Quad}$). For these studies, viral-based gene transfer into isolated cardiac myocytes is used to replace endogenous cTnI, and then myocytes are monitored for expression, sarcomere incorporation and contractile function. These results demonstrate cTnI Ser43/45 produces a dominant reduction in myocyte shortening, although Ser23/24 also plays a subtle but complex role in modulating function. The present studies also demonstrate $cTnIAsp_{Quad}$ activates adaptive signaling in intact myocytes, although the signaling

differs from the adaptive responses observed with cTnISer43/45Asp alone. In agreement with earlier work, the present results also bridge the gap between *in vitro* and *in vivo* work and are consistent with conclusions drawn from both approaches.

METHODS

Gene transfer into isolated cardiac myocytes

Site-directed mutagenesis is used to replace cTnISer23/24 and cTnISer43/45 with negatively charged aspartic acid (Asp) in full-length, wild-type cTnI cDNA (rat) (QuikChange; Invitrogen) [83, 85, 99]. The cTnIAsp$_{Quad}$ construct is produced with and without a FLAG-tag using the following primers: cTnISer23/24Asp 5'-ctgctcctgtccgacgtcgc**gatgatg**ccaactaccgagcctatg-3' (sense, mutated residues are bolded/underlined) and 5'-cataggctcggtagttgg**catcatc**gcgacgtcggacaggagcag-3' (anti-sense). cTnISer43/45Asp 5'aaagtctaagatc**gat**gcc**ga**cagaaa**gc**ttcagttgaagactctg-3' (sense) and 5'-cagagtcttcaactgaa**gc**tttctg**tc**ggc**atc**gatcttagacttt-3' (anti-sense). Each cDNA was cloned into a pDC315 shuttle vector. Recombinant adenovirus used for gene transfer is produced by homologous recombination of the adenoviral backbone pBHGLoxΔE1, 3Cre (Microbix) and the pDC315 shuttle vector in HEK293 cells [85, 100].

Ca^{2+}-tolerant adult rat myocytes (Sprague-Dawley female rats; 200g) are isolated using the protocol described earlier (Ch. 2) [85, 99]. Experiments with rats are carried out according to guidelines developed by the University Committee for the Use and Care of Animals (UCUCA) at the University of Michigan [85, 99]. Recombinant adenovirus with wild-type cTnI (±FLAG), cTnISer43/45Asp or cTnIAsp$_{Quad}$ (±FLAG) is diluted in serum-free media and incubated with Ca^{2+}-tolerant myocytes plated onto laminin-coated coverslips as previously described [85] [99]. Myocytes treated with DMEM+P/S without adenovirus serve as controls. Following isolation and gene transfer, cells are cultured in M199+P/S. Coverslips used for functional measurements are transferred to a stimulation chamber and paced at 0.2Hz 24hr after gene transfer, and media

is replaced every 12 hr. Media on non-stimulated cells is changed 24hr post-gene transfer and then every other day for up to 7 days.

Expression analysis: Western blotting and immunohistochemistry

Western blot analysis is used to monitor replacement of endogenous cTnI with FLAG-tagged wild-type cTnI or cTnIAsp$_{Quad}$, maintenance of myofilament stoichiometry, and protein phosphorylation as previously described (Ch. 2 and Ch. 3) [99]. Similar comparisons are performed for cTnISer43/45Asp in chapter 3. Replacement and stoichiometry are monitored at days 2 and 4 while analysis of protein phosphorylation is measured at day 4 as previously described (Ch. 2 and Ch. 3). For each Western blot, proteins are separated on a 12% SDS polyacrylamide gel and electrophoretically transferred to PVDF membranes, which are then probed with the primary and secondary antibody pairs described in Table 4.1. Quantification and normalization of bands from the Western blot are carried out as previously described (Ch. 2 and Ch. 3) [99].

Primary Antibodies	Secondary Antibodies
Total troponin I (mAb, 1:4000, MAB1691, Millipore)	GAM-HRP (1:2000)
Tropomyosin (mAb, 1:1000, Sigma Aldrich)	GAM-HRP (1:2000)
Phospho-cTnI Ser23/24 (pAb, 1:1000)	GAR-HRP (1:2000)
Total cMyBP-C (pAb, 1:1000, Santa Cruz Biotechnology)	GAR-HRP (1:2000)
Phospho-cMyBP-C Ser273 (pAb, 1:2500)*	GAR-HRP (1:2000)
Phospho-cMyBP-C Ser282 (pAb, 1:2500)*	GAR-HRP (1:2000)
Phospho-cMyBP-C Ser302 (pAb, 1:5000)*	GAR-HRP (1:2000)
Total Phospholamban (pAb: 1:1000, Sigma Aldrich)	GAR-HRP (1:2000)
Phospho-phospholamban Ser16 (pAb, 1:1000, Upstate Biologicals)	GAR-HRP (1:2000)
Phospho-phospholamban Thr17 (mAb, 1:5000, Badrilla)	GAM-HRP (1:2000)

Table 4.1. Primary and secondary antibodies used for Western blot analysis. Primary (right column) and HRP-linked secondary (left column) antibodies are described. The antibody and dilution used are listed. The source of the antibody is also noted. Goat-anti-mouse (GAM), goat-anti-rabbit (GAR), horseradish-peroxidase (HRP). Antibodies were purchased from Cell Signaling Technology unless otherwise noted. *Site-specific cMyBP-C phospho-antibodies were a kind gift of Dr. Sadayappan [101].

Indirect immunofluorescence with dual monoclonal antibodies is used to confirm localization of FLAG-tagged cTnI constructs into the myofilament, as described in earlier work

(Ch. 2 and Ch. 3) [99]. Detergent- permeabilized myocytes are stained with a troponin-I specific monoclonal antibody (mAb, 1:500, MAB1691, Millipore) and a secondary antibody conjugated to fluorescein isothiocyanate (FITC, 1:500, Invitrogen) to detect total TnI. A FLAG-specific mAb (1:500, Invitrogen) and a secondary antibody conjugated to Texas Red (TR, 1:500, Sigma) are used to detect exogenous cTnI. Projection images of immunostained myocytes are obtained using a Fluoview 500 laser scanning confocal microscope (Olympus) and de-convoluted using Auto quant X software (Media Cybernetics).

Cellular function: sarcomeric shortening and Ca^{2+} transient measurements

Basal cell shortening measurements are performed in electronically paced myocytes in a heated (37ºC) perfusion chamber 2 and 4 days after gene transfer. Resting sarcomere length, peak shortening amplitude (% baseline), time to peak (TTP), shortening rate, re-lengthening rate, time to 25% re-lengthening ($TTR_{25\%}$), time to 50% re-lengthening ($TTR_{50\%}$), and time to 75% re-lengthening ($TTR_{75\%}$) are calculated from signal-averaged traces measured with a video-based CCD camera system (Ionoptix) as previously described (Ch. 2 and Ch. 3) [99].

Ca^{2+} transients and sarcomere shortening are simultaneously measured in Fura-2AM-loaded, electronically stimulated myocytes with the same CCD-camera system used for basal shortening measurements (Ch. 2 and Ch. 3) [99]. The basal Ca^{2+} ratio, peak Ca^{2+} ratios, the rates of Ca^{2+} rise and decay, the time to 25% decay ($TTD_{25\%}$), the time to 50% decay ($TTD_{50\%}$), and the time to 75% decay ($TTD_{75\%}$), are calculated from signal-averaged traces 4 days after gene transfer (Ch. 2 and Ch. 3) [99] [86].

Data analysis and statistics

All data are presented as the mean±SEM. Statistical significance was set to $p<0.05$ (*). Unless otherwise noted, data are analyzed using a one-way analysis of variance (ANOVA) and Newman-Keuls post-hoc tests.

RESULTS

cTnIAsp$_{Quad}$ increasingly replaces endogenous cTnI in the myofilament

Structural studies demonstrated the cTnIAsp$_{Quad}$ (±FLAG) construct is expressed and replaces endogenous cTnI in the sarcomere of intact myocytes. The FLAG-tagged cTnIAsp$_{Quad}$ replaced < 50% endogenous cTnI 2 days after gene transfer, matching the replacement achieved by cTnIFLAG. Increasing temporal expression also developed for both cTnIFLAG and cTnIAsp$_{Quad}$FLAG, with >80% replacement observed by day 4 (Figs. 4.1A,B). These results are comparable to the expression pattern obtained for cTnISer43/45AspFLAG in earlier work (Figs. 3.1A,B; Figs. 4.1A,B). Western analysis of tropomyosin (Tm) expression indicated the temporal increase in cTnIAsp$_{Quad}$ expression did not alter myofilament stoichiometry compared to controls (Fig. 4.1C). Expression of cTnIFLAG and cTnIAsp$_{Quad}$FLAG also produced the striated immunostaining pattern indicative of sarcomeric localization in myocytes (Fig. 4.2). These expression and immunostaining results demonstrate cTnIAsp$_{Quad}$ (±FLAG) replacement of endogenous cTnI is comparable to work with other cTnI constructs (Ch.2 and Ch.3).

Myocyte contractile performance with cTnIAsp$_{Quad}$ expression

Partial replacement of endogenous cTnI with <50% cTnIAsp$_{Quad}$ 2 days after gene transfer significantly reduced peak shortening amplitude and slowed shortening rate without altering resting sarcomere length in intact myocytes (Fig 4.3). This limited replacement with cTnIAsp$_{Quad}$ also resulted in a faster time to peak shortening (TTP) and time to 50% re-lengthening (TTR$_{50\%}$). In contrast, these measured intervals remained comparable between controls and myocytes expressing cTnISer43/45Asp (Fig. 4.3). As previously observed, the shortening amplitude in cTnISer43/45Asp-expressing myocytes also remained similar to control values at day 2 (Figs. 3.3, 4.3). Based on these results, the presence of cTnISer23/24

phosphorylation or phospho-mimetic substitution may cause sufficient conformational changes in cTnI to enhance the ability of low amounts of negative charge located at cTnISer43/45 (e.g. phosphorylation or phospho-mimetic substitution) in the same cTnI to negatively modulate function.

The reduction in peak shortening amplitude and accelerated $TTR_{50\%}$ observed in myocytes expressing $cTnIAsp_{Quad}$ continued to be detected with more extensive $cTnIAsp_{Quad}$ expression at day 4 (Fig. 4.4). Interestingly, the faster TTP and slowed shortening rates observed 2 days after $cTnIAsp_{Quad}$ gene transfer were no longer significantly different from controls, although the shortening rate remained slower than the rate in myocytes expressing cTnIFLAG. The restoration of TTP with $cTnIAsp_{Quad}$ is worth noting, as this result is opposite from the changes in TTP observed in myocytes expressing cTnISer43Asp and cTnISer45Asp 2 and 4 days after gene transfer (Figs. 3.3, 3.4, 4.3, 4.4). More extensive replacement with cTnISer43/45Asp on day 4 also reduced peak shortening amplitude and slowed shortening rate compared to controls, although TTP and $TTR_{50\%}$ remained unchanged from the control values (Fig. 4.4). A final observation in this set of experiments was the slightly reduced resting sarcomere length detected with cTnIFLAG 4 days post-gene transfer, although shortening amplitude and/or the rates of shortening and re-lengthening were not impaired compared to non-treated controls. Overall, the functional studies performed 2 and 4 days after gene transfer demonstrated the presence of negative charge at cTnISer43/45 produces a dominant influence to reduce contractile function, while cTnISer23/24 is likely responsible for the faster $TTR_{50\%}$ observed with $cTnIAsp_{Quad}$. This later conclusion is consistent with the known ability of Ser23/24 phosphorylation to increase the Ca^{2+} dissociation rate from troponin and indicates this cluster

independently influences function when both cTnISer23/24 and cTnISer43/45 are phosphorylated on a single cTnI [42].

$cTnIAsp_{Quad}$ generates adaptive responses

The return of TTP and shortening rate toward control values suggests adaptive responses contribute to the functional differences on days 2 versus 4 in myocytes expressing $cTnIAsp_{Quad}$. Alterations in Ca^{2+} cycling could restore the TTP and/or shortening rate in $cTnIAsp_{Quad}$-expressing myocytes back toward control values. Thus, Ca^{2+} transients and sarcomeric shortening were measured simultaneously in Fura-2AM loaded controls, and myocytes expressing wild-type cTnI, cTnISer43/45Asp, or $cTnIAsp_{Quad}$ 4 days after gene transfer (Fig.4.5). In these experiments, there were no significant differences detected in peak shortening amplitude or in the release and decay rates of the Ca^{2+} transient among these groups of myocytes (Fig. 4.5). However, $cTnIAsp_{Quad}$ expression diminished peak shortening amplitude and slowed both shortening and re-lengthening rates under these conditions. The impact of cTnISer43/45Asp on shortening amplitude and the rates of shortening and re-lengthening were comparable to earlier observations, although the previously observed increase in $TTD_{50\%}$ was not detected here (Fig. 3.6 vs. Fig. 4.5). In these studies, $cTnIAsp_{Quad}$ also reduced peak shortening and slowed the rates of shortening and re-lengthening significantly more than cTnISer43/45Asp. The enhanced impact of $cTnIAsp_{Quad}$ versus cTnISer43/45Asp observed in this set of experiments supports the idea phosphorylation and/or negatively charged cTnISer23/24 enhances the ability of cTnISer43/45 to modulate contractile function. Fura-2-mediated Ca^{2+} buffering may explain the more dramatic ability of $cTnIAsp_{Quad}$ to reduce contractile function and minimize the influence of this construct on $TTR_{50\%}$ in the current experiments.

While alterations in the Ca^{2+} transient are not detected, it remains possible there are adaptations in the phosphorylation level of individual Ca^{2+} cycling proteins, such as phospholamban (PLB). Thus, PLB phosphorylation at Ser16 and Thr17 is measured in parallel studies (Table 4.1, Fig. 4.6). In contrast to the tendency for cTnISer43/45Asp to enhance Ser16 phosphorylation, a set of initial experiments indicated $cTnIAsp_{Quad}$ tended to reduce Thr17 phosphorylation on PLB (Fig. 3.9 vs. Fig. 4.6). This reduction is not significantly different, although additional experiments are needed for a comparison with adequate statistical power (Fig. 4.6). Currently, the results with PLB phosphorylation levels are consistent with the lack of change in the cellular Ca^{2+} transient. The variability of data observed here also indicates an observed change in PLB phosphorylation may be transient and/or may depend on the long-term presence of cTnISer23/24 and cTnISer43/45 phosphorylation on the same cTnI and in a majority of cTnI proteins within the myofilament. Based on these findings, the restoration of shortening rate and TTP observed 4 days after gene transfer is likely mediated by another mechanism (Fig. 4.4).

Previously, sarcomeric protein phosphorylation correlated with the adaptive changes in shortening and re-lengthening rate produced in myocytes expressing cTnISer43Asp and/or Ser45Asp (Figs. 3.4, 3.7, 3.8). Increased phosphorylation of a third PKC-targeted site on cTnI, Thr144, and cMyBP-C phosphorylation could modulate cross-bridge cycling rates, which could in turn lead to the adaptive changes in TTP and shortening rate [109, 110, 116] [59]. Therefore, site-specific phospho-antibodies were used to evaluate phosphorylation of both cTnIThr144 and cMyBP-C by Western analysis (Table 4.1, Fig. 4.7). Indeed, significantly enhanced cTnIThr144 phosphorylation was detected in myocytes expressing $cTnIAsp_{Quad}$ 4 days after gene transfer (Fig. 4.7). Earlier work demonstrated a phospho-mimetic Glu substitution for Thr144 reduced

the Ca^{2+} sensitivity of thin filament sliding speed [68]. This reduction could contribute to the slowing of TTP back toward control levels in the 4 day myocytes expressing $cTnIAsp_{Quad}$, but does not explain the faster shortening rate adaptation [68].

Further analysis also demonstrated enhanced phosphorylation of the cardiac-specific m-motif of cMyBP-C (Table 4.1, Fig 4.7). Both Ser273 and Ser282 in cMyBP-C were substantially phosphorylated in myocytes expressing $cTnIAsp_{Quad}$ compared to cTnI-expressing controls while there were no detected changes in the Ser302 phosphorylation level (Fig 4.7). Cross-bridge cycling rates increase when cMyBP-C is phosphorylated in this m-motif, and the increased phosphorylation of Ser273 and Ser282 is consistent with phosphorylated cMyBP-C working to return the slowed shortening observed with $cTnIAsp_{Quad}$ observed at day 2 back toward control levels at day 4 (Figs. 4.3,4.4) [109, 110]. Taken together, the elevated phosphorylation level of cTnIThr144 and cMyBP-C Ser273 and Ser282 indicate myofilament expression of a phospho-mimetic substitution at Ser23/24 and Ser43/45 on the same cTnI protein stimulates adaptive signaling response to preserve contractile function in intact myocytes.

DISCUSSION

The current studies demonstrate PKC-targeted Ser43/45 cluster in cTnI produces a dominant reduction in contractile function, while cTnISer23/24 modulates function via a separate mechanism. In addition, there is evidence phospho-mimetic substitutions at Ser43/45 and Ser23/24 on the same cTnI communicate to influence cellular contractile function. This conclusion is based on the potentiated functional effect produced by cTnISer23/24Asp in combination with cTnISer43/45Asp, and the reduced shortening amplitude produced 2 days after gene transfer of $cTnIAsp_{Quad}$. However, more extensive cTnISer43/45Asp expression is required to achieve the same change in function (Figs. 3.4, 4.3). In agreement with earlier work on cTnISer43/45Asp, adaptive changes in myofilament protein phosphorylation also develop with extensive expression of $cTnIAsp_{Quad}$. However, the specific adaptations are unique to $cTnIAsp_{Quad}$ expression.

The current structural model of cTn can be used to predict a mechanism for the intensified effects of cTnISer43/45 within $cTnIAsp_{Quad}$ (Fig. 1.2A) [25]. Phosphorylation or phospho-mimetic substitutions at Ser23/24 in cTnI is predicted to stabilize the cardiac-specific N-terminal domain of the protein [117] [118]. Conversely, cTnISer43 and cTnISer45 are located in the H1(I) α-helix in the more rigid, highly conserved I-T arm, and the phosphorylation or phospho-mimetic substitutions at these sites may rotate this helix away from the N-lobe of cTnC and/or change the rigidity of the I-T arm (Fig.1.2A) [25, 70, 71, 119]. The addition of phospho-mimetic substitutions at cTnISer23/24 to form $cTnIAsp_{Quad}$ may further reposition the rotated I-T arm and accentuate the functional impact of cTnISer43/45Asp (Figs. 3.4, 4.4) [25, 70, 71, 117-119]. Conformational differences also are expected to produce separate functional responses. Specifically, cTnISer43/45 phosphorylation is proposed to slow Ca^{2+} association or binding to

cTnC and/or delay cross-bridge detachment from the myofilament [67, 105] [68]. The observed reduction in peak shortening and slowing of shortening rate in Fura-2-loaded myocytes expressing $cTnIAsp_{Quad}$ could result from slower kinetics for Ca^{2+} binding to cTnC, while a reduction in cross-bridge detachment rates would slow re-lengthening rate. In contrast, phosphorylation of cTnISer23/24 enhances Ca^{2+} dissociation from cTnC, which should accelerate relaxation [42]. The presence of slowed re-lengthening rate in the presence but not the absence of Fura-2AM is probably related to Ca^{2+} buffering by Fura-2AM in these myocytes [103]. This buffering would mask the faster Ca^{2+} dissociation from cTnC by cTnISer23/24 phosphorylation and accentuate the slowing of cross-bridge detachment and/or cTnC Ca^{2+} binding produced by cTnISer43/45Asp substitutions. The more dramatic functional influences of $cTnIAsp_{Quad}$ on shortening and re-lengthening rate and peak shortening amplitude observed in Fura-2AM-loaded myocytes is expected if cTnISer23/24 and cTnISer43/45 work through the proposed mechanisms (Fig.4.5). Previously, phospho-mimetic replacement of all 5 PKC-targeted cTnI residues ($cTnI_{AllP}$) was predicted to reduce Ca^{2+} accessibility to the hydrophobic patch more than cTnISer23/24Asp alone [49 248]. The $cTnIAsp_{Quad}$ construct should similarly reduce Ca^{2+} accessibility more than cTnISer43/45Asp. However, the slowing of re-lengthening rate observed in Fura-2AM-loaded myocytes expressing $cTnIAsp_{Quad}$ suggests cTnISer43/45 substitutions also reduce cross-bridge detachment rate.

Expression of $cTnIAsp_{Quad}$ is predicted to produce a similar change in function as cTnISer43/45Asp, based on earlier experiments showing cTnISer43/45Asp expression augmented cTnISer23/24 phosphorylation (Fig. 3.7). However, these 2 constructs have different influences on peak shortening amplitude, TTP, and $TTR_{50\%}$ at both 2 and 4 days after gene transfer, which indicates different mechanism(s) may be involved in producing the functional

response (Figs. 4.3, 4.4). In myocytes expressing cTnIAsp$_{Quad}$, both clusters are modified on the same cTnI while adaptive cTnISer23/24 phosphorylation occurred more stochastically along the myofilament with cTnISer43/45Asp expression (Ch. 3). Studies with cTnIAsp$_{Quad}$ also indicate cTnISer23/24 promotes the functional impact of cTnISer43/45 when present within the same cTnI. Moreover, modification of these 2 phosphorylation sites within the same cTnI allows Ser23/24 to independently produce the well-known acceleration of cellular re-lengthening, which was measured here as TTR$_{50\%}$ (Figs. 4.3, 4.4) [43, 46]. In contrast, adaptive cTnI Ser23/24 phosphorylation observed with cTnISer43/45Asp expression failed to change TTR$_{50\%}$ or other indicators of re-lengthening rate (Fig.4.4). Thus, these differences in contractile function could result from conformational differences in the thin filament when modified Ser23/24 is present on the same versus different cTnI as Ser43/45 phospho-mimetic substitutions or phosphorylation.

Alternatively, the functional difference could be explained by the presence of phosphorylation turnover at cTnI Ser23/24 for myocytes expressing cTnISer43/45Asp compared to the absence of turnover at this site in myocytes expressing cTnIAsp$_{Quad}$. In previous studies, PKC activation of downstream kinase and phosphatase activity accelerated phosphorylation turnover at Ser23/24 and on other proteins [102, 114]. Accelerated turnover of phosphorylation on end-targets such as Ser23/24 proved to be highly sensitive to cellular environment and influenced the functional response. Thus, this mechanism also may explain the current contractile function response better than a change in the magnitude of phosphorylation [120, 121]. If Ser23/24 phosphorylation turnover is responsible for functional differences, the absence of turnover at cTnI Ser23/24 could influence the slower phase of re-lengthening rate in myocytes expressing cTnIAsp$_{Quad}$ and have no detected impact with more rapid phosphorylation turnover in myocytes expressing cTnISer43/45Asp. There is little evidence to indicate whether

phosphorylation on the same/different cTnI or phosphorylation turnover are responsible for the functional differences attributed to Ser23/24 in cTnISer43/45Asp- versus $cTnIAsp_{Quad}$-expressing myocytes. Clearly, further experiments are necessary to distinguish between these two possible explanations for the different functional impact observed with cTnISer43/45Asp versus $cTnIAsp_{Quad}$.

In addition to directly modifying contractile function, the restoration of shortening rate and TTP toward control values on day 4 demonstrates adaptive signaling develops in myocytes expressing $cTnIAsp_{Quad}$ (Figs. 4.6, 4.7). Phosphorylation of the m-motif in cMyBP-C increases cross-bridge cycling rate, and the enhanced cMyBP-C phosphorylation detected with $cTnIAsp_{Quad}$ expression could contribute toward the restoration of shortening rate observed in my studies (Fig. 4.4)[109, 110]. The functional impact of elevated cTnIThr144 phosphorylation is more controversial. Increased phosphorylation of Thr144 in cTnI reduced Ca^{2+}-activated actomyosin ATPase activity, which indicates the adaptive phosphorylation at this residue may diminish cross-bridge cycling and return TTP toward control values [59, 116]. However, it appears counterintuitive for adaptive phosphorylation to further slow cross-bridge cycling if cTnISer43/45 directly decreases cross-bridge detachment rate [68]. Phosphorylation of Thr144 in cTnI also is proposed to destabilize Ca^{2+} binding to the N-domain of cTnC and may add to the ability of Ser23/24 to enhance Ca^{2+} dissociation from cTnC [49]. If so, enhanced cTnIThr144 phosphorylation may slow TTP but also work as a secondary mechanism to preserve relaxation when cTnISer23/24 modulation is no longer available in $cTnIAsp_{Quad}$-expressing myocytes. Overall, these increases in cTnI and cMyBP-C phosphorylation are consistent with the functional adaptations, although further studies are needed to prove the extent each residue contributes to the adaptive response.

Interestingly, the adaptive signaling response observed with cTnIAsp$_{Quad}$ is unique compared to adaptations previously observed with cTnI Ser43 and/or Ser45 Asp substitutions (Figs. 3.6-3.9, 4.5-4.7). For example, no differences in the Ca^{2+} transient are detected between controls and myocytes expressing cTnIAsp$_{Quad}$, while a faster decay of the Ca^{2+} transient develops in myocytes expressing Asp substitutions at cTnISer43 and/or cTnISer45 compared to controls (Figs. 3.6, 3.9, 4.5). Phosphorylation of the Ca^{2+} cycling protein PLB at Ser16 remained unchanged and Thr17 phosphorylation tended to decrease in myocytes expressing cTnIAsp$_{Quad}$, although some additional experiments are needed to achieve adequate statistical power for this comparison (Fig. 4.6). In contrast, cTnISer43 and cTnISer45Asp increased PLB Ser16 phosphorylation compared to controls (Fig. 3.9). In addition, cTnIAsp$_{Quad}$ expression also caused extensive increases in cTnIThr144, cMyBP-CSer273, and cMyBP-CSer282 phosphorylation while cTnISer43/45Asp expression only influenced cMyBP-CSer282 phosphorylation (Figs. 3.7, 3.8, 4.7A, 4.7B). These differences in the adaptive responses are consistent with the possibility cTnISer23/24 and cTnISer43/45 modifications on the same cTnI produce a conformational difference compared to cTnISer43/45 alone. Conformational-induced structural changes in the thin filament could differentially modify the access of kinases and/or phosphatases to specific sites within myofilament proteins, such as cTnI and cMyBP-C, as well as Ca^{2+} cycling proteins, such as PLB, to produce the unique adaptations observed with cTnIAsp$_{Quad}$.

Based on the current findings, phosphorylation of Ser43/45 with and without Ser23/24 in cTnI also is predicted to play a physiologically important role in the myofilament by acting as a brake. This brake may be a modulatory signal to counteract increases in sympathetic drive over longer periods and/or with chronic stress. For example, increased β-AR activation increases cardiac contractility and heart rate [32] [1, 122]. While sympathetic stimulation and downstream

β-AR signaling are expected to maintain cardiac function over brief time periods, persistent elevations in sympathetic activity may be energetically unfavorable. This type of sustained stress also is expected to result in sympathetic activation of α-adrenergic receptors (α-ARs) and/or produce changes in other neurohormones such as endothelin (ET) or the renin-angiotensin-aldosterone system [54, 123] [55]. Adult cardiac myocytes express α-AR, ET receptors (ETR) and angiotensin II receptors (ATR), and each of these neurohormones activates PKC in myocytes [54] [53, 55]. Thus, the initial neurohormonal activation of PKC in cardiac myocytes may act as a brake in response to longer term or sustained sympathetic activation and/or other environmental stressors. The detection of cTnISer23/24, but not cTnISer43/45 phosphorylation in cTnI under physiological conditions in human and animal models is consistent with this idea [30, 35-37]. Moreover, this idea agrees with earlier predictions cTnISer43/45 phosphorylation reduces cross-bridge cycling to preserve ATP stores in the heart [64] [47].

The additional phosphorylation of cTnISer23/24 could be a sign of a compensatory state of cardiac dysfunction if cTnISer43/45 phosphorylation acts as a modulatory brake within the myofilament. Based on my results, the added presence of cTnISer23/24 phosphorylation is anticipated to enhance the ability of cTnISer43/45 to act as a systolic brake while preserving relaxation (Figs.4.3-4.4). Consistent with this idea, enhanced phosphorylation of both cTnISer23/24 and cTnISer43/45 is observed in a rat model of spontaneous hypertension [30]. Heightened sympathetic drive also could be a contributing factor in the development of phosphorylation at both Ser23/24 and Ser43/45 in cTnI. Indeed, augmented sympathetic drive is an early-stage marker of the compensated state of cardiac dysfunction [124] [5]. The adaptive phosphorylation of Thr144 in cTnI and residues in the m-motif of cMyBP-C observed here may

work to further fine tune cardiac performance during the early stages of heart failure (Figs. 4.6, 4.7).

Over time, the sustained activation of the cTnISer43/45 modulatory brake on myofilament function could be a critical element contributing to systolic and diastolic dysfunction and/or the transition to end-stage heart failure. Down-regulation of β-AR signaling and/or deterioration in compensatory signaling pathways may result in the diminished cTnISer23/24 phosphorylation observed in end-stage heart failure [27, 29]. Previous studies indicate Ser43/45 phosphorylation in cTnI is present as the heart transitions from compensatory to decompensatory heart failure and persists in end-stage heart failure [27] [30, 31]. Increased phosphatase activity and reduced cMyBP-C phosphorylation also develop with decompensated heart failure [125] [126] [127-129]. These changes indicate the adaptive signaling observed in the present study, is diminished in the later stages of heart failure. At this point, cTnISer43/45 phosphorylation likely contributes directly to dysfunction.

In summary, the present group of experiments demonstrates the dominance of cTnISer43/45 and a functional role for cross-talk between Ser23/24 and Ser43/45 within the same cTnI. The cTnISer43/45 cluster is predicted to work as a modulatory brake on contractile function. Conformational changes within cTnI are postulated to produce the enhanced functional response observed with cTnIAsp$_{Quad}$ compared to cTnISer43/45Asp. Compensatory signaling also is detected in myocytes expressing cTnIAsp$_{Quad}$, although this response differed from cTnISer43/45Asp alone. Overall, adaptive signaling is thought to temper the modulatory brake of cTnISer43/45, and heart failure my result when similar adaptive signaling responses are absent.

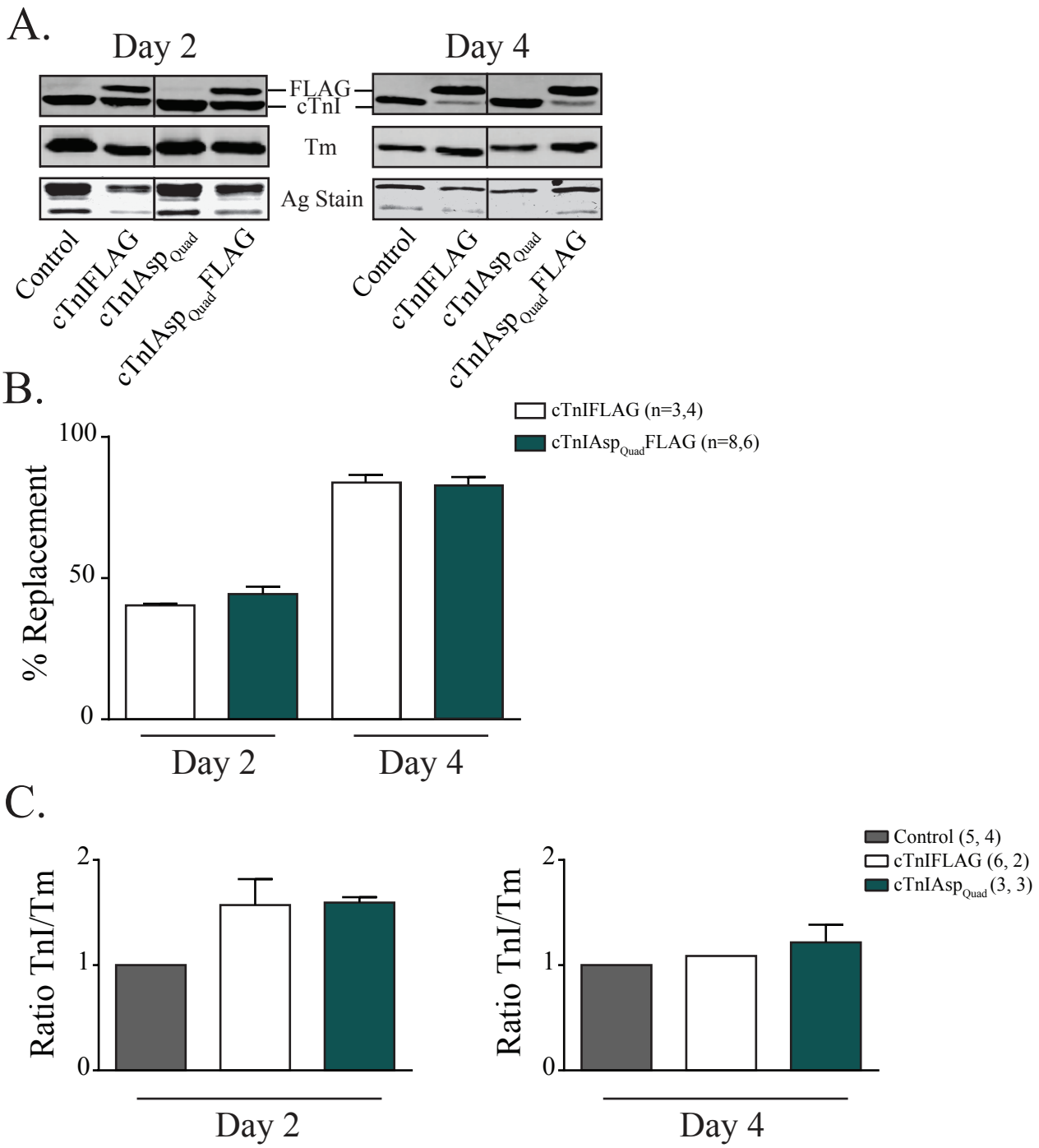

Fig. 4.1 cTnIAsp$_{Quad}$FLAG increasingly replaces endogenous cTnI in the myofilament over time. **A.** Representative Western blot of cTnI(±FLAG) and cTnIAsp$_{Quad}$(±FLAG) expression 2 (left panel) and 4 (right panel) days after gene transfer. A troponin I-specific Ab detected both endogenous and FLAG-tagged cTnI constructs (upper panels, Table 4.1). Tropomyosin levels were measured to determine if cTnIAsp$_{Quad}$ expression alters myofilament stoichiometry (middle panels). A section of silver (Ag)-stained gel is included to demonstrate protein loading in each lane (lower panels). All samples were run on the same gel, and the black line indicates a separation between these lanes by additional samples. **B.** Quantitative analysis showing cTnIAsp$_{Quad}$ replacement of endogenous cTnI 2 (left side) and 4 (right side) days post-gene transfer. Replacement is calculated from the ratio of FLAG-tagged/total cTnI protein detected and is expressed as the percentage of endogenous cTnI replaced by each construct. **C.** The ratio of total cTnI/Tm protein was calculated for control, cTnIFLAG, or cTnIAsp$_{Quad}$FLAG-expressing myocytes. The normalized protein ratios were quantified 2 (left panel) and 4 (right panel) days after gene transfer. There were no statistical differences in expression compared controls in B and C (*p>0.05).

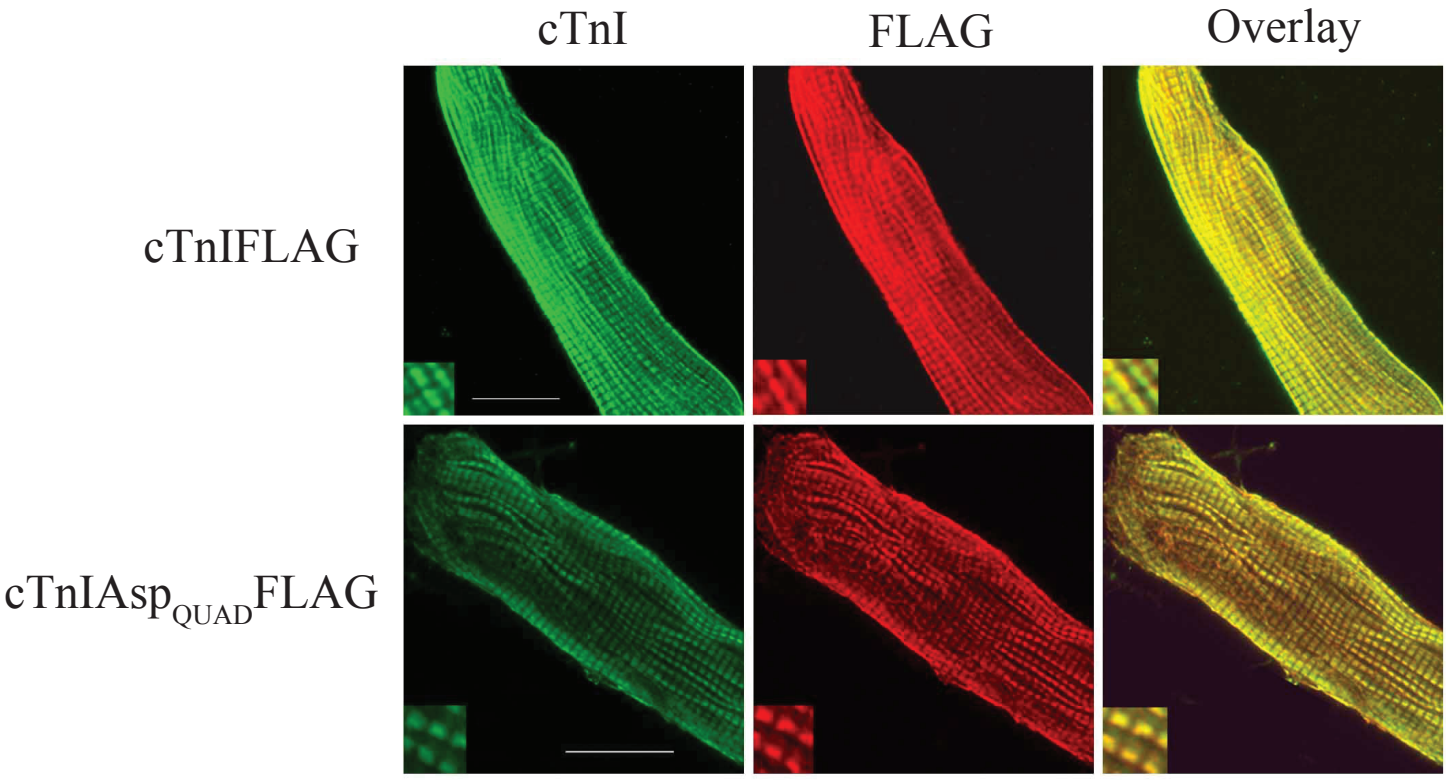

Fig. 4.2 cTnIAsp$_{Quad}$ localizes to the sarcomere. Permeabilized myocytes from each sample group were stained with monoclonal antibodies specific for TnI and FLAG to monitor both endogenous and exogenous cTnI localization. Projection confocal images of cTnIFLAG and cTnIAsp$_{Quad}$FLAG-expressing myocytes exhibited a striated pattern when probed with a TnI 1°Ab and a FITC-conjugated 2°Ab (left column). Myocytes stained with a FLAG-specific 1°Ab and a Texas Red-conjugated 1°Ab (middle column) showed cTnIFLAG and cTnIAsp$_{Quad}$FLAG produced the same striated patterning. Overlays of these images showed co-localization of the two antibodies, confirming myofilament incorporation of the phospho-mimetic cTnI. A magnified section of each myocyte inserted into each panel illustrates the striated patterning produced by cTnI expression in the myofilament. Bars shown in each FITC channel represents 25μm.

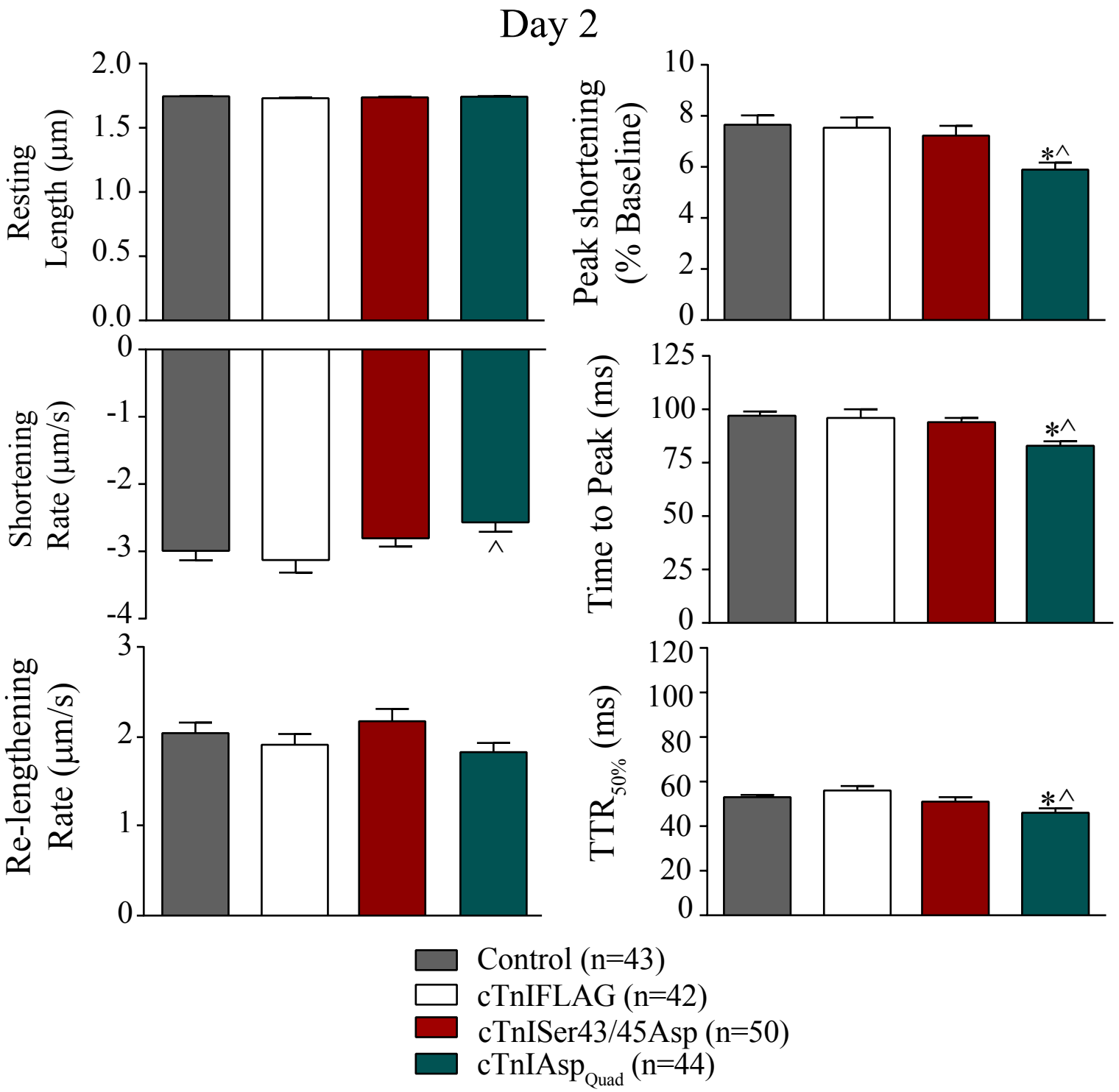

Fig. 4.3 Analysis of basal shortening and re-lengthening in control, cTnIFLAG, cTnISer43/45Asp, and cTnIAsp$_{Quad}$-expressing myocytes 2 days after gene transfer. Signal-averaged traces of contractile shortening and re-lengthening were recorded in individual myocytes 2 days after gene transfer. Then, resting sarcomere length, peak shortening amplitude, shortening rate, time to peak (TTP), re-lengthening rate, and the time to 50% re-lengthening ($TTR_{50\%}$) were determined for each trace. A $p<0.05$ was considered to be statistically significant, where * indicates a difference from controls and ^ indicates a difference from cTnIFLAG-expressing myocytes.

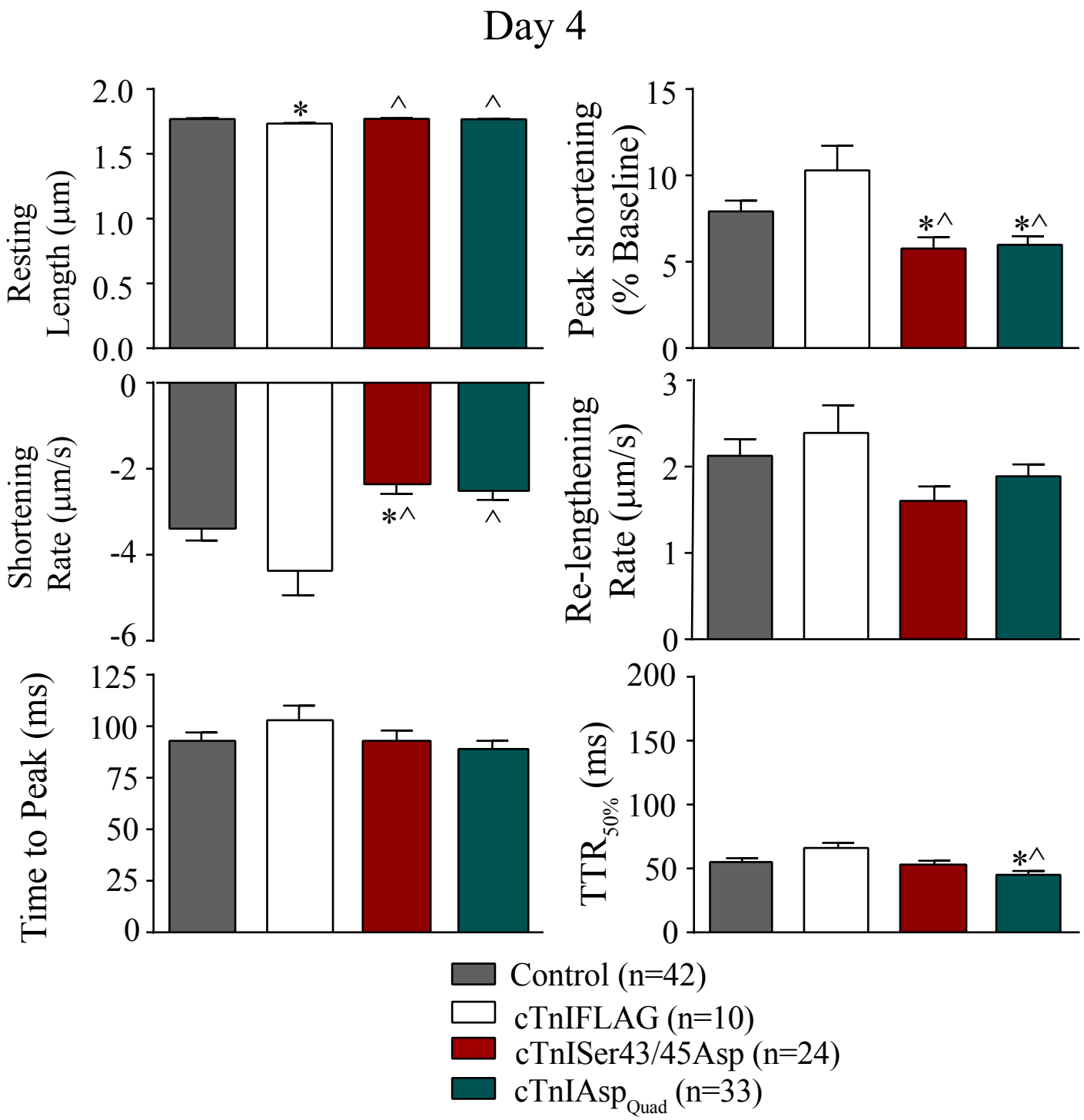

Fig. 4.4 Extensive replacement of endogenous cTnI with cTnIAsp$_{Quad}$ modulates contractile function. Signal averaged traces of basal shortening and re-lengthening were measured in each group of myocytes 4 days after gene transfer, as described in Fig. 4.3. The quantitative analysis of resting length, peak shortening amplitude, shortening and re-lengthening rates along with the time to peak (TTP) and time to re-lengthening 50% (TTR$_{50\%}$) are shown, and there were no changes in other measures of shortening or re-lengthening. Statistical differences ($p<0.05$) from controls (*) or cTnIFLAG (^) are indicated in each panel.

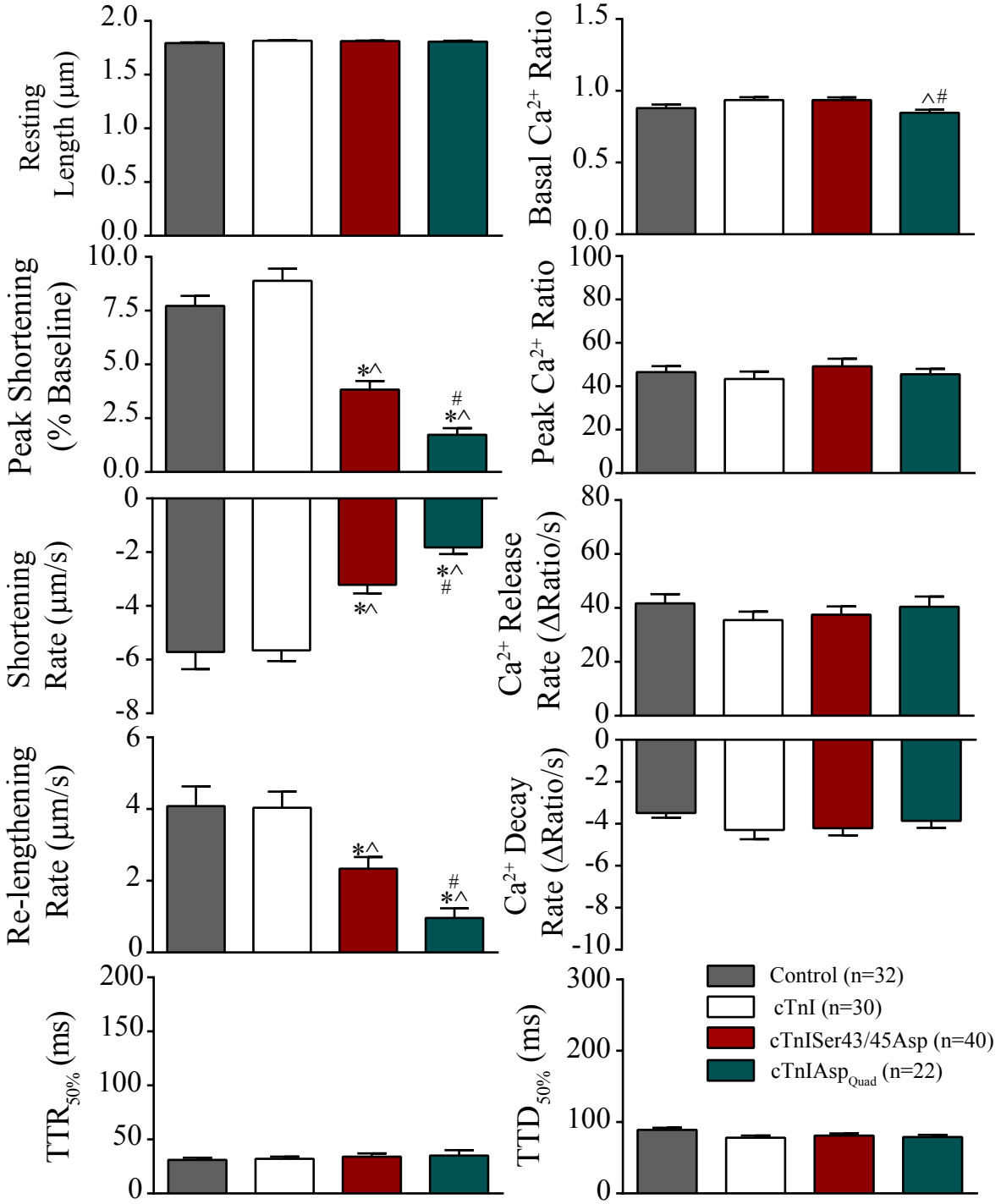

Fig. 4.5 Contractile function and Ca^{2+} transients in control, cTnI, cTnISer43/45Asp and $cTnIAsp_{Quad}$-expressing, Fura-2AM-loaded myocytes 4 days after gene transfer. Basal shortening and Ca^{2+} transients were simultaneously measured in Fura-2AM-loaded myocytes in each group 4 days after gene transfer. Signal-averaged traces were analyzed for resting length, peak shortening amplitude, shortening rate, re-lengthening rate, and the time to 50% re-lengthening ($TTR_{50\%}$) along with the corresponding analysis of the Ca^{2+} transient. The Ca^{2+} transient measurements included the basal and peak Ca^{2+} ratios, rate of Ca^{2+} release, rate of Ca^{2+} decay, and time to 50% Ca^{2+} decay ($TTD_{50\%}$). *p<0.05 indicates statistically different from controls, ^p<0.05 indicates statistically different from cTnI, and #<0.05 indicates statistically different from cTnISer43/45Asp.

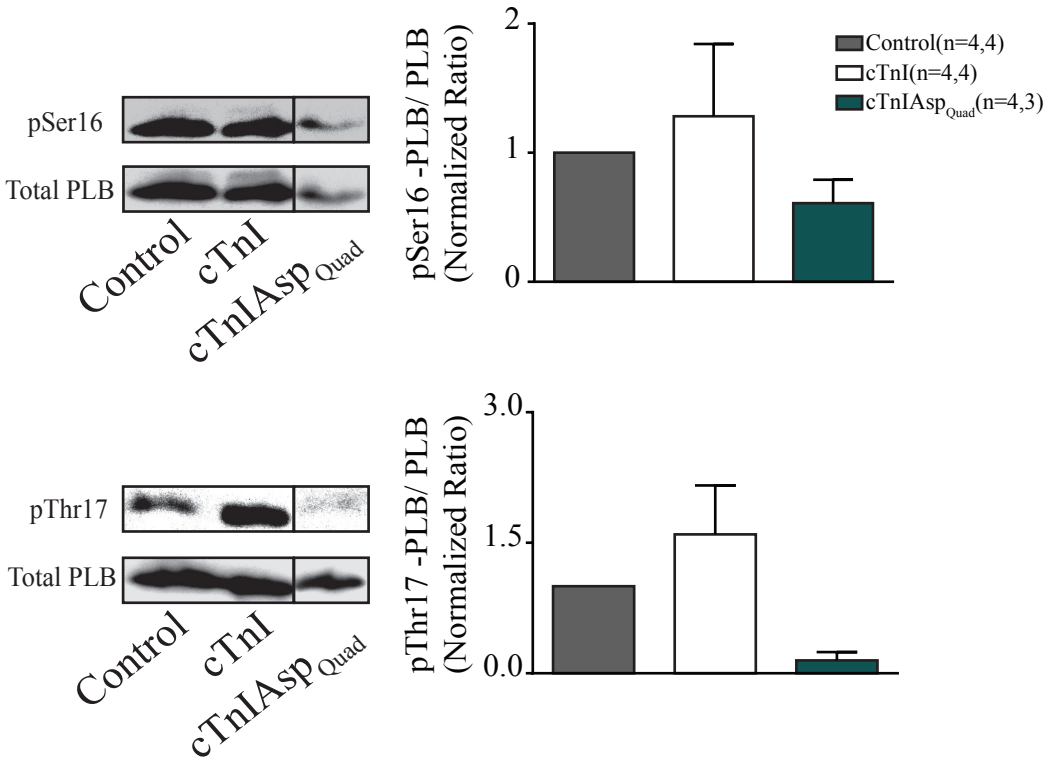

Fig. 4.6 Phospholamban phosphorylation in control, cTnI, and cTnIAsp$_{Quad}$-expressing myocytes 4 days after gene transfer. Representative Western blot analysis of phospholamban (PLB) phosphorylation at PLBSer16 (upper panel) and PLBThr17 (lower panel) using site-specific phospho-antibodies (upper blots) compared to total PLB expression (lower blots). Black lines between lanes indicate groups were separated by additional samples run on the same gel. The phospho-PLB/total PLB protein ratio is quantified for each residue (right panels). The current data indicates no statistical differences compared to control values (*p>0.05) for either phosphorylated residue in PLB.

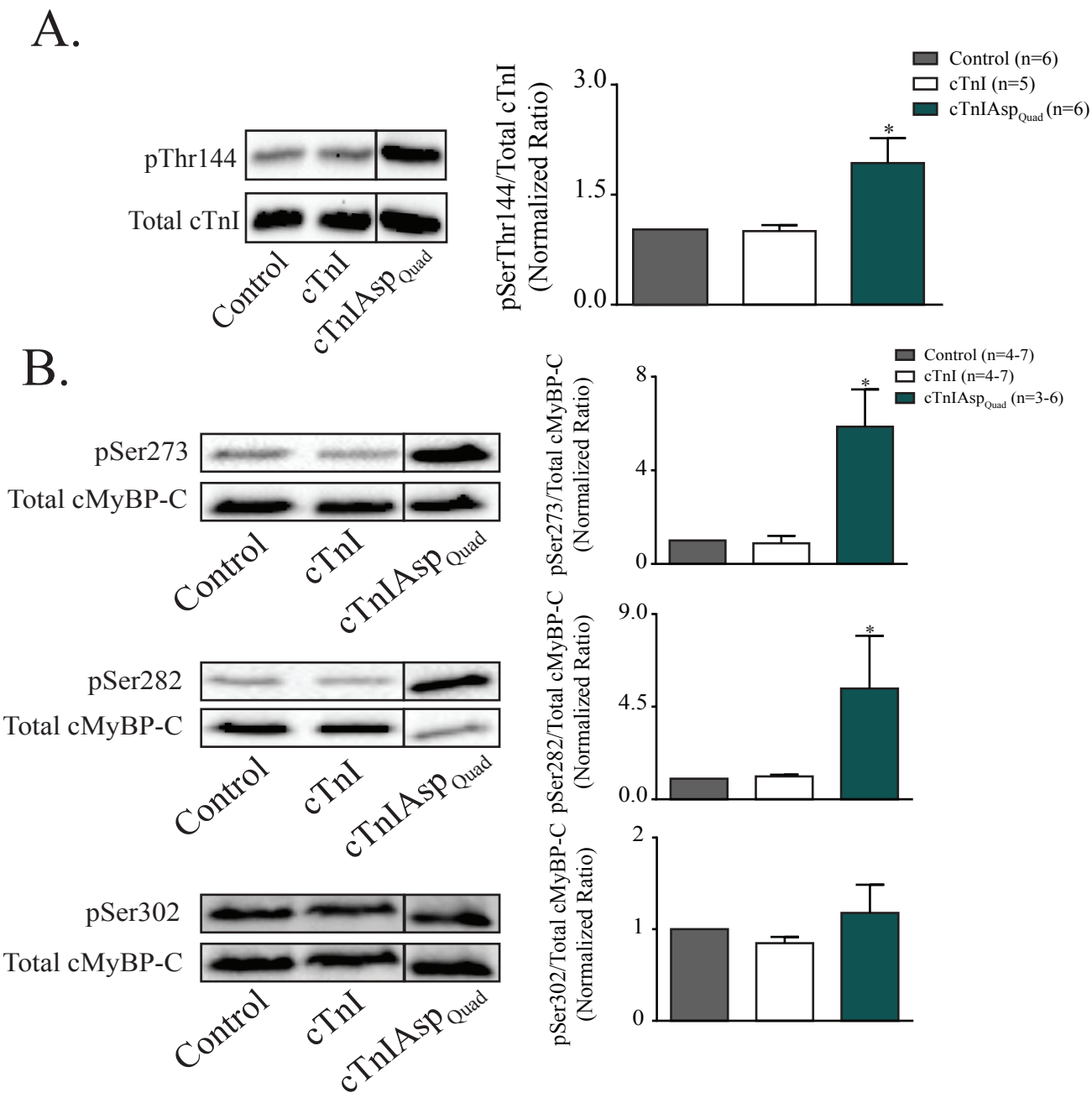

Fig. 4.7 Myofilament protein phosphorylation in control, cTnI, and cTnIAsp$_{Quad}$-expressing myocytes 4 days after gene transfer. A. Representative Western blot analysis of cTnIThr144 phosphorylation in myocytes 4 days after gene transfer (left panel). A site-specific phospho-antibody is used to detect cTnIThr144 phosphorylation in control, wild-type cTnI, and cTnIAsp$_{Quad}$-expressing myocytes (upper blot). Total cTnI protein levels were also monitored (lower blot). The normalized phospho-cTnIThr144/total cTnI ratios are shown for each sample (right panel; mean SEM, n=5-6), and statistical differences ($p<0.05$) from control are indicated by *. **B.** Representative Western blot showing site-specific phospho-antibody detection of cMyBP-CpSer273 (upper panels), cMyBP-CpSer282 (middle panels), and cMyBP-CpSer302 (lower panels). Total cMyBP-C protein levels are shown in the lower rows of each panel. The black line between lanes indicates additional samples separated the lanes shown on the same gel for Westerns shown in A and B. The normalized phospho/total protein ratios were quantified for each sample (right panel), and $p<0.05$ was considered to be significantly different from controls (*).

CHAPTER 5

CONCLUSIONS

OVERVIEW

Phosphorylation of cardiac troponin I (cTnI) plays an important role in modulating myocardial contractile performance [3, 6]. Moreover, alterations in protein kinase C (PKC) activation and downstream cTnI phosphorylation are linked to cardiac dysfunction [27] [56, 65] [28-31]. Thus, understanding the role(s) of each cTnI residue targeted by PKC and the functional interplay between residues are important issues in the modulation of contractile function by cTnI under physiological and pathophysiological conditions. Multiple *in vitro* and *in vivo* studies attempted to address these questions. However, the results are complex, and different approaches gave rise to divergent interpretations. Currently, there is a lack of consensus about the role played by PKC-targeted cTnISer43/45 phosphorylation in the myocardium.

Experiments in this dissertation addressed the role PKC-mediated cTnISer43/45 phosphorylation plays and the influence cTnISer23/24 and cTnISer43/45 communication has in modulating contractile function in isolated adult rat cardiac myocytes. The first aim in this study was to determine whether cTnISer43/45 acts as a modulatory brake on contractile function. These studies were performed using gene transfer of phospho-null (Ala) or phospho-mimetic (Asp) substitutions at cTnISer43 and/or cTnISer45 into adult myocytes. Overall, results from this work demonstrated cTnISer43/45 reduces the amplitude and rate of myocyte shortening (Ch. 2 and Ch. 3). In addition, Ser43 and Ser45 in cTnI independently reduced contractile function, and results from this work were consistent with each residue working via separate mechanisms within the myofilament (Ch. 3).

Expression of cTnISer43/45 substitutions in myocytes also produced adaptive changes in function. Thus, the idea adaptive signaling within the myofilament contributes to the overall

functional response was tested in a second aim of this dissertation (Ch.3 and Ch.4). These adaptive changes produced a functional response comparable to results obtained in intact animal models. Thus, extensive cTnISer43/45Asp expression levels produced dynamic signaling modulation across the myofilament. To better understand adaptive signaling, experiments then focused on the relationship between Ser23/24 and Ser43/45 in cTnI, which are both targets for PKC. Phospho-mimetic cTnISer43/45 expression increased cTnISer23/24 phosphorylation, and yet the impact of this cTnI substitution produced a different functional response than cTnI containing Asp substitutions at all 4 residues (e.g. cTnIAsp$_{Quad}$; Ch. 3 vs. Ch. 4). Results from this study indicate myofilament function is sensitive to the distribution and/or turnover of adaptive phosphorylation (Ch. 4). In summary, results from the present study provided insight into the direct role of cTnISer43/45 and the dynamic adaptive responses contributing to cTnI modulation of contractile function. Moreover, this work showed the cellular approach used here is an important bridge for resolving controversies arising from earlier myofilament and genetic animal model studies.

SIGNIFICANT FINDINGS

Chemical properties of substitutions at cTnISer43/45 influence contractile function

The functional modulatory role of cTnISer43/45 phosphorylation is examined in the present group of studies by expressing phospho-null cTnISer43/45Ala and phospho-mimetic cTnISer43/45Asp substitutions in adult cardiac myocytes (Chs.2-4). Both substitutions are expressed and incorporated into the sarcomere of myocytes after gene transfer to a comparable extent as cTnI. The Ala substitution is functionally conservative at other sites, including Ser23/24 in cTnI, and not anticipated to change contractile function compared to controls [43, 78]. In contrast, expression of cTnISer43/45Asp should mimic phosphorylation at this site and

reduce contractile function. Indeed, comparable contractile function is observed in controls and in myocytes with <50% cTnISer43/45Ala replacement of endogenous cTnI. These results are in keeping with the lack of change in cardiac function observed in a transgenic (tg) cTnISer43/45Ala mouse model with ≈50% replacement of endogenous cTnI (Table 1.1)[72]. However, myofilament Ca^{2+} sensitivity of tension in permeabilized myocytes and peak shortening amplitude in intact myocytes decreased while the later stages of re-lengthening became faster (e.g. $TTR_{50\%}$) with more extensive cTnISer43/45Ala expression. These findings could result if hydrogen bonding by hydroxyl groups present in Ser is lost when Ala, which contains a less polar methyl side chain, replaces this residue. The cTnISer45 residue is predicted to interact with cTnC Glu10 via this type of weak ionic interaction, and the functional alterations observed with cTnISer43/45Ala could result from disruption of this interaction [71]. The dramatic rightward shift in myofilament Ca^{2+} sensitivity of tension observed in the knock-out/knock-in $cTnIAla_5^{nb}$ mice, with complete replacement of endogenous cTnI, further reinforces this conclusion [64] (Table 1.1).

An additional component of this study focused on the role cTnISer43/45 plays during PKC activation by the agonist, endothelin-1 (ET-1, Ch. 2). If PKC targets cTnISer43/45 in response to activation by ET-1, the accelerated relaxation rate attributed to cTnI phosphorylation during this response should be absent [78, 86]. While the re-lengthening rate, measured as $TTR_{50\%}$, is significantly slowed with cTnISer43/45Ala compared to controls during ET-1 treatment, a more indirect process also may explain this experimental outcome. This conclusion is based on the accelerated basal re-lengthening produced by cTnISer43/45Ala as well as evidence phospho-mimetic cTnISer43/45Asp slows re-lengthening (Ch. 2 and Ch. 3). Taken together, the observations made in the present study could indicate cTnISer43/45Ala prevents

PKC from phosphorylating other cTnI residues and/or blocks the phosphorylation-induced thin filament transduction necessary for the ET-1-mediated acceleration of re-lengthening. The altered basal and ET-1-induced contractile function observed with cTnISer43/45Ala suggests the Ser residues in this cluster play an essential role in defining the 3-dimensional orientation or structure of cTnI under basal conditions and in response to neurohormonal PKC activation. Due to the chemical properties of Ala, the current studies with cTnISer43/45Ala are unable to definitively demonstrate the contribution of this cluster to neurohormonal modulation by PKC in myocytes.

While the Ala substitutions produced unanticipated changes in contractile function, the reduced rate and amplitude of peak shortening as well as the rightward shift in Ca^{2+} sensitivity observed with Asp substitutions at cTnISer43/45 are in agreement with the consensus ideas derived from biochemical studies about the functional impact of PKC-mediated phosphorylation this residue cluster (Ch. 3). Previous studies demonstrated reconstitution of exhaustively phosphorylated cTnI into myofibrils reduced Ca^{2+} sensitivity and maximum actomyosin ATPase activity, and cTnISer43/45 phosphorylation levels strongly correlated with the functional response relative to the levels of cTnI phosphorylation at Ser23/24 and Thr144 [68] [51] [60, 61]. Further work established phospho-mimetic Asp or Glu substitutions at Ser43/45 reduced cross-bridge cycling rate and actomyosin Ca^{2+} sensitivity [49, 68]. To date, only the impact on maximum isometric tension observed in the current studies differs from published work with cTnISer43/45Glu, which reduces peak isometric tension [68]. A smaller number of attached cross-bridges was proposed as a likely reason to explain the differential influence of Glu versus Asp in chapter 3, which could result from a subtle change in tropomyosin (Tm) positioning to prevent complete myofilament activation. In keeping with this idea, peak tension and thin

filament conformation also differ slightly in the presence of rigor versus cycling cross-bridges [130]. Besides the difference in maximum tension, the present studies are consistent with earlier work on PKC-mediated cTnI phosphorylation and studies with phospho-mimetic substitutions at Ser43/45 in cTnI [49, 61 204, 62, 67, 68]. In addition, the current work adds to this research area by showing there is a length-dependent component to the influence of cTnISer43/45Asp on myofilament Ca^{2+} sensitivity of tension (Ch. 3). Collectively, studies with cTnISer43/45Asp indicate phosphorylation of this cluster acts as a modulatory brake on function, and the length-dependent response observed with cTnISer45Asp suggests the greatest influence of phosphorylation in this cluster should be observed with increased preload.

Myocyte studies provide insight into the divergent functions attributed to cTnI phosphorylation

My work in isolated myocytes provides insight into the often divergent conclusions reached in myofilament and genetic animal model studies. Thus, this approach helped to resolve controversies about the modulatory role of cTnISer43/45 phosphorylation on function, which are due in large part to divergent functions observed when phospho-null Ala is substituted for Ser/Thr at PKC-targeted residues [47, 64]. Overall, the functional changes produced by cTnISer43/45Ala expression in this work are consistent with the majority of myofilament studies on cTnISer43/45 phosphorylation and/or work with cTnISer43/45Ala in myofilaments and transgenic (tg) animals [45, 72]. The diminished function observed after more extensive replacement with cTnISer43/45Ala in the present study also is in agreement with basal myocyte function measured in the $cTnIAla_5^{nb}$ mouse model [64]. Endogenous cTnI is completely replaced by cTnI containing Ala at all 5 PKC-targeted residues (i.e. Ser23/24, Ser43/45 and Thr144) in this mouse model [47, 64]. The present studies show cTnISer43/45Ala caused a

decrease in myofilament Ca^{2+} sensitivity, which is also evident in $cTnIAla_5^{nb}$ myocytes [64]. The controversy arising from the $cTnIAla_5^{nb}$ study is primarily caused by the interpretation of cTnISer43/45 function in this mouse model, with important contributing factors being the absence of *in vivo* cardiac function measurements, failure of the authors to discuss the physiological significance of the rightward shift in Ca^{2+} sensitivity in $cTnIAla_5^{nb}$ myocytes and lack of consideration given to alternative data interpretations [64].

My studies show the cTnISer43/45Ala substitution is not functionally conservative and could therefore cause cardiac dysfunction, which is a significant consideration for the $cTnIAla_5^{nb}$ studies [47] [45, 64]. This functional change also impacts the interpretation of results obtained with ET-1 activation of PKC in $cTnIAla_5^{nb}$ myocytes. In functional studies with wild-type and $cTnIAla_5^{nb}$ myocytes, ET-1 increased myofilament Ca^{2+} sensitivity and slowed re-lengthening rate in wild-type myocytes in the presence of a phosphatase inhibitor, and this response is attenuated in $cTnIAla_5^{nb}$ myocytes [64]. The authors concluded their results are explained by PKC phosphorylation of cTnI and proposed this phosphorylation produced an increase rather than a decrease in myofilament Ca^{2+} sensitivity [47, 64]. The findings suggest the observed response may not be an accurate measure of PKC signaling in myocytes and could result from impaired responses to environmental conditions and/or confounding factors such as cTnISer43/45Ala-induced changes in conformational positioning of Tn in the myofilament. The current work with cTnISer43/45 substitutions shows there is a delicate balance between kinase and phosphatase activity (Chs. 2-4). Different functional responses should be expected with the addition of a phosphatase inhibitor and/or when baseline function changes, as is observed in $cTnIAla_5^{nb}$ myocytes [64]. Higher doses of ET-1 produce a similar functional response as phosphatase inhibition using low ET-1 doses, and high ET-1 produces a significant cellular

alkalosis and sensitizes cTnI to Ca^{2+} [86] [77, 92]. Thus, it remains possible functional responses attributed to ET-1-induced cTnI phosphorylation are instead due to alterations in the pH sensitivity of $cTnIAla_5^{nb}$ in the myofilament. Moreover, pharmacological levels of PKC activation are known to increase myofilament Ca^{2+} sensitivity of tension independent from changes in cTnISer43/45 phosphorylation and are mediated by myosin light chain kinase (MLCK) phosphorylation of myosin light chain 2 (MLC_2) [97]. In studies with $cTnIAla_5^{nb}$ myocytes, there is also some evidence of compromised MLCK signaling [15, 47]. In addition, the Ca^{2+} transient response to ET-1 is elevated in intact $cTnIAla_5^{nb}$ myocytes compared to wild-type controls, and this mouse develops a dilated cardiomyopathy [64]. Collectively, the current work provides insights into the ability of Ala substitution at cTnISer43/45 to directly alter function and the potential for adaptive signaling to develop in cardiac myocytes. Thus, the presence of both direct and adaptive mechanisms should be considered when interpreting the roles(s) played by PKC-mediated cTnI phosphorylation on the modulation of contraction.

Direct role of cTnISer43/45 to modulate cardiac contractile function

Overall, the current work with cTnISer43/45Asp substitutions provided significant insight into the role this cluster plays in modulating contractile function. In previous work, cTnISer43/45 phosphorylation and/or phospho-mimetic substitution reduced cross-bridge cycling and myofilament Ca^{2+} sensitivity [45] [51, 68]. Thus, diminished peak shortening amplitude and accelerated cellular re-lengthening were anticipated in adult myocytes expressing cTnISer43/45Asp. The expected decrease in peak shortening is observed, but there is also a slowing of shortening rate. Fura-2AM-loaded myocytes also exhibits a slowing of re-lengthening rate compared to controls (Ch. 3). The slowed shortening rate is consistent with slowing of pressure development in multiple genetic animal models containing phospho-mimetic

substitutions at cTnISer43/45 [49, 62]. These studies also demonstrate cTnISer43Asp and cTnISer45Asp independently modulate function, exerting a brake-like effect on myocyte contraction. Both cTnI Ser23 and Ser24 phosphorylation are required to modulate cardiac relaxation, but these results demonstrate this is not true for cTnISer43/45 [40, 41]. In addition, cTnISer45Asp expression has a greater influence on cardiac myocyte contractile function based on the larger decrease in peak shortening and the slowed shortening and re-lengthening rates with comparable levels of cTnISer43Asp and cTnISer45Asp expression (Ch. 3). Moreover, the absence of diminished peak shortening in myocytes expressing cTnISer43/45Asp indicates the individual residues may counterbalance one another at low levels of replacement, and there is evidence of communication between cTnISer23/24 and cTnISer43/45.

The potential molecular mechanisms responsible for Asp substitutions at cTnISer43 and/or Ser45 to function as a brake are discussed in chapter 3. The most likely mechanisms include a reduction in Ca^{2+} binding to cTnC and a slowed cross-bridge detachment rate (Figs. 5.1A, B). The slowing of Ca^{2+} binding is consistent with the diminished myofilament Ca^{2+} sensitivity in permeabilized myocytes as well as the reduced amplitude and rate of shortening in intact myocytes (Fig. 5.1A). Recent biochemical studies also provide evidence modifications at cTnISer45 reduce the Ca^{2+} binding rate to cTnC, which may be mediated via functionally relevant interactions identified between this residue and the N- and/or C-lobes of cTnC [49, 70, 71] [67]. The cTnISer43 residue resides on a different face of the α-helix than Ser45, and while relevant Ser43 interactions are not yet known, this residue is in close proximity to upstream cTnI residues adjacent to the regulatory cTnC Ca^{2+} binding site in the cTn structural model [25]. It remains possible the reduced Ca^{2+} sensitivity produced by cTnISer43/45 also results from inhibited signal transduction following Ca^{2+} binding to the regulatory site in cTnC. The

molecular changes responsible for this possibility likely depend on changes in the flexibility of the I-T arm within cTn and/or an overall conformational change to re-position the inhibitory peptide (IP) and H3/H4 helical domains, which form a significant component of the molecular switch and transmit the Ca^{2+} signal within cTn (Fig. 1.2A) [25, 119].

The reduced Ca^{2+} binding rate and/or signal transduction mechanism is unable to explain the slowing of re-lengthening rate, which became more apparent with Ca^{2+} buffering in Fura2-AM-loaded myocytes (Ch. 3 and Ch. 4). This observation suggests cTnISer43/45 works to reduce cross-bridge detachment rates, which also may depend on conformational changes within the cTn I-T arm and/or the domains responsible for the switching mechanism in cTnI (e.g. IP and H3/H4 helices) (Fig. 5.1B). This possibility is difficult to explain based on the current 3 state-model of thin filament activation [22]. A slowing of cross-bridge detachment rate should also translate into faster cross-bridge attachment. If so, the kinetics of this process should counteract the influence of cTnISer43/45 on Ca^{2+} binding, and there should be no change in shortening or pressure development rates. However, a 4-state model of thin filament activation has been recently proposed to explain hysteresis mediated by the thin filament to differentially influence cross-bridge attachment and detachment rates [131]. Further evidence to support this new model and experimental proof for slowed cross-bridge detachment in response to cTnI Ser43/45 phosphorylation will need to be addressed in future studies.

The independent influence of cTnISer43Asp or cTnISer45Asp on myocyte shortening also suggests cTnISer43 and cTnISer45 exert their effects through separate mechanisms. As discussed above, cTnISer43 and cTnISer45 likely interact with different components of cTnC and/or cTnI to modulate function [119] [25]. If future experiments validate this idea, additional studies are needed to test whether the separate cTnISer43- and cTnISer45-mediated mechanisms

could prevent the overall conformational change needed to diminish peak shortening in myocytes with limited expression of cTnISer43/45Asp. The ability of cTnISer43 and cTnISer45 to counter the other residue after extensive replacement with cTnISer43/45Asp appears to be more subtle by day 4, when only a faster TTP is observed between the individual substitutions and is absent with cTnISer43/45Asp. The diminished function produced by extensive cTnISer43/45Asp replacement is intriguing, and this effect could be explained if a threshold level of cTnISer45Asp exerts a dominant influence on either Ca^{2+} binding to cTnC or induces an overall conformational change in the thin filament, reducing myofilament Ca^{2+} sensitivity. The later idea is possible if extensive replacement with cTnISer43/45Asp allows neighboring functional units to adopt the necessary conformational change to reduce overall myofilament Ca^{2+} sensitivity [3] [22]. The comparable functional influence of cTnISer43/45Asp and cTnISer45Asp on day 4 supports this idea. Increased phospho-mimetic replacement at either cTnISer43 or cTnISer45 also could increase phosphorylation of the other residue, mimicking the effect of cTnISer43/45Asp. However, this scenario is unlikely because the individual residues produce slightly different effects on cardiomyocyte contraction with low and high levels of replacement at each site. Moreover, if phosphorylation increases at the neighboring residues after individual replacement, comparable contractile responses should have been observed with the individual substitutions and cTnISer43/45Asp, which is not the case (Ch. 3).

Augmented phosphorylation at cTnISer23/24 in myocytes expressing cTnISer43/45Asp substitutions raised the question of whether neighboring, but spatially distinct, Ser clusters communicate to modulate contractile function (Ch. 3 and Ch. 4). To test this idea, function was measured in myocytes expressing $cTnIAsp_{Quad}$, and the functional outcome was expected to be comparable to function observed with cTnISer43/45Asp replacement. Instead, slightly different

functional responses are observed with each construct, providing important insight about communication between these Ser clusters. One significant difference was the ability of limited $cTnIAsp_{Quad}$ expression (e.g. <50%) to reduce function, which remained unchanged from controls at comparable cTnISer43/45Asp expression levels (Ch. 4). The continued slowing of myocyte re-lengthening rate after more extensive $cTnIAsp_{Quad}$ replacement, but not cTnISer43/45Asp expression, also was not anticipated given cTnISer23/24 phosphorylation accelerates relaxation [40, 43, 70, 71, 78]. This conclusion is based on cTnISer23/24 phosphorylation having little effect on Ca^{2+} association with the N-lobe of TnC but having a significant influence on promoting Ca^{2+} release from TnC [42]. These results suggest either cTnISer23/24Asp stabilizes the cTnISer43/45Asp structural response when present in the same cTnI and/or is necessary for cTnISer43/45 to reduce peak shortening amplitude and accelerate re-lengthening. Recent studies also showed two substitutions in the same myofilament protein can produce contradictory effects on Ca^{2+} binding and Ca^{2+} dissociation [105]. Thus, this data support the idea communication occurs between individual residues within a single cluster and between neighboring residue clusters within the same protein. This work also shows myofilament communication is dynamic and able to influence phosphorylation at other sites in the same protein.

Communication between the N-terminal residues cTnISer23/24 and cTnISer43/45 as well as the distal cTnIThr144 could have a significant impact on contractile function, but the consequences of this communication are not yet defined. Thr144 is specific to the cardiac isoform of TnI and is positioned in the inhibitory peptide domain adjacent to the H3 and H4 domains, and all 3 domains act as “molecular switch” peptides. The positioning of cTnIThr144 within cTnI suggests phosphorylation is an important mechanism for regulating the ability of the

switch peptide to transition between actin and TnC [25, 119] [3, 78]. If this is true, cTnIThr144 phosphorylation could position the IP region to favor either myofilament activation or deactivation. The physiological importance of this residue seems obvious, and yet the functional role of cTnIThr144 phosphorylation remains controversial. In early *in vitro* work, phospho-mimetic replacement at cTnIThr144 failed to influence maximal isometric tension or thin filament sliding speed in reconstituted myofibrils, indicating this residue was not functionally relevant [68]. In contrast, reduced maximum tension and slowed cross-bridge cycling developed in skinned myofibrils treated with Src-activated PKCδ, which phosphorylates cTnI Thr144 [59, 78, 86]. Therefore, it is reasonable to predict cTnIThr144 phosphorylation positions cTnI to interact with actin. Moreover, Thr144 may position cTnI to enhance the functional influence of cTnISer23/24 phosphorylation on Ca^{2+} dissociation [116] [49]. Further work is needed to determine if cTnIThr144 phosphorylation also influences cTnISer43/45-dependent function.

cTnISer43/45 substitutions produce adaptive signaling in isolated myocytes

Another major outcome from the current work is the idea adaptive and dynamic myofilament signaling, produced by chronic cTnI phosphorylation at residues such as Ser43/45, plays an important role in modulating contractile function. Functional adaptations were first identified in cTnI with phospho-mimetic Asp substitutions at Ser43 and/or Ser45 (Ch. 3). More extensive studies demonstrated the presence of adaptations in cellular protein phosphorylation and Ca^{2+} handling, consistent with an adaptive functional response (Ch. 3 and Ch. 4). Although several potential target proteins were investigated here, additional proteins should be examined in the future. Interestingly, I also found different phospho-mimetic substitutions produced specific adaptations within cardiac myocytes (Ch.4). For example, cTnISer43/45Asp enhanced phosphorylation of cTnISer23/24 and cMyBP-CSer282 while cTnIAsp$_{Quad}$ increased

phosphorylation at cTnIThr144, cMyBP-CSer273 and cMyBP-CSer282. As discussed in chapter 4, these adaptive differences may be due to the distribution of the adaptive response along the myofilament and/or to phosphorylation turnover within an individual protein. The preliminary evidence suggests PKD targeting to cTnISer23/24 is up-regulated while phosphatase activity is diminished in myocytes expressing Asp substitutions at cTnISer43/45 (Ch. 3). In addition, the specific compensatory response observed with cTnISer43/45Asp compared to $cTnIAsp_{Quad}$, along with some *in vivo* data, suggests there may be an organized layering to the adaptive response. This organized layering could be spatially or temporally regulated and/or dependent on other environmental factors. Further work will be necessary to identify the signaling pathways and mechanism responsible for the adaptive responses.

Additional modifications within cTnI and cMyBP-C cannot be precluded from contributing to the adaptive response. Within cTnI, 14 residues, including 6 novel sites, have been identified by improved mass spectroscopy techniques (Table 5.1)[27]. Many of the novel sites identified are located in the N and C terminal domains of cTnI and could be important for coordinating the influence of cTnISer43/45 on either Ca^{2+} binding or cross-bridge dissociation. For example, the AMP-activated protein kinase (AMPK)-targeted residue cTnISer150 produces a leftward shift in myofilament Ca^{2+} sensitivity, which may counter the slowed Ca^{2+} binding to TnC with cTnISer43/45Asp substitutions (Ch.3 and Ch.4) [132]. Additionally, 14 candidate sites phosphorylated by AGC and/or Ca^{2+}/Calmodulin-dependent (CaMK) kinases were identified as *in vivo* targets for rat cMyBP-C, and many are located in the functionally relevant N-terminus (Table 5.1)[125, 133]. However, analysis of site-specific phosphorylation at these residues is limited by a lack of commercially available phospho-antibodies. Overall, it will be critical to identify the signaling pathways responsible for mediating phosphorylation at each of the sites

targeted during the adaptive signaling response. Eventually, studies to investigate adaptive signaling *in vivo* will be needed after a more comprehensive understanding of the adaptations, signaling pathways and conditions contributing to compensation is achieved in a less complex model, such as the cardiac myocyte.

Dynamic signaling is likely not limited to the changes identified in cTnI and cMyBP-C in the present study. Multiple sarcomeric and Ca^{2+} handling proteins are phosphorylated by the AGC and CaMK families of kinases, and work to modulate contractile function and Ca^{2+} cycling (Table 5.1, Fig. 5.2)[134]. For example, myosin light chain (MLC) phosphorylation in the thick filament accelerates cross-bridge detachment from the myofilament and could counteract the slowed cross-bridge detachment proposed to explain results with cTnISer43/45Asp [15]. Alternatively, phosphorylation at troponin T (TnT) may be elevated in myocytes expressing $cTnIAsp_{Quad}$. Augmented cTnT diminishes cross-bridge cycling, mitigating the probability phosphorylation increases when cTnISer43/45Asp is expressed [135]. However, increased TnT phosphorylation also could counteract the accelerated TTP at day 2 in myocytes expressing $cTnIAsp_{Quad}$ (Ch. 4). Moreover, augmented PLB phosphorylation can contribute to the accelerated Ca^{2+} decay in these studies, but the lack of statistical significance indicates other Ca^{2+} handling proteins may also be involved in the adaptive response. Increased expression of the Na^{+}-Ca^{2+} exchanger (NCX) and enhanced Ca^{2+} expulsion from the cytosol is also possible, but further work is necessary to confirm this hypothesis [136, 137].

The current studies also indicate it will be important to identify the kinases and phosphatases contributing to the adaptive response. Myofilament phosphorylation is coordinated by a large regulatory network, and multiple Ser/Thr kinases phosphorylate cTnI (Figs. 5.2A-C). Preliminary experiments addressed potential mechanisms underlying adaptive cTnISer23/24

phosphorylation (Ch. 3). Protein kinase A (PKA), activated via β-AR signaling, phosphorylates cTnI (Ser23/24), cMyBP-C (Ser273, Ser282, and Ser302), and PLB (Ser16) [5, 32, 104, 113, 138]. I investigated whether phospho-mimetic substitution at cTnISer43/45 enhanced PKA-mediated phosphorylation at cTnISer23/24, but PKA inhibition in preliminary work did not mitigate the adaptive cTnISer23/24 phosphorylation (Fig. 3.10). PKA also inhibits protein phosphatase 1 (PP1) activity and could increase cTnI phosphorylation via this indirect mechanism (Fig. 5.2A) [5]. However, other kinases could contribute to this adaptive response.

Recently, PKD emerged as an important mediator of stress-activated signaling in cardiac myocytes and is capable of phosphorylating cTnISer23/24 and cMyBP-CSer302 (Fig. 5.2C) [93, 139] [94, 111, 140]. Preliminary analysis showed protein kinase D (PKD) inhibition also partially restored cTnISer23/24 phosphorylation to control levels with increased cTnISer43/45 phospho-mimetic replacement (Figs. 3.7, 3.10). Moreover, the preliminary work is consistent with PKD activating a phosphatase, as phosphorylation at cTnISer23/24 increased in all groups following PKD inhibition (Fig. 3.10). Currently, PKD-mediated regulation of phosphatase activity has not yet been reported in a cardiac myocyte [5, 141]. Direct and indirect modulation by PKD suggests this kinase may participate in bifurcated signaling, whereby a single stimulus activates kinase and phosphatase activity which serves to amplify a signal [114, 120, 121]. A bifurcated mechanism would explain altered phosphorylation at both cTnISer23/24 and cMyBP-CSer273/282, since these cMyBP-C residues are not directly phosphorylated by PKD [93, 94, 114]. Alternatively, protein kinase G (PKG), a cyclic-GMP activated kinase, also phosphorylates (cTnI Ser23/24) and cMyBP-C (Ser273) in response to oxidative stress [95, 96] [142-144](Table 5.1; Figure 5.2C). PKG may play a prominent role in the adaptive response observed in the

current studies, but further work with pharmacological inhibitors are needed to confirm this hypothesis [95, 96].

Protein kinase C (PKC) is another possible kinase which could play a critical role in modulating cTnI and cMyBP-C phosphorylation, but the role of this kinase was not experimentally addressed here. Classical and novel PKCs are the primary isoforms present in the heart, and the activity of these isoforms is up-regulated during cardiac dysfunction [57, 58] [56, 65]. The novel class kinases are thought to directly phosphorylate myofilament proteins, including both cTnI and cMyBP-C (Fig. 5.2B) [56-58] [60, 61, 145]. Both *in vitro* and *in vivo* studies show novel class PKCs phosphorylate cTnI Ser43/45 and Thr144, with PKCδ favoring cTnISer23/24, as well as cMyBP-C at Ser273 and Ser302 [60] [59, 61, 146] [147, 148]. Conversely, classical PKC isoforms coordinate kinase/phosphatase targeting to the myofilament and do not necessarily execute their functional effects via direct phosphorylation of myofilament targets. Instead, they are proposed to function as a mini-processor to modulate multiple pathways within a cardiac myocyte (Fig. 5.2B) [50] [102, 114, 141, 149, 150]. Hwang ***et al.*** proposed $PKC\beta_{II}$ activates a bifurcative pathway by simultaneously activating PKD and phosphatases [114, 141]. Aside from the ability of PKA to target sarcomeric proteins and reduce phosphatase activity, the contribution of other kinases to the complex phosphorylation pattern observed with cTnISer43/45 phospho-mimetic expression is not yet determined. However, amplification of the adaptive signal by a "processor" kinase such as PKC could work to produce a sustained adaptive response. If so, this pathway could provide the basis for a central mechanism underlying the adaptive signaling identified in the present studies.

In the present model, enhanced cTnISer23/24 phosphorylation was predicted to result from increased kinase activity (Fig. 3.7). However, preliminary analysis utilizing the

phosphatase inhibitor calyculin A (Cal A) indicated phosphatase activity may be reduced in myocytes expressing cTnISer43/45 substitutions (Fig. 3.10). Cyclic regulation, or turnover, of phosphorylation is as equally important for normal cardiac function as the phosphorylation state. Phosphatases serve as a critical regulatory mechanism to produce phosphorylation turnover (Fig. 5.2) [114, 121]. In the heart, the Ser/Thr phosphatase protein phosphatase 1 (PP1) and protein phosphatase 2A (PP2A) are active and target a large array of cardiac proteins [5, 128, 129]. Three isoforms of PP1's catalytic subunit are expressed in cardiac tissue including PP1α, PP1β/δ, and PP1γ, and the catalytic subunit associates with a diverse network of regulatory subunits to provide either substrate specificity or regulation of enzyme activity [129]. One well characterized regulatory protein for PP1 is inhibitor-1 (I-1), and its post-translational modification by both kinases and phosphatases regulate the ability of I-1 to inhibit PP1 activity [5, 129]. PKA-mediated phosphorylation at Ser35 on I-1 causes increased association between I-1 and PP1, and reduces phosphatase activity in order to maintain the positive inotropic response induced by PKA activation. Conversely, PKCα phosphorylates I-1 at Ser67, which inhibits I-1 interactions with PP1, and results in elevated phosphatase activity [5, 141].

Protein phosphatase 2A also targets many myofilament proteins including cTnI, and *in vitro* phosphorylation assays indicate PP2A uniformly dephosphorylates the protein [151]. Unlike PP1, PP2A forms a heterotrimeric protein consisting of a catalytic subunit (PP2A-C) dimerized with a scaffolding subunit (PP2A-A), but not an inhibitory subunit [128, 129]. Instead, phosphorylation at tyrosine 307 (Tyr307) on the catalytic subunit inactivates the phosphatase [128, 151]. In contrast, increased methylation at leucine 309 (Leu309) in the catalytic subunit actives PP2A, which enhances heterotrimer formation with a scaffolding subunit [128] [152]. There are 4 families of regulatory proteins, and many function within the heart, although their

expression is species and chamber-specific [128, 129]. Among these regulatory subunits, B56α directs PP2A targeting to myofilament proteins [128, 129, 151, 153]. Collectively, the data shows increased replacement at cTnISer43/45 with Asp substitutions produces adaptive signaling with preliminary indication there may be increased kinase and reduced phosphatase activity. However, additional studies are needed to obtain adequate statistical power. This work also did not directly address the underlying mechanism for the altered kinase/phosphatase balance. Further studies are necessary to determine whether a similar change in kinase and phosphatase activity is produced by cTnIAsp$_{Quad}$. Moreover, it will be important to determine if the adaptive response originates from a structural change within cTnI or a reduction in phosphorylation turnover introduced by a phospho-mimetic substitution.

The cTnIAsp$_{Quad}$ and cTnISer43/45Asp constructs were expected to produce functionally similar outcomes due to the adaptive cTnISer23/24 phosphorylation arising from extensive cTnISer43/45Asp expression. However, the individual responses produced by the two constructs suggest there are different mechanisms contributing to the overall function response, which could be attributed to differences within a single cTnI versus across the myofilament and/or to a loss of phosphorylation turnover at cTnISer23/24 (Ch. 4). While the current work is unable to distinguish between these possibilities, the results provide evidence for a multi-layered signaling mechanism utilizing a distinct pattern of local, regional and/or distal adaptive responses. When one component of the signaling pathway is removed, the pathway is able to modify other protein targets to maintain cellular function. For example, when cTnISer23/24 is no longer available for phosphorylation in cTnIAsp$_{Quad}$, phosphorylation increases in other local and regional targets, such as cTnIThr144 and cMyBP-C, while decreasing at more distal targets, such as PLB. Changes in kinase and phosphatase distribution throughout the cell may underlie this change.

Movement of a phosphatase away from the myofilament and towards PLB would explain the phosphorylation pattern produced by cTnIAsp$_{Quad}$. Conversely, a kinase may be recruited to cTnI and cMyBP-C to enhance phosphorylation at a target residue, such as cTnIThr144.

Physiological and pathophysiological role of cTnISer43/45 on contractile function

The distinct phosphorylation pattern produced by the cTnI phospho-mimetics indicates there are specific signaling mechanisms in play to respond to changes in the cellular environment, which may be mediated via both spatial and temporal regulation. For example, localization of signaling components could change in response to neurohormonal input to the cell. In agreement with this prediction, the PP2A regulatory protein B56α moved away from the myofilament in ventricular myocytes following treatment with the PKA agonist isoproterenol. The same protein remained associated with the myofilament after treatment with the PKC-agonist ET-1 [154]. This spatio-temporal localization also may be important during the progression of heart failure. Global phosphatase activity increases in end-stage heart failure, and more recent work suggested enhanced activity may be localized to specific subdomains within the cell [129, 153] [5, 127]. Additionally, temporal regulation of signaling also appears to be important for responding to cellular changes. In the heart, up-regulation of PKA develops during the early stages of cardiac stress, and as cardiac dysfunction progresses, PKA activity is reduced and phosphatase activity increases [5, 32, 124, 127, 153]. The present studies suggest adaptive signaling is an important part of maintaining physiological function in the heart. Signaling adaptations are modulated by environmental factors, such as the physiological state of the heart, and loss of adaptive modulation is expected to accelerate the transition to heart failure. Therefore, dissecting out the precise signaling mechanism(s) contributing to the adaptive

response in cellular and *in vivo* models is essential for identifying the role adaptive signaling plays in both cardiac physiology and pathophysiology.

A significant portion of the current work focused on the ability of cTnISer43 and cTnISer45 to act as a modulatory brake on cardiac function. However, changes in the myocardium during cardiac stress may alter compensatory signaling so cTnISer43/45 phosphorylation becomes maladaptive. In a healthy heart, the ability of cTnISer43/45 to function as a brake is postulated to be important for short-term regulation (e.g. beat to beat; Fig.5.3A). Sudden changes in hemodynamic load could activate PKC signaling [155, 156]. Transiently, increased PKC activity is predicted to directly target the myofilament, and phosphorylate proteins, such as cTnISer43/45, to reduce ATPase activity, unloaded shortening velocity and pressure development in an effort to preserve cardiac energy stores and/or reduce arterial pressure [51, 64, 68, 73, 74, 114]. The resulting reduction in myocyte contraction could shorten the ejection phase of the cell cycle to reduce stroke volume, decrease cardiac output, and restore arterial pressure back toward previous steady-state levels [1]. Short-term functional regulation by cTnISer43/45 phosphorylation is not expected to stimulate adaptive signaling, but neurohormonal inputs released by mechanical stretch and sustained hypertension, such as angiotensin II, could activate multiple signaling pathways, including PKC, to produce a different response [155, 157]. The data are consistent with adaptive signaling playing a more prominent role during chronic cTnISer43/45 phosphorylation, which could develop during compensated cardiac dysfunction.

The effects of cTnISer43Asp/Ser45Asp on contractile function closely match the cellular alterations produced by short-term acidosis, an early and critical element of myocardial ischemia [9, 158 372]. Therefore, it is reasonable the observations made in the present study could

provide insight into the mechanism activated during an early, compensatory stage of cardiac dysfunction (Fig.5.3B) [9, 158 372]. Chronic β-AR signaling in the heart helps maintain cardiac pump function in the compensatory state [32] [124]. While this response may be initially beneficial for preserving contractile function, it depletes cardiac ATP levels [47, 159] [79]. As in healthy hearts, increased cTnISer43/45 phosphorylation could act as a brake to reduce the enhanced cross-bridge cycling produced by β-AR activation in an effort to preserve cardiac energy stores (Ch. 3 and Ch. 4) [159, 160] [79]. Increased cTnISer43/45 phosphorylation is expected to reduce cardiac ejection of blood, but the data also suggest the adaptive increases in cTnI, cMyBP-C, and PLB phosphorylation observed with cTnISer43/45Asp and in acidotic hearts are part of a compensatory signaling mechanism designed to maintain systolic and diastolic function [79, 158, 159].

Over time, metabolic demands may compete against and dominate over these adaptive, compensatory responses. At this transition point, the heart progresses into decompensatory heart failure characterized by diminished force production and contractile function (Fig. 5.3C) [122, 124]. PKC expression and activity are persistently elevated in failing hearts while PKA activity decreases during end-stage heart failure [5, 30, 56, 65]. In addition, PKD and PKG are known stress-activated kinases which may further contribute to the transition into a decompensatory state [142, 161]. Dysregulation of phosphatase activity also is gaining recognition as a prominent contributor to the development of heart failure [5, 127-129, 153]. Increased phosphatase activity could result from sustained activation by classical PKC isoforms and/or other kinases along with a loss in PP1 inactivation by PKA (Ch.3) [5, 127, 141]. However, PP2A activity is reduced in failing hearts with ischemic cardiomyopathy, supporting the idea specific environmental factors may produce spatio-temporal differences in the overall phosphorylation state [128]. Indeed,

samples from patients in end-stage heart failure exhibit increased phosphatase activity and reductions in both cTnI and cMyBP-C phosphorylation [125-128, 153]. However, cTnISer43/45 phosphorylation remains elevated in human and animal models of heart failure [27, 30, 31] [65]. Based on the present findings, the loss of phosphorylation turnover at cTnISer43/45 may eliminate the ability of this cluster to function as a modulatory brake, and could eventually contribute to contractile dysfunction if and when adaptive mechanisms are lost and/or no longer functional. Thus, loss of signaling modulation within the heart could result in cTnISer43/45 phosphorylation-mediated reductions in both systolic and diastolic dysfunction, which would accelerate the progression to end-stage heart failure [49, 62] [24, 42, 68, 105].

Current *in vivo* models of PKC-mediated cTnI phosphorylation highlight the importance of maintaining the balance between kinase and phosphatase activity. In addition, disruption of this balance is expected to impact the phenotypes observed in animal models with phospho-mimetic substitutions at the PKC sites. Mice expressing $cTnI_{PKC\text{-}P}$ exhibited compromised systolic function and diastolic function, similar to those anticipated in end-stage heart failure [62]. These results are puzzling given the severe cardiac phenotype observed with minimal expression and the lack of compensatory adaptations detected in this mouse. In contrast to the $cTnI_{PKC\text{-}P}$ mouse, the preservation of peak pressure in the $cTnI_{AllP}$ mouse suggests compensatory adaptations are present in this model [49]. Future work is needed to identify the role adaptive signaling plays in producing the phenotypic differences between the $cTnI_{PKC\text{-}P}$ and $cTnI_{AllP}$ mouse models, though compensatory signaling was not detected in $cTnI_{AllP}$ mice [49]. However, Ca^{2+} handling and cMyBP-C phosphorylation were not evaluated in the $cTnI_{AllP}$ model, and treatment with the PKA agonist, dobutamine, produced a heightened acceleration of relaxation, arguing for the presence of adaptive signaling in these mice [49]. Loss of cTnISer23/24

phosphorylation turnover and altered adaptive signaling in the $cTnI_{AllP}$ model could mean this mouse is more susceptible to heart failure in response to stressors such as myocardial ischemia and/or hypertension. Future work is necessary to determine whether this idea is correct.

FUTURE DIRECTIONS

Chemical properties and substitutions at cTnISer43/45 influence contractile function

The cTnISer43/45Ala results indicate future work is needed to gain insight into the key interactions between Ser43/45 and other residues within cTnI and/or cTnC, their influence on thin filament function under basal conditions and their influence in response to PKC activation. Ala replacement at cTnISer43/45 is predicted to disrupt polar interactions with TnC and cause the functional changes observed with cTnISer43/45Ala expression. Thus, gene transfer of cTnI containing a more polar residue such as asparagine (Asn) should either produce no change and/or the opposite influence on function compared to Ala. At the biophysical level, studies with FRET-labeled cTnC also are needed to evaluate the impact of cTnISer43/45 Ala versus Asn substitutions on ionic interactions between cTnI and the N- and C-lobes of cTnC in reconstituted myofilaments. Another focus for molecular studies would include efforts to distinguish between cTnISer43 versus cTnISer45 phosphorylation during PKC activation. Currently, it is often difficult to distinguish between these residues by mass spectrometry, and efforts to generate phospho-specific antibodies by a number of investigators have been unsuccessful [30] [27, 162]. The cTnISer43 site conforms to the most popular consensus sequence for phosphorylation by PKC while the sequences flanking cTnISer45 form a less recognized motif [163]. The identification of the most likely residue targeted for phosphorylation will require continued improvements and advances in mass spectrometry approaches. The knowledge gained from the proposed biophysical and cellular studies is expected to be important for the development of small molecule therapeutics if *in vivo* work proposed later in this chapter demonstrates cTnISer43/45 phosphorylation plays a significant role in producing contractile dysfunction during heart failure.

The controversies arising from studies performed with the $cTnIAla_5^{nb}$ mouse point to the need for additional work in this animal model. Studies are needed to determine *in vivo* cardiac function, the nature of adaptive signaling, and the progression to heart failure produced by expression of $cTnIAla_5^{nb}$. Results from this work could lead to studies focused on gaining further insight into adaptive signaling patterns and determining if $cTnIAla_5^{nb}$ hearts are more susceptible to heart failure induced by other environmental stressors such as myocardial ischemia and/or hypertension. In addition, cellular gene transfer studies with the same construct should mimic the responses observed in myocytes from the genetic animal model. Direct versus adaptive influences of $cTnIAla_5^{nb}$ on function could be uncovered in the event divergent outcomes are observed between cellular and *in vivo* studies.

Direct role of cTnISer43/45 in the modulation of contractile function

Important gaps remain in our understanding of cTnI inter-domain interactions and cTnC/cTnT interactions with the region around cTnISer43/45. Understanding the molecular structural changes within cTnI and neighboring Tn subunits will be important to investigate using substitutions at cTnISer43 and cTnISer45, which produce diverse functional responses. Further work utilizing molecular modeling techniques and biochemical approaches also is necessary to predict potential residue contacts between cTnISer43/45 and additional cTn subunits [25, 119]. Less is known about the molecular contacts between cTnISer43 and other cTn domains, and molecular modeling could help to predict the most likely proximal residues for interaction within the cTn core. Additional modeling also could predict how interactions could modify the response to cTnISer43 phosphorylation. The relevance of the predicted interactions should then be evaluated using biochemical approaches such as actomyosin MgATPase activity and FRET-measurements of Ca^{2+} association/ dissociation with cTnC [42, 67, 70, 105].

Phosphorylation at cTnISer43Asp also could increase IT arm rigidity and diminish interactions with TnC, reducing both MgATPase activity and Ca^{2+}association with TnC. These molecular approaches are less complex and more efficient for testing prior to the transition to cellular or *in vivo* models. However, the increased phosphorylation of cTnISer43/45 under pathological conditions indicates these ideas also need further analysis in more complex models.

Adaptive signaling by cTnISer43/45 substitutions

My results also demonstrate changes within the cTnI backbone can modify function and adaptive signaling in response to amino acid substitutions at cTnISer43/45 with and without substitutions at cTnISer23/24 (e.g. $cTnIAsp_{Quad}$ vs. cTnISer43/45Asp). However, the influence of structural positioning on function caused by multi-residue replacement within cTnI or the loss of turnover at cTnISer23/24 has led to controversies. Previous molecular modeling studies revealed the cTnI-specific, N-terminal extension interacts with the N-lobe of TnC, and this interaction is reduced by phosphorylation or phospho-mimetic substitution at Ser23/24 [117] [118]. Phosphorylation at cTnISer43/45 is predicted to increase I-T arm rigidity, and the combined Ser23/24 modification in the same cTnI (e.g. $cTnIAsp_{Quad}$) may target multiple molecular changes within cTn as well as kinase and phosphatase targeting of residues within a single cTnI. Conformation changes along the myofilament also could contribute to altered kinase and phosphatase activity throughout the sarcomere and/or could amplify the functional and signaling responses caused by the structural changes induced by cTnISer23/24 and cTnISer43/45 modifications. Molecular modeling techniques, especially 3D reconstruction, along with biochemical studies will be important approaches needed to study and prove this idea [164]. Moreover, modeling the interaction between the N-terminal domain of cTnI and kinases and/or phosphatases via molecular dynamics could allow a more accurate prediction signaling

components which interact with Tn. Immunoprecipitation, *in vitro* binding assays, and myofilament FRET assays to evaluate Ca^{2+} binding are relevant approaches for confirming the modeling results. These approaches also may help identify additional molecular players contributing to compensatory signaling as well as the structural alterations responsible for modulating cellular communication.

The mechanism underlying individual adaptive responses produced by cTnISer43/45Asp compared to $cTnIAsp_{Quad}$ could also be addressed in physiologically relevant cellular and animal models. If the adaptive response is modulated by negative charge distribution along the myofilament, dual gene transfer of cTnISer23/24Asp and cTnISer43/45Asp cTnI constructs into isolated cardiac myocytes should produce a functional response similar to cTnISer43/45Asp (e.g. increased cMyBP-CSer282). However, if loss of phosphorylation turnover determines the adaptive response, the adaptations and function measured in these myocytes is expected to resemble the functional response produced by $cTnIAsp_{Quad}$ (e.g. enhanced cTnIThr144 and cMyBP-CSer302 phosphorylation). Phosphatase inhibition with Cal A also would be a direct approach for identifying the role of altered phosphorylation turnover. An additional approach, such as siRNA-mediated inhibition of a specific phosphatase, could be used to identify the precise cellular components participating in the adaptive response. A set of *in vivo* experiments should also be performed to determine whether loss of functional modulation at specific PKC-targeted residues within cTnI changes compensatory phosphorylation and/or if global disruption of phosphorylation turnover is sufficient to produce this response. In addition, a comparison of adaptations observed in the $cTnI_{PP}$ and $cTnI_{AllP}$ mice could further address the importance cTnISer43/45 phosphorylation in stimulating compensatory signaling *in vivo*. Dynamic modulation of myofilament phosphorylation is a requirement for maintaining normal

physiological function. Significant alterations to cTnISer23/24 phosphorylation and kinase/phosphates activity occur during cardiac stress, and the proposed experiments in animal models could identify therapeutic targets to prevent or ameliorate the progression to cardiac dysfunction [27, 56, 65, 127] [29, 31].

Though preliminary studies provided some candidate signaling components important in the cTnISer43/45Asp-induced adaptation, further clarification of the kinases and phosphatases is necessary to gain mechanistic insight. The putative alterations in kinase/phosphatase activity in response to cTnISer43/45 phospho-mimetic replacement are illustrated in the lower panel of Fig. 5.4. Based on preliminary studies, increased PKD activity and diminished phosphatase activation are expected to result in the observed augmentation of cTnISer23/24 phosphorylation with cTnISer43 and/or cTnISer45 containing Asp substitutions (Fig. 5.4). However, the inability of PKD inhibition to completely restore cTnISer23/24 phosphorylation to control levels warrants additional investigation into the role of other kinases, such as PKG and PKC. The use of dual gene transfer of a dominant negative PKC isoform with cTnISer43Asp and/or cTnISer45Asp into isolated myocytes is one potential approach. Based on previous work, this approach will require extensive controls to demonstrate the expression and activation of other PKC isoforms are not influenced by this change [102]. If PKC directly targets cTnISer23/24 in myocytes expressing these Asp substituted cTnIs and dominant negative PKC, reduced phosphorylation is expected, which could be detected by Western blot. Alternatively, PKC could modulate a phosphatase, and PKC inhibition would reduce phosphatase activity, resulting in enhanced cTnISer23/24 phosphorylation. Another candidate kinase is protein kinase G (PKG), which is activated in response to oxidative stress and nitric oxide production in the heart [142] [95, 96]. Myocytes could be treated with a commercially available PKG inhibitor, KT5823, prior to evaluating the

phosphorylation level of target residues with site-specific phospho-antibodies via Western blot. Cells treated with individual inhibitors targeting a range of kinases also could be used to determine whether these kinases participate in the adaptive response. For example, treatment with the PKC inhibitor bisindolylmalemide (Bis-I) or kb-Nb-142-70 (PKD) could each attenuate adaptive cTnISer23/24 phosphorylation if PKC is working upstream of PKD. However, if both inhibitors need to be added together to obtain restoration of cTnISer23/24 phosphorylation to control values, it would indicate the target kinases are working through separate signaling pathways. Because PKC, PKD, and PKG also are associated with a cardiac dysfunction, this work may provide insight into whether a specific stress signal works through a single pathway or if multiple signaling cascades can be activated by an individual change within the myofilament.

The present studies investigating the adaptive communication pathway fail to identify the phosphatase contributing to cellular communication (Fig. 5.4). Further studies will be needed to investigate if PP2A activity is reduced by phospho-mimetic replacement in cTnI. PP2A is inactivated in ischemic human heart failure suggesting PP2A is important for regulating cardiac function [128]. Western blot analysis using site-specific antibodies for methylation of the activation site Leu309 and phosphorylation of the deactivation site Tyr307 could be used to monitor phosphatase activation states [128]. If cTnISer43/45 replacement diminishes phosphatase activity, Tyr307 phosphorylation should increase and/or Leu309 methylation should decrease [128]. Co-immunoprecipitation assays employing PP2A-specific antibodies can also be used to test whether cTnI phospho-mimetic replacement inhibits physical coupling between PP2A and the myofilament. Defining the contributions of kinase and phosphatase activity to the adaptive signaling response initiated by phospho-mimetic substitution at cTnISer43/45 and the potential for this signaling mechanism to be a common cellular response to other environmental

changes (e.g. cellular pH, energy availability, or reactive oxygen species) are expected to provide insight into the physiological importance of adaptive communication. In addition, studies focused on kinase/phosphatase may be able to determine whether this communication becomes altered during the process of cardiac dysfunction and/or end-stage heart failure. Insights into adaptive communication gained from cellular work are expected to be critical for identifying signaling components as therapeutic targets.

Acute Asp replacement at cTnISer23/24 and cTnISer43/45 generates compensatory Thr144 phosphorylation, and yet the modulatory role of Thr144 *in silico*, in isolated myocytes and *in vivo* was not explored here. Molecular modeling could predict the effects of Thr144 phosphorylation on cTn structure. If the increased phosphorylation at cTnISer43/45 exerts its functional effects through rotation of the I-T arm, there should be evidence to show cTnT and/or Tm hold the myofilament in the blocked state. Increased phosphorylation at cTnIThr144 could alternatively influence myofilament activation by modulating the position and/or anchoring of the cTnI H4 helix and/or carboxy-terminal mobile domain on the actin filament to effect the cTn-Tm position. Maximum MgATPase activity assays in reconstituted thin filaments using cTnIThr144Asp alone or in combination with cTnISer23/24Asp or cTnISer43/45Asp could be compared to the functional effects predicted by modeling. Additionally, the effects of Thr144 phosphorylation on Ca^{2+} binding to TnC should be evaluated due to the proximity of cTnIThr144 to the N-lobe of cTnC in the apo state [25]. A cTnIThr144Asp construct also could be utilized to evaluate the physiological effects of phosphorylation at this residue on sarcomere incorporation of cTnI and myofilament function. Studies in isolated myocytes using approaches similar to the ones utilized for the current work could be used for the initial studies. Based on cellular studies with the cTnIThr144Pro construct, increased replacement with Thr144Asp is expected to

accelerate re-lengthening without altering Ca^{2+} handling [78, 86]. A genetic mouse model with this substitution would provide insight into the more chronic effect of Asp replacement at cTnIThr144 on contractile function and allow the effects of cTnIThr144Asp on whole heart function to be evaluated. As in the cellular studies, relaxation is expected to be affected under basal conditions compared to non-transgenic controls. These studies will provide insight into the importance of cTnIThr144 phosphorylation in biophysical, cellular, and whole heart function.

Physiological and pathophysiological role of cTnISer43/45 on contractile function

The present results indicate adaptive signaling and/or phosphorylation turnover are important mechanisms for maintaining normal physiological function (Ch. 3 and Ch. 4). However, I did not explore whether the compensatory signaling mechanism identified in present study is a common response to environmental changes produced by cardiac stress, such as ischemia. To test whether the compensatory signaling mechanism identified in present study is a common response to cardiac stress, preliminary studies were performed in myocytes incubated with a transient acidosis similar to the pH change produced by acute myocardial ischemia after 30min (Fig. 5.5)[9, 158 372]. These studies indicate treatment with an ischemic mimetic restored phosphorylation in myocytes expressing cTnISer43/45 substitutions toward control values, similar to the effects of PKD and phosphatase inhibition (Fig. 5.5A, Ch.3). While these results provide evidence adaptive signaling is stimulated by a cellular acidosis stressor, myofilament protein phosphorylation patterns in human patients or in animal models of ischemic injury may be more complex than the results obtained in isolated cells due to divergent alterations in kinase and phosphatase activity which may be specific for the disease state (Fig. 5.5B) [27, 29-31, 153] [56, 128].

Therefore, it seems reasonable to address the response to ischemic injury in a genetic mouse model expressing cTnISer43/45Asp. Under basal conditions, cardiac morphometry, morphology, histochemistry, and function are not expected to differ from non-transgenic controls. Myocytes isolated from these hearts can be compared to the results from the gene-transfer studies presented in this body of work to determine whether additional compensatory mechanisms are present in the animal model. However, mice expressing cTnISer43/45Asp are expected to transition into end-stage heart failure more quickly than non-transgenic controls in response to cardiac injury, such as myocardial infarction. The reason for this prediction is the slowed cross-bridge cycling predicted for cTnISer43/45 phosphorylation becomes energetically unfavorable at an earlier time point. However, a compensatory period should be observed in cTnISer43/45Asp mice because cTnISer23/24 is still able to be modified. Alternatively, the adaptive phosphorylation occurring in these mice prior to injury may serve a protective role in response to cardiac stress similar to the effects of ischemic pre-conditioning [79, 159]. The more intriguing studies would involve comparing the effects of ischemia on cTnISer43/45Asp mouse model to the $cTnI_{AllP}$ mice [49]. Because cTnISer23/24 can no longer be adaptively phosphorylated in the $cTnI_{AllP}$ model, these mice are expected to have an even higher mortality rate in response to stress, such as MI. However, an improved response to myocardial ischemia and prolonged survival observed in $cTnI_{AllP}$ mice, this result would suggest the presence of a sustained negative charge at cTnISer23/24, cTnISer43/45, or cTnIThr144 is sufficient to maintain cardiac pump performance. In summary, the current experiments provided significant insight into the functional contribution and adaptive response produced by Ser43/45 phosphorylation in cTnI. These studies also provided ideas for future molecular, cellular and *in*

vivo studies to provide more insight and a greater understanding of the role played by post-translational modifications in the sarcomere.

Kinase	Troponin I	Troponin T	^cMyBP-C	MLC_2
AGC Family				
PKA	S23[34], S24[34], S40[168], S167[168], **S78**[27,37], **T79**[27,37], **T144**[27], **S151**[132], **T181**[27]*, T124, **T285**[162,170]	S69, **S181**[162,170], **T195**[162,170], S199[113], **T204**[162,170], S240	**S47**[125], **T56**[125], **S105**[125], S273[138], S282[138], **T290**[125], S302[138], **S307**[125], **S474**[133]	
PKC	S23[26], S24[26], S43[26], S45[26], S78[50], T144[26], **S40**[168], **T79**[37], **S167**[27], **T181**[27*]	T195[60], S199[60], T204[60], T276, T278, T285[60]	S302[147,148]	
PKG	S23[169], S24[169], **T79**[37], **S167**[27]	None identified		
ROCKII	S23[171], S24[171], T144[171]	S69, S276[171], T278[171]		
RSK1	S23[172], S24[172], **S78**[27,37]	None identified		
S6K	**S78**[27,37]	None identified		
CaMKII Family				
PKD	S23[93], S24[93], S198[93]	None identified	S302[139]	
AMPK	S23[173], S151[132]	None identified		
CaMKII	None identified	T195[174]	**S25**[125], **S47**[125], **T50**[125], **S105**[125], **S210**[125], S273[125], S282[125], **T290**[125], S302[125,177], S307[125], **S327**[125], **T380**[125], **S410**[125]	
PHK	S23[175], T79[175], T144[175], S167[175]	S2[176], S181[176]		
MLCK				S14[15,178]** S15[15,178]
ZIPK(DAPK3)				S15[179]

Table 5.1. Documented and predicted phosphorylation of rat Tn, cMyBP-C and MLC_2 by signaling kinases. Phosphorylation is predicted based on the presence of consensus phosphorylation motifs for each kinase. phosphorylation sites (S for Ser, T for Thr, Y for Tyr) targeted by each kinase are underlined. Sites known to be phosphorylated without proof the specified kinase targets this residue are shown in bold. Predicted, but non-verified sites (probability >0.50) are not bolded or underlined. Sites are consistently predicted by multiple tools including NetPhosK, Scansite, and NetPhorest [168-170].
^ **Note:** For cMyBP-C only, mouse numbering is used for phosphorylation sites. All other residues listed in the table are rat sequence. *T181 in human sequence, not present in rat sequence; **S14 only present in rodent MLC_2.
The references for this table include: [15, 26, 27, 35, 38, 51, 61, 94, 115, 127, 134, 135, 140, 141, 165, 171-182]

A.

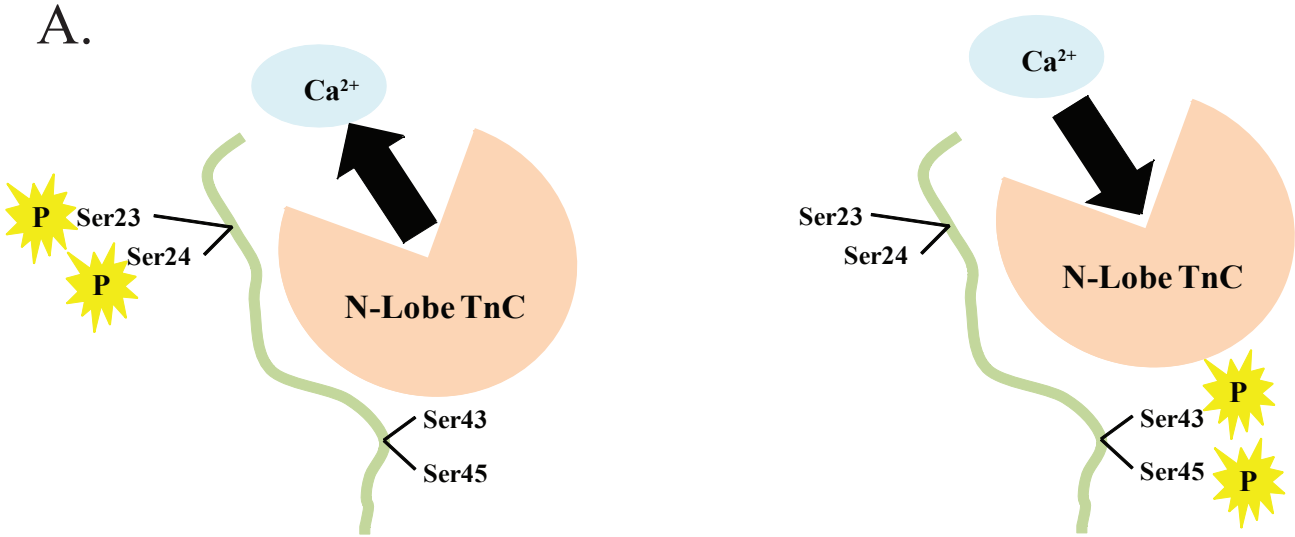

cTnISer23/24 Phosphorylation: Accelerated Ca^{2+} Dissociation

cTnISer43/45 Phosphorylation: Slowed Ca^{2+} Binding

B.

cTnISer43/45 Phosphorylation: Slowed Crossbridge Detachment

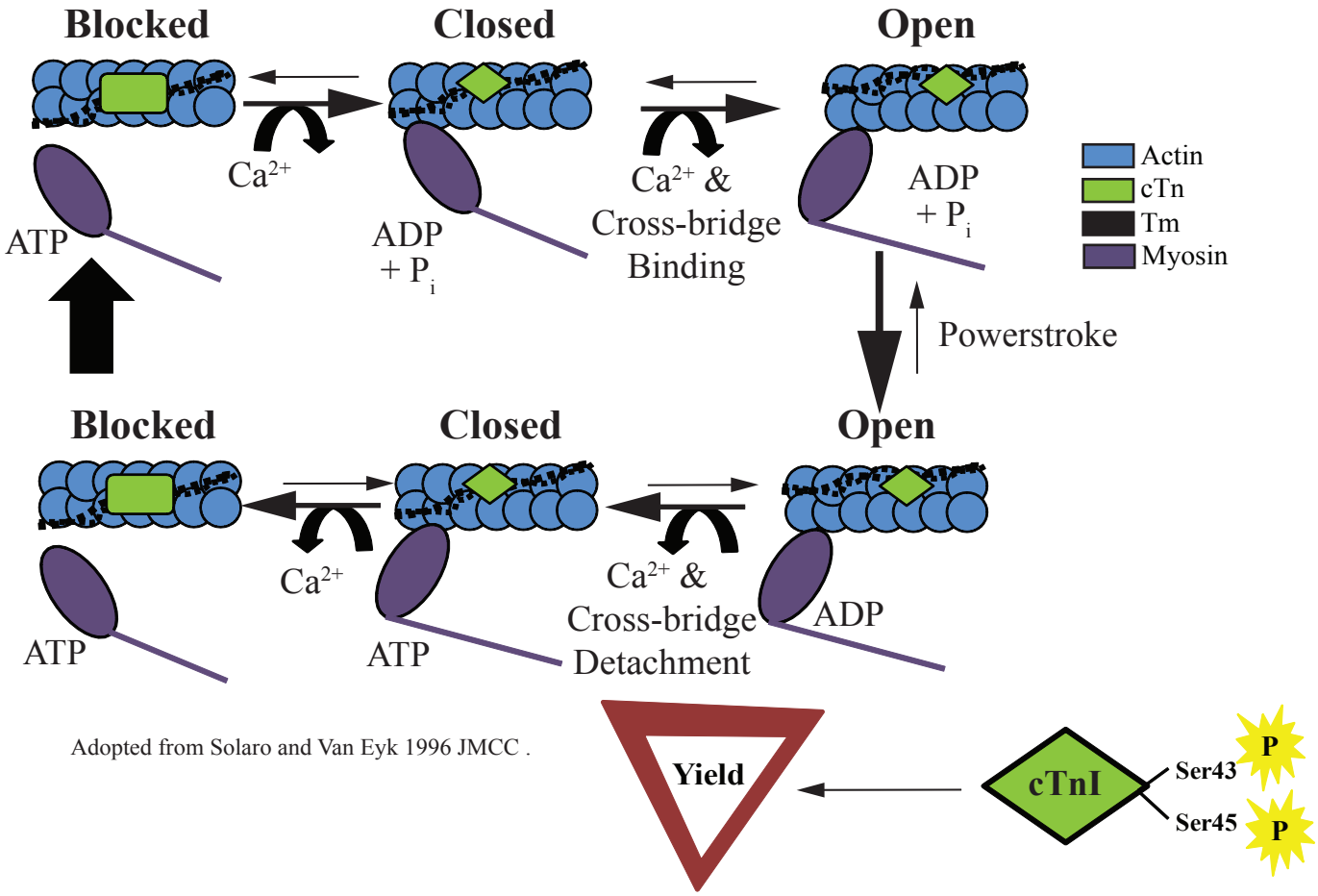

Adopted from Solaro and Van Eyk 1996 JMCC .

Fig. 5.1. Predicted mechanisms for contractile function modulation by cTnISer23/24 and cTnISer43/45 phosphorylation A. Illustration of Ca^{2+} (blue) association with troponin C (TnC; orange) after cTnI (green) phosphorylation (yellow) at cTnISer23/24 (left panel) and cTnISer43/45 (right panel). The N-lobe contains the regulatory Ca^{2+} binding site in TnC. The illustration of cTnI depicts the N-terminus (residues 1-32) and the beginning of the amino-terminal H1 helix residues (residues 33-50) to indicate the location of cTnISer23/24 and cTnISer43/45, respectively. Arrows in the figure show the direction of Ca^{2+} movement relative to the Ca^{2+} binding site within the N-lobe of TnC. Phosphorylation at cTnISer23/24 accelerates Ca^{2+} release while cTnISer43/45 phosphorylation is predicted to slow Ca^{2+} binding to TnC. **B.** Illustration of one cycle of interactions between thick and thin filaments during a single cross-bridge cycle. Components of the thick and thin filament are shown including the myosin cross-bridge (purple), actin (blue), troponin (green), and tropomyosin (black). In addition, the cycling and cleavage of ATP into ADP and P_i by the cross-bridge is shown for each step. Arrows between steps indicate the proposed transitions through each step of myofilament activation (Fig. 1.2C), as proposed for the 3-state model. A "yield" sign indicates a possible step in cross-bridge detachment from the thin filament which could be slowed by cTnISer43/45 phosphorylation and prevent the myofilament transition from an "open" to "closed" state.

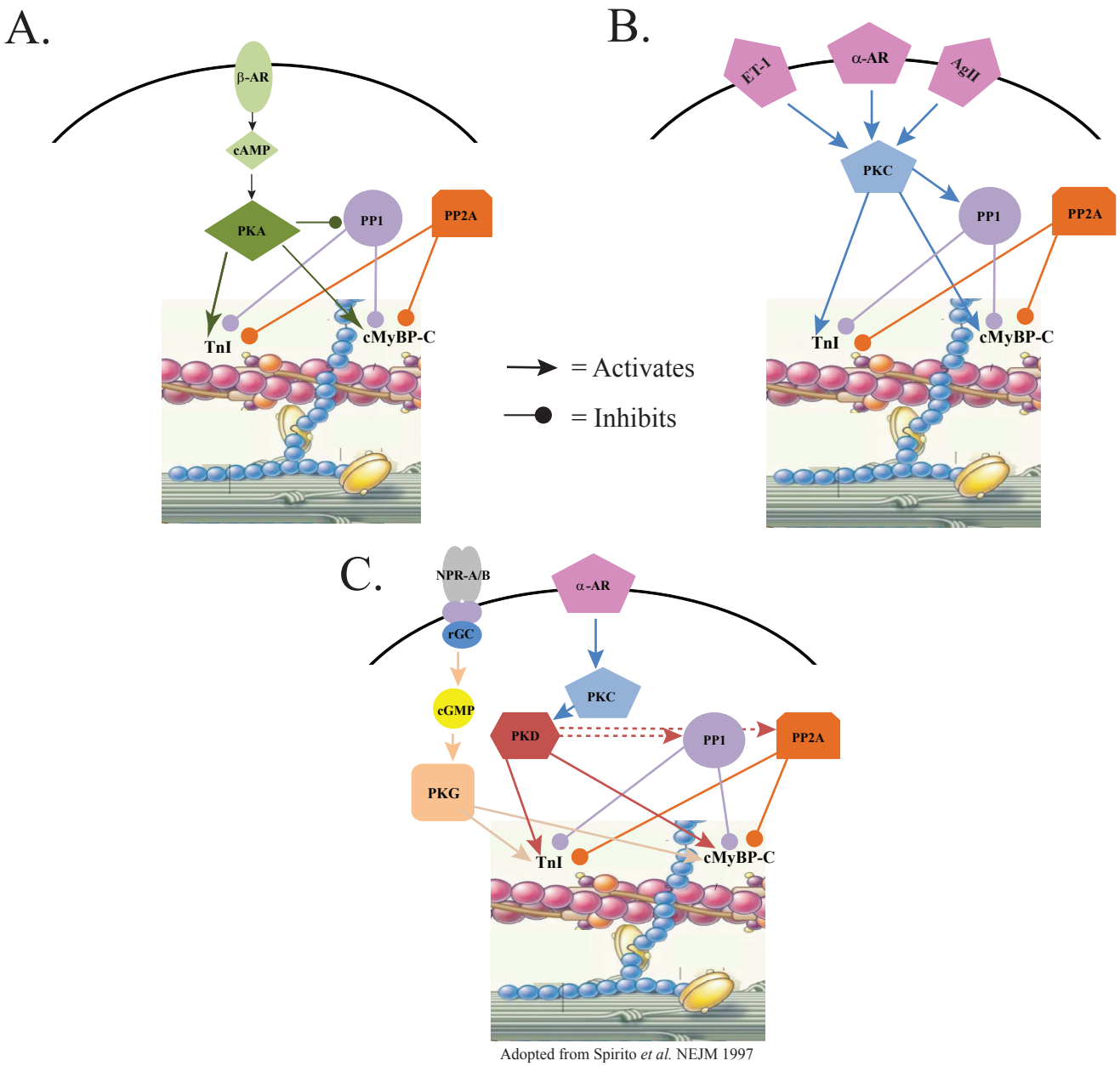

Fig. 5.2 Signaling cascades targeting sarcomeric cardiac troponin I (cTnI) and cardiac myosin binding protein C (cMyBP-C) A magnified portion of thick and thin filament proteins in the sarcomere is shown for each illustration. Signaling modulation targeting cTnI and cMyBP-C were chosen as representative proteins targeted by multiple kinases and phosphatases in myocytes. **A.** Illustration of β-adrenergic receptor (light green) activation of cAMP production (light green) and downstream PKA (dark green) activation, which targets cTnI and cMyBP-C for phosphorylation. PKA also inhibits PP1 (purple) activity, and both PP1 and PP2A (orange) are capable of de-phosphorylating cTnI and cMyBP-C. **B.** Illustration of the PKC signaling pathway. Multiple sarcolemmal receptors activate PKC, as indicated by the ET-1, α-adrenergic receptor (α-AR) and angiotensin II (AngII) receptors shown in pink. The activation of PKC directly and indirectly modulates cTnI and cMyBP-C phosphorylation by direct phosphorylation (blue arrows) and by activating PP1 (purple). **C.** Illustration of PKD (red) and PKG (peach)-mediated phosphorylation of cTnI and cMyBP-C. PKD can be directly activated by α-adrenergic receptor (α-AR) (pink) activation or activated by PKC (blue). Preliminary results indicate PKD may up-regulate phosphatase activity (dotted red) in myocytes expressing cTnISer43/45Asp. PKG (peach) is activated by the natriuretic peptide receptor A/B (NPR-A/B; grey/purple), which stimulates a receptor guanylate cyclase (rGC) to produce cGMP followed by PKG (peach arrows). PKG can directly target cTnI and cMyBP-C for phosphorylation (peach arrows).

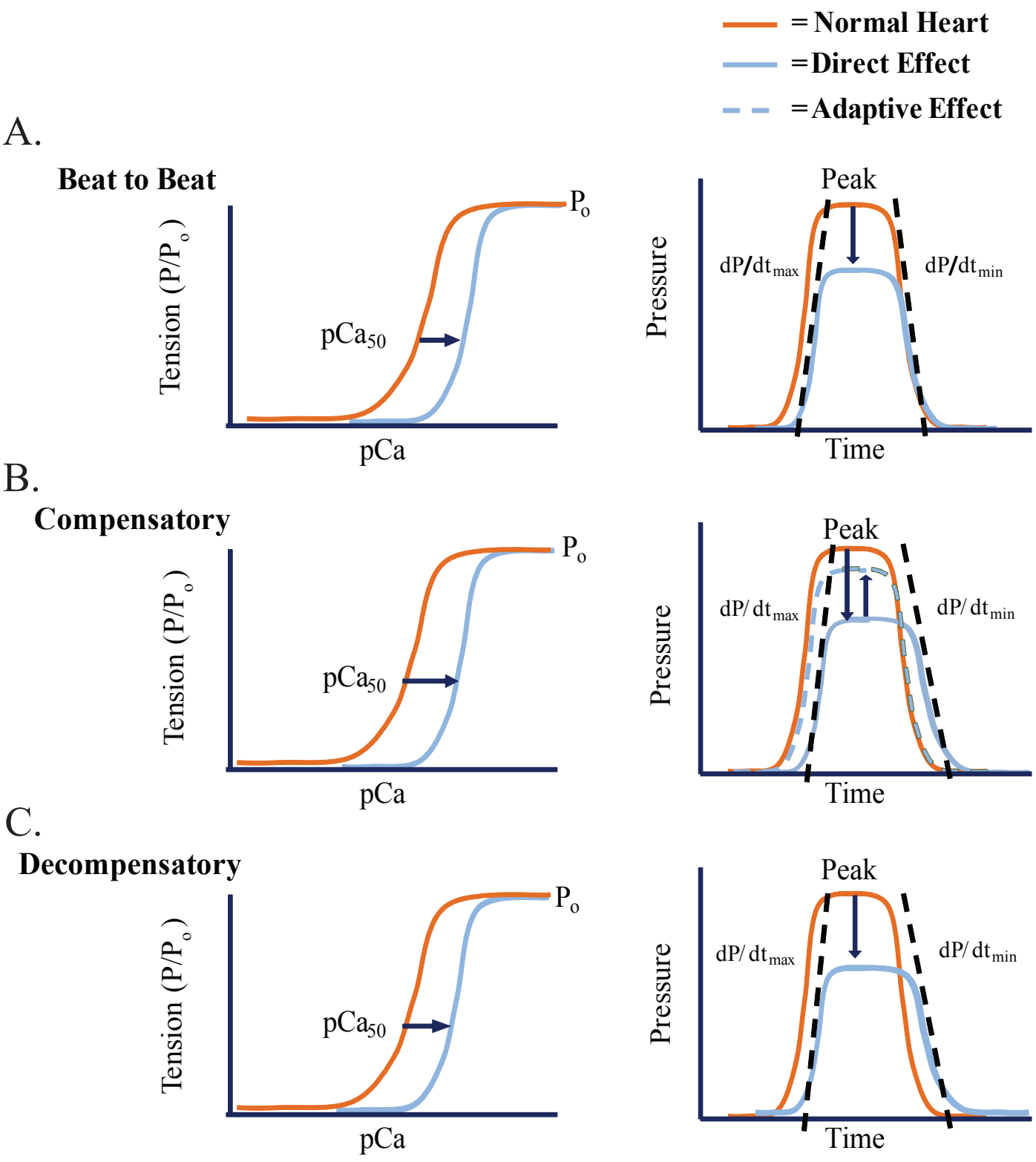

Fig. 5.3 Predicted physiological and pathophysiological effects of cTnISer43/45 phosphorylation. Predicted changes in tension generation in isolated myocytes (left) and pressure development of whole hearts (right) with increased cTnISer43/45 phosphorylation. Isometric tension (P) is measured over a range of Ca^{2+} concentrations (-log[Ca^{2+}] = pCa). The myofilament Ca^{2+} sensitivity (amount of Ca^{2+} required to generate 50% of the maximum tension [P_o]) and P_o are measured in permeabilized myocytes. Note: the adaptive response is not expected to influence tension measurements due to the loss of the cellular environment. Pressure is measured by *in vivo* hemodynamic measurements in the left ventricle over time. The rate of systolic pressure development (dP/dt_{max}), relaxation rate (dP/dt_{min}), and peak pressure (P_o) are included in the pressure trace.

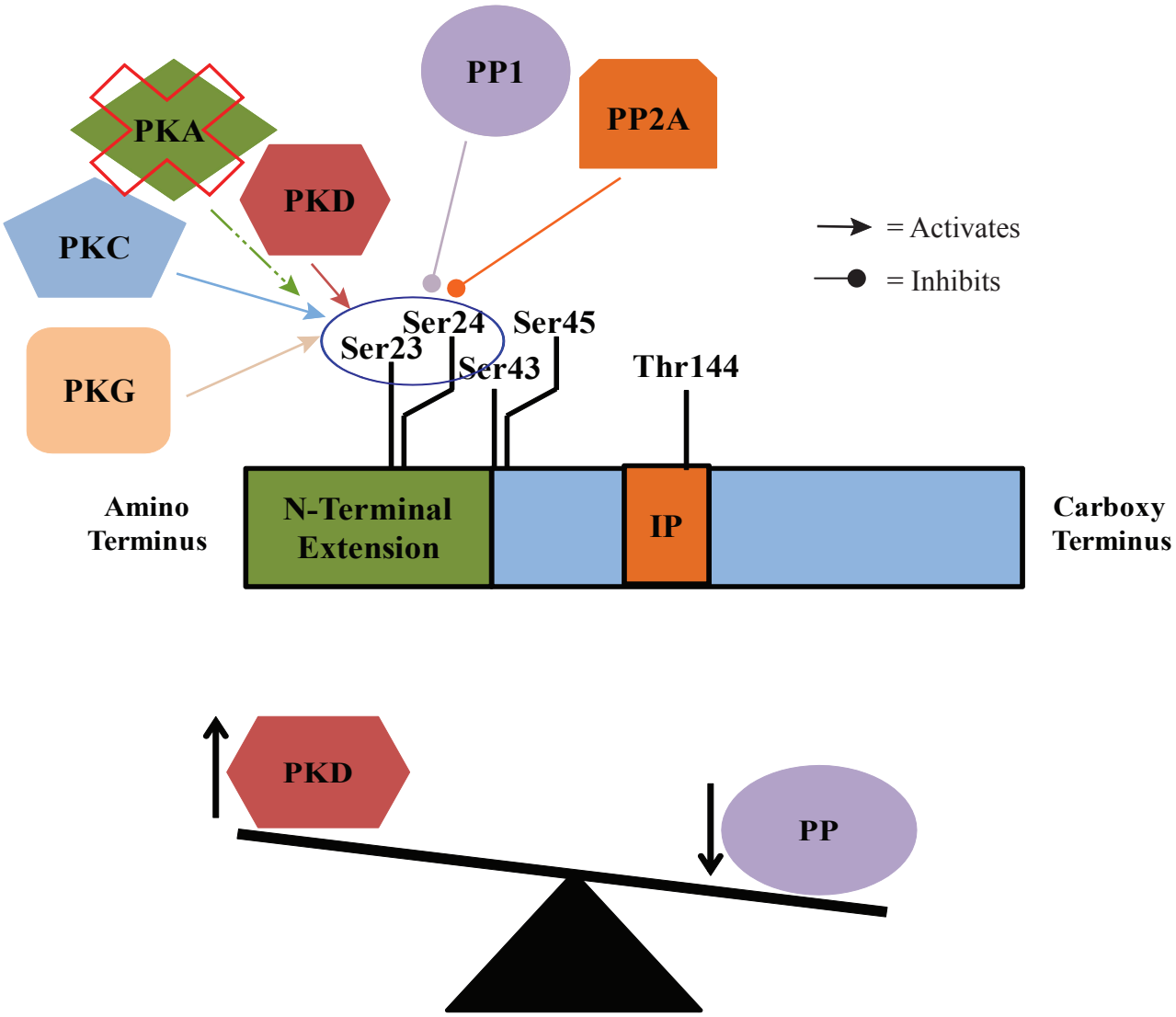

Fig. 5.4 Potential pathways for adaptive cTnISer23/24 phosphorylation. Upper panel. An illustration of the cTnI structure showing the PKC-targeted residue clusters. The amino and carboxy termini are labeled. The cardiac-specific N-terminal extension (residues 1-32) is shown in green and contains cTnISer23/24. The amino terminus containing the cTnISer43/45 residues (residues 33-80), regulatory domain (residues 147-167), and carboxyl terminus (residues 168-211) are shown in blue. The inhibitory peptide (IP; orange) contains cTnIThr144. PKA (dark green), PKD (red), PKC (blue), and PKG (peach) are candidate kinases for being part of the compensatory signaling cascade activated by cTnISer43Asp/Ser45Asp. Preliminary studies suggest PKA is not responsible for adaptive cTnISer23/24 phosphorylation (red X). PP1 (purple) and PP2A (orange) can also modulate cTnISer23/24 phosphorylation. **Lower panel.** The increased phosphorylation suggests the balance between kinase and phosphatase activity (turnover) is shifted and favors increased kinase activity and/or reduced phosphatase activity.

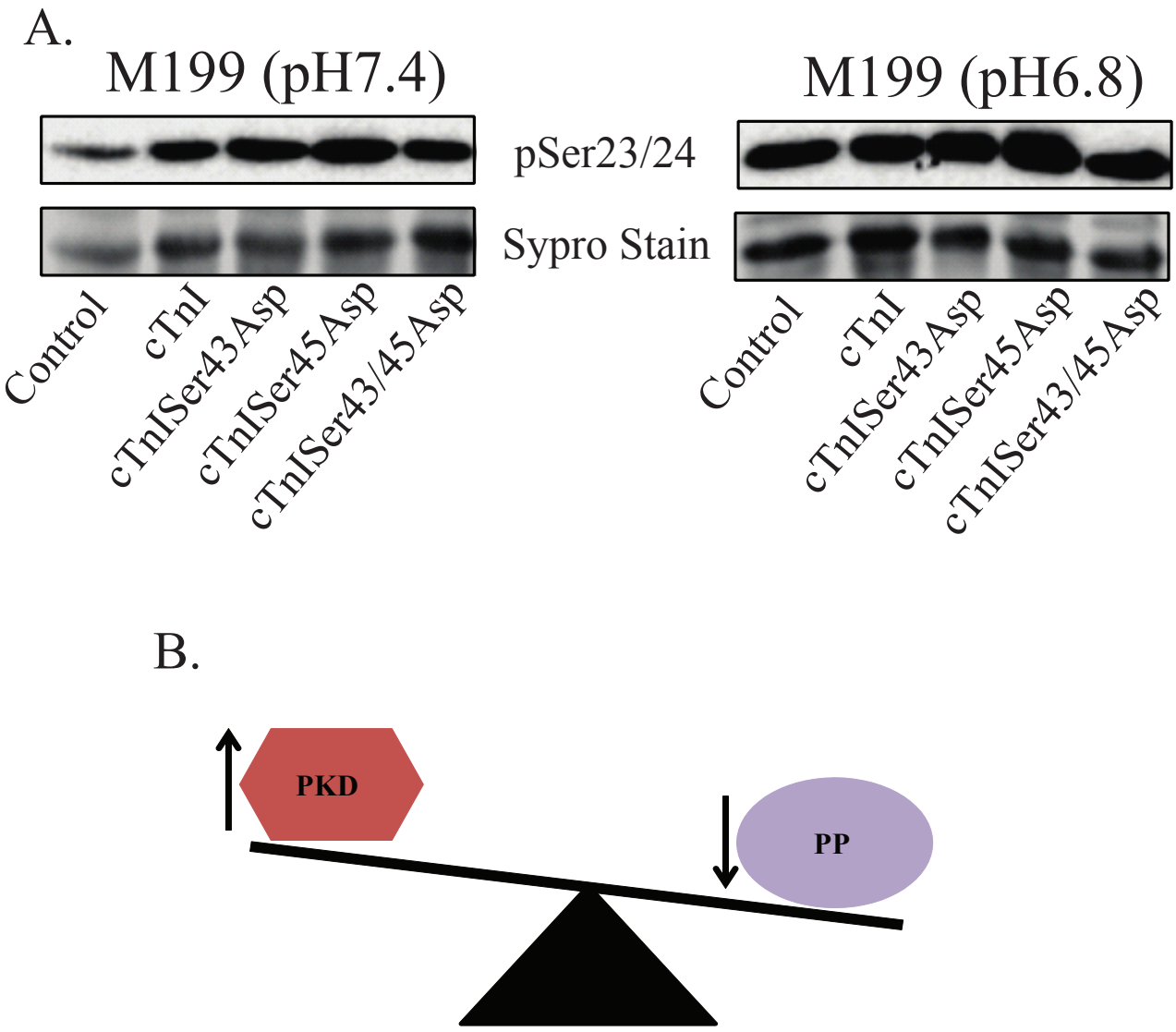

Fig. 5.5 Acidosis mimetic produces a similar adaptive response to cTnISer43/45Asp. A. Representative Western blot analysis of cTnISer23/24 phosphorylation in myocytes treated with M199 at physiological pH (pH 7.4; left columns; top row) and in response to cellular acidosis (pH 6.8; right columns; top row). Myocytes were treated with M199 alone. A section of sypro-stained blot illustrates protein loading in each lane. **B.** Potential mechanism(s) for ischemia-induced alterations to cTnISer23/24 phosphorylation. Kinase (red) activity may be up-regulated or phosphatase activity reduced following cellular acidosis. Both alterations would increase cTnISer23/24 phosphorylation.

REFERENCES

1. Widmaier, R., Strang, *Vander's Human Physiology* 10th ed. 2006, Boston: McGraw-Hill. 827.
2. Berne, L., *Cardiovascular Physiology*. 4th ed. 1981, St Louis: CV Mosby. 286.
3. Solaro, R.J., M. Henze, and T. Kobayashi, *Integration of troponin I phosphorylation with cardiac regulatory networks.* Circ Res, 2013. **112**(2): p. 355-66.
4. Solaro, R.J. and T. Kobayashi, *Protein phosphorylation and signal transduction in cardiac thin filaments.* J Biol Chem, 2011. **286**(12): p. 9935-40.
5. Wittkopper, K., et al., *Phosphatase-1 inhibitor-1 in physiological and pathological beta-adrenoceptor signalling.* Cardiovasc Res, 2011. **91**(3): p. 392-401.
6. Kass, D.A. and R.J. Solaro, *Mechanisms and use of calcium-sensitizing agents in the failing heart.* Circulation, 2006. **113**(2): p. 305-15.
7. Davis, J., et al., *Designing heart performance by gene transfer.* Physiol Rev, 2008. **88**(4): p. 1567-651.
8. Bers, D.M. and T. Guo, *Calcium signaling in cardiac ventricular myocytes.* Ann N Y Acad Sci, 2005. **1047**: p. 86-98.
9. Day, S.M., M.V. Westfall, and J.M. Metzger, *Tuning cardiac performance in ischemic heart disease and failure by modulating myofilament function.* J Mol Med (Berl), 2007. **85**(9): p. 911-21.
10. Bers, D.M., *Cardiac excitation-contraction coupling.* Nature, 2002. **415**(6868): p. 198-205.
11. Previs, M.J., et al., *Molecular mechanics of cardiac myosin-binding protein C in native thick filaments.* Science, 2012. **337**(6099): p. 1215-8.
12. Tajsharghi, H., *Thick and thin filament gene mutations in striated muscle diseases.* Int J Mol Sci, 2008. **9**(7): p. 1259-75.
13. Murphy, A.M., *Heart failure, myocardial stunning, and troponin: a key regulator of the cardiac myofilament.* Congest Heart Fail, 2006. **12**(1): p. 32-8; quiz 39-40.
14. Geeves, M.A. and P.B. Conibear, *The role of three-state docking of myosin S1 with actin in force generation.* Biophys J, 1995. **68**(4 Suppl): p. 194S-199S; discussion 199S-201S.
15. Scruggs, S.B. and R.J. Solaro, *The significance of regulatory light chain phosphorylation in cardiac physiology.* Arch Biochem Biophys, 2011. **510**(2): p. 129-34.
16. Barefield, D. and S. Sadayappan, *Phosphorylation and function of cardiac myosin binding protein-C in health and disease.* J Mol Cell Cardiol, 2010. **48**(5): p. 866-75.
17. Flashman, E., et al., *Cardiac myosin binding protein C: its role in physiology and disease.* Circ Res, 2004. **94**(10): p. 1279-89.
18. Mun, J.Y., et al., *Electron microscopy and 3D reconstruction of F-actin decorated with cardiac myosin-binding protein C (cMyBP-C).* J Mol Biol, 2011. **410**(2): p. 214-25.
19. Colson, B.A., et al., *Differential roles of regulatory light chain and myosin binding protein-C phosphorylations in the modulation of cardiac force development.* J Physiol, 2010. **588**(Pt 6): p. 981-93.
20. Gordon, A.M., M. Regnier, and E. Homsher, *Skeletal and cardiac muscle contractile activation: tropomyosin "rocks and rolls".* News Physiol Sci, 2001. **16**: p. 49-55.
21. Dong, W.J., et al., *Conformation of the regulatory domain of cardiac muscle troponin C in its complex with cardiac troponin I.* J Biol Chem, 1999. **274**(44): p. 31382-90.
22. McKillop, D.F. and M.A. Geeves, *Regulation of the interaction between actin and myosin subfragment 1: evidence for three states of the thin filament.* Biophys J, 1993. **65**(2): p. 693-701.
23. Solaro, R.J. and J. Van Eyk, *Altered interactions among thin filament proteins modulate cardiac function.* J Mol Cell Cardiol, 1996. **28**(2): p. 217-30.
24. Little, S.C., et al., *The rates of Ca2+ dissociation and cross-bridge detachment from ventricular myofibrils as reported by a fluorescent cardiac troponin C.* J Biol Chem, 2012. **287**(33): p. 27930-40.

25. Takeda, S., et al., *Structure of the core domain of human cardiac troponin in the Ca(2+)-saturated form.* Nature, 2003. **424**(6944): p. 35-41.
26. Noland, T.A., Jr., R.L. Raynor, and J.F. Kuo, *Identification of sites phosphorylated in bovine cardiac troponin I and troponin T by protein kinase C and comparative substrate activity of synthetic peptides containing the phosphorylation sites.* J Biol Chem, 1989. **264**(34): p. 20778-85.
27. Zhang, P., et al., *Multiple reaction monitoring to identify site-specific troponin I phosphorylated residues in the failing human heart.* Circulation, 2012. **126**(15): p. 1828-37.
28. Bodor, G.S., et al., *Troponin I phosphorylation in the normal and failing adult human heart.* Circulation, 1997. **96**(5): p. 1495-500.
29. Christopher, B., et al., *Reduced force production during low blood flow to the heart correlates with altered troponin I phosphorylation.* J Muscle Res Cell Motil, 2009. **30**(3-4): p. 111-23.
30. Dong, X., et al., *Augmented phosphorylation of cardiac troponin I in hypertensive heart failure.* J Biol Chem, 2012. **287**(2): p. 848-57.
31. Walker, L.A., et al., *Stage-specific changes in myofilament protein phosphorylation following myocardial infarction in mice.* J Mol Cell Cardiol, 2010. **48**(6): p. 1180-6.
32. Wachter, S.B. and E.M. Gilbert, *Beta-adrenergic receptors, from their discovery and characterization through their manipulation to beneficial clinical application.* Cardiology, 2012. **122**(2): p. 104-12.
33. Perry, S.V. and H.A. Cole, *Phosphorylation of troponin and the effects of interactions between the components of the complex.* Biochem J, 1974. **141**(3): p. 733-43.
34. Swiderek, K., et al., *Cardiac troponin I, isolated from bovine heart, contains two adjacent phosphoserines. A first example of phosphoserine determination by derivatization to S-ethylcysteine.* Eur J Biochem, 1988. **176**(2): p. 335-42.
35. Zhang, J., et al., *Deciphering modifications in swine cardiac troponin I by top-down high-resolution tandem mass spectrometry.* J Am Soc Mass Spectrom, 2010. **21**(6): p. 940-8.
36. Ayaz-Guner, S., et al., *In vivo phosphorylation site mapping in mouse cardiac troponin I by high resolution top-down electron capture dissociation mass spectrometry: Ser22/23 are the only sites basally phosphorylated.* Biochemistry, 2009. **48**(34): p. 8161-70.
37. Zabrouskov, V., et al., *Unraveling molecular complexity of phosphorylated human cardiac troponin I by top down electron capture dissociation/electron transfer dissociation mass spectrometry.* Mol Cell Proteomics, 2008. **7**(10): p. 1838-49.
38. Mittmann, K., K. Jaquet, and L.M. Heilmeyer, Jr., *Ordered phosphorylation of a duplicated minimal recognition motif for cAMP-dependent protein kinase present in cardiac troponin I.* FEBS Lett, 1992. **302**(2): p. 133-7.
39. Keane, N.E., et al., *The ordered phosphorylation of cardiac troponin I by the cAMP-dependent protein kinase--structural consequences and functional implications.* Eur J Biochem, 1997. **248**(2): p. 329-37.
40. Zhang, R., J. Zhao, and J.D. Potter, *Phosphorylation of both serine residues in cardiac troponin I is required to decrease the Ca2+ affinity of cardiac troponin C.* J Biol Chem, 1995. **270**(51): p. 30773-80.
41. Wattanapermpool, J., X. Guo, and R.J. Solaro, *The unique amino-terminal peptide of cardiac troponin I regulates myofibrillar activity only when it is phosphorylated.* J Mol Cell Cardiol, 1995. **27**(7): p. 1383-91.
42. Dong, W.J., et al., *Effects of PKA phosphorylation of cardiac troponin I and strong crossbridge on conformational transitions of the N-domain of cardiac troponin C in regulated thin filaments.* Biochemistry, 2007. **46**(34): p. 9752-61.
43. Yasuda, S., et al., *Cardiac transgenic and gene transfer strategies converge to support an important role for troponin I in regulating relaxation in cardiac myocytes.* Circ Res, 2007. **101**(4): p. 377-86.
44. Robertson, S.P., et al., *The effect of troponin I phosphorylation on the Ca2+-binding properties of the Ca2+-regulatory site of bovine cardiac troponin.* J Biol Chem, 1982. **257**(1): p. 260-3.

45. Noland, T.A., Jr., et al., *Cardiac troponin I mutants. Phosphorylation by protein kinases C and A and regulation of Ca(2+)-stimulated MgATPase of reconstituted actomyosin S-1.* J Biol Chem, 1995. **270**(43): p. 25445-54.
46. Zhang, R., et al., *Cardiac troponin I phosphorylation increases the rate of cardiac muscle relaxation.* Circ Res, 1995. **76**(6): p. 1028-35.
47. Pi, Y., et al., *Protein kinase C and A sites on troponin I regulate myofilament Ca2+ sensitivity and ATPase activity in the mouse myocardium.* J Physiol, 2003. **552**(Pt 3): p. 845-57.
48. Takimoto, E., et al., *Frequency- and afterload-dependent cardiac modulation in vivo by troponin I with constitutively active protein kinase A phosphorylation sites.* Circ Res, 2004. **94**(4): p. 496-504.
49. Sakthivel, S., et al., *In vivo and in vitro analysis of cardiac troponin I phosphorylation.* J Biol Chem, 2005. **280**(1): p. 703-14.
50. Steinberg, S.F., *Cardiac actions of protein kinase C isoforms.* Physiology (Bethesda), 2012. **27**(3): p. 130-9.
51. Noland, T.A., Jr. and J.F. Kuo, *Protein kinase C phosphorylation of cardiac troponin I and troponin T inhibits Ca(2+)-stimulated MgATPase activity in reconstituted actomyosin and isolated myofibrils, and decreases actin-myosin interactions.* J Mol Cell Cardiol, 1993. **25**(1): p. 53-65.
52. Rohde, S., et al., *The alpha(1)-adrenoceptor subtype- and protein kinase C isoform-dependence of Norepinephrine's actions in cardiomyocytes.* J Mol Cell Cardiol, 2000. **32**(7): p. 1193-209.
53. Sugden, P.H., *An overview of endothelin signaling in the cardiac myocyte.* J Mol Cell Cardiol, 2003. **35**(8): p. 871-86.
54. Egger, M. and A.A. Domenighetti, *Adaptive and maladaptive remodeling of cardiomyocyte excitation-contraction coupling by angiotensin II.* Trends Cardiovasc Med, 2010. **20**(3): p. 78-85.
55. Steinberg, S.F., *Structural basis of protein kinase C isoform function.* Physiol Rev, 2008. **88**(4): p. 1341-78.
56. Bowling, N., et al., *Increased protein kinase C activity and expression of Ca2+-sensitive isoforms in the failing human heart.* Circulation, 1999. **99**(3): p. 384-91.
57. Rybin, V.O. and S.F. Steinberg, *Protein kinase C isoform expression and regulation in the developing rat heart.* Circ Res, 1994. **74**(2): p. 299-309.
58. Bogoyevitch, M.A., P.J. Parker, and P.H. Sugden, *Characterization of protein kinase C isotype expression in adult rat heart. Protein kinase C-epsilon is a major isotype present, and it is activated by phorbol esters, epinephrine, and endothelin.* Circ Res, 1993. **72**(4): p. 757-67.
59. Sumandea, M.P., et al., *Tyrosine phosphorylation modifies protein kinase C delta-dependent phosphorylation of cardiac troponin I.* J Biol Chem, 2008. **283**(33): p. 22680-9.
60. Jideama, N.M., et al., *Phosphorylation specificities of protein kinase C isozymes for bovine cardiac troponin I and troponin T and sites within these proteins and regulation of myofilament properties.* J Biol Chem, 1996. **271**(38): p. 23277-83.
61. Noland, T.A., Jr., et al., *Differential regulation of cardiac actomyosin S-1 MgATPase by protein kinase C isozyme-specific phosphorylation of specific sites in cardiac troponin I and its phosphorylation site mutants.* Biochemistry, 1996. **35**(47): p. 14923-31.
62. Kirk, J.A., et al., *Left ventricular and myocardial function in mice expressing constitutively pseudophosphorylated cardiac troponin I.* Circ Res, 2009. **105**(12): p. 1232-9.
63. Noland, T.A., Jr. and J.F. Kuo, *Protein kinase C phosphorylation of cardiac troponin I or troponin T inhibits Ca2(+)-stimulated actomyosin MgATPase activity.* J Biol Chem, 1991. **266**(8): p. 4974-8.
64. Pi, Y., et al., *Phosphorylation of troponin I controls cardiac twitch dynamics: evidence from phosphorylation site mutants expressed on a troponin I-null background in mice.* Circ Res, 2002. **90**(6): p. 649-56.
65. Noguchi, T., et al., *Thin-filament-based modulation of contractile performance in human heart failure.* Circulation, 2004. **110**(8): p. 982-7.

66. Walker, L.A., D.A. Fullerton, and P.M. Buttrick, *Contractile protein phosphorylation predicts human heart disease phenotypes.* Am J Physiol Heart Circ Physiol, 2013. **304**(12): p. H1644-50.
67. Mathur, M.C., T. Kobayashi, and J.M. Chalovich, *Negative charges at protein kinase C sites of troponin I stabilize the inactive state of actin.* Biophys J, 2008. **94**(2): p. 542-9.
68. Burkart, E.M., et al., *Phosphorylation or glutamic acid substitution at protein kinase C sites on cardiac troponin I differentially depress myofilament tension and shortening velocity.* J Biol Chem, 2003. **278**(13): p. 11265-72.
69. Wang, H., et al., *PKC-betaII sensitizes cardiac myofilaments to Ca2+ by phosphorylating troponin I on threonine-144.* J Mol Cell Cardiol, 2006. **41**(5): p. 823-33.
70. Finley, N.L. and P.R. Rosevear, *Introduction of negative charge mimicking protein kinase C phosphorylation of cardiac troponin I. Effects on cardiac troponin C.* J Biol Chem, 2004. **279**(52): p. 54833-40.
71. Kobayashi, T., et al., *Effects of protein kinase C dependent phosphorylation and a familial hypertrophic cardiomyopathy-related mutation of cardiac troponin I on structural transition of troponin C and myofilament activation.* Biochemistry, 2004. **43**(20): p. 5996-6004.
72. MacGowan, G.A., et al., *Troponin I protein kinase C phosphorylation sites and ventricular function.* Cardiovasc Res, 2004. **63**(2): p. 245-55.
73. Montgomery, D.E., et al., *alpha-Adrenergic response and myofilament activity in mouse hearts lacking PKC phosphorylation sites on cardiac TnI.* Am J Physiol Heart Circ Physiol, 2002. **282**(6): p. H2397-405.
74. Pyle, W.G., et al., *Troponin I serines 43/45 and regulation of cardiac myofilament function.* Am J Physiol Heart Circ Physiol, 2002. **283**(3): p. H1215-24.
75. Hinken, A.C., et al., *Protein kinase C depresses cardiac myocyte power output and attenuates myofilament responses induced by protein kinase A.* J Muscle Res Cell Motil, 2012. **33**(6): p. 439-48.
76. Michele, D.E., et al., *Cardiac dysfunction in hypertrophic cardiomyopathy mutant tropomyosin mice is transgene-dependent, hypertrophy-independent, and improved by beta-blockade.* Circ Res, 2002. **91**(3): p. 255-62.
77. Westfall, M.V., E.M. Rust, and J.M. Metzger, *Slow skeletal troponin I gene transfer, expression, and myofilament incorporation enhances adult cardiac myocyte contractile function.* Proc Natl Acad Sci U S A, 1997. **94**(10): p. 5444-9.
78. Westfall, M.V. and A.R. Borton, *Role of troponin I phosphorylation in protein kinase C-mediated enhanced contractile performance of rat myocytes.* J Biol Chem, 2003. **278**(36): p. 33694-700.
79. Pyle, W.G., J.W. Lester, and P.A. Hofmann, *Effects of kappa-opioid receptor activation on myocardium.* Am J Physiol Heart Circ Physiol, 2001. **281**(2): p. H669-78.
80. Lester, J.W., et al., *Effects of adenosine and protein kinase C stimulation on mechanical properties of rat cardiac myocytes.* Am J Physiol, 1996. **271**(5 Pt 2): p. H1778-85.
81. Sumandea, M.P., et al., *Molecular and integrated biology of thin filament protein phosphorylation in heart muscle.* Ann N Y Acad Sci, 2004. **1015**: p. 39-52.
82. MacGowan, G.A., et al., *Ischemic dysfunction in transgenic mice expressing troponin I lacking protein kinase C phosphorylation sites.* Am J Physiol Heart Circ Physiol, 2001. **280**(2): p. H835-43.
83. Murphy, A.M., et al., *Molecular cloning of rat cardiac troponin I and analysis of troponin I isoform expression in developing rat heart.* Biochemistry, 1991. **30**(3): p. 707-12.
84. Michele, D.E., F.P. Albayya, and J.M. Metzger, *Thin filament protein dynamics in fully differentiated adult cardiac myocytes: toward a model of sarcomere maintenance.* J Cell Biol, 1999. **145**(7): p. 1483-95.
85. Westfall, M.V., et al., *Adenovirus-mediated myofilament gene transfer into adult cardiac myocytes.* Methods Cell Biol, 1997. **52**: p. 307-22.

86. Westfall, M.V., A.M. Lee, and D.A. Robinson, *Differential contribution of troponin I phosphorylation sites to the endothelin-modulated contractile response.* J Biol Chem, 2005. **280**(50): p. 41324-31.
87. Sweitzer, N.K. and R.L. Moss, *The effect of altered temperature on Ca2(+)-sensitive force in permeabilized myocardium and skeletal muscle. Evidence for force dependence of thin filament activation.* J Gen Physiol, 1990. **96**(6): p. 1221-45.
88. Metzger, J.M., et al., *Effects of myosin heavy chain isoform switching on Ca2+-activated tension development in single adult cardiac myocytes.* Circ Res, 1999. **84**(11): p. 1310-7.
89. Reitz, F.B. and G.H. Pollack, *Labview virtual instruments for calcium buffer calculations.* Comput Methods Programs Biomed, 2003. **70**(1): p. 61-9.
90. Westfall, M.V., et al., *Myofilament calcium sensitivity and cardiac disease: insights from troponin I isoforms and mutants.* Circ Res, 2002. **91**(6): p. 525-31.
91. Westfall, M.V. and J.M. Metzger, *Single amino acid substitutions define isoform-specific effects of troponin I on myofilament Ca2+ and pH sensitivity.* J Mol Cell Cardiol, 2007. **43**(2): p. 107-18.
92. Kramer, B.K., T.W. Smith, and R.A. Kelly, *Endothelin and increased contractility in adult rat ventricular myocytes. Role of intracellular alkalosis induced by activation of the protein kinase C-dependent Na(+)-H+ exchanger.* Circ Res, 1991. **68**(1): p. 269-79.
93. Haworth, R.S., et al., *Protein kinase D is a novel mediator of cardiac troponin I phosphorylation and regulates myofilament function.* Circ Res, 2004. **95**(11): p. 1091-9.
94. Cuello, F., et al., *Protein kinase D selectively targets cardiac troponin I and regulates myofilament Ca2+ sensitivity in ventricular myocytes.* Circ Res, 2007. **100**(6): p. 864-73.
95. Jin, C.Z., et al., *Myofilament Ca2+ desensitization mediates positive lusitropic effect of neuronal nitric oxide synthase in left ventricular myocytes from murine hypertensive heart.* J Mol Cell Cardiol, 2013. **60**: p. 107-15.
96. Layland, J., R.J. Solaro, and A.M. Shah, *Regulation of cardiac contractile function by troponin I phosphorylation.* Cardiovasc Res, 2005. **66**(1): p. 12-21.
97. Clement, O., et al., *Protein kinase C enhances myosin light-chain kinase effects on force development and ATPase activity in rat single skinned cardiac cells.* Biochem J, 1992. **285 (Pt 1)**: p. 311-7.
98. Noland, T.A., Jr. and J.F. Kuo, *Phosphorylation of cardiac myosin light chain 2 by protein kinase C and myosin light chain kinase increases Ca(2+)-stimulated actomyosin MgATPase activity.* Biochem Biophys Res Commun, 1993. **193**(1): p. 254-60.
99. Lang, S.E., et al., *Myofilament incorporation and contractile function after gene transfer of cardiac troponin I Ser43/45Ala.* Arch Biochem Biophys, 2013. **535**(1): p. 49-55.
100. Kampert, S.E., E. Devaney, and M.V. Westfall, *Gene Transfer and Expression in Animal Cells*, in *Handbook of Molecular and Cellular Methods in Biology and Medicine*, A.K. LJ Cseke, PB Kaufman, and MV Westfall, Editor. 2011, CRC Press: Boca Raton, Florida. p. 557-578.
101. Sadayappan, S., et al., *Cardiac myosin binding protein-C phosphorylation in a {beta}-myosin heavy chain background.* Circulation, 2009. **119**(9): p. 1253-62.
102. Hwang, H., et al., *PKCbetaII modulation of myocyte contractile performance.* J Mol Cell Cardiol, 2012. **53**(2): p. 176-86.
103. Haworth, R.A. and D. Redon, *Calibration of intracellular Ca transients of isolated adult heart cells labelled with fura-2 by acetoxymethyl ester loading.* Cell Calcium, 1998. **24**(4): p. 263-73.
104. Kranias, E.G. and R.J. Hajjar, *Modulation of cardiac contractility by the phospholamban/SERCA2a regulatome.* Circ Res, 2012. **110**(12): p. 1646-60.
105. Tikunova, S.B., et al., *Effect of calcium-sensitizing mutations on calcium binding and exchange with troponin C in increasingly complex biochemical systems.* Biochemistry, 2010. **49**(9): p. 1975-84.

106. Morimoto, S., et al., *A pH-sensitive interaction of troponin I with troponin C coupled with strongly binding cross-bridges in cardiac myofilament activation.* Biochem Biophys Res Commun, 2001. **282**(3): p. 811-5.
107. McDonald, K.S. and R.L. Moss, *Strongly binding myosin crossbridges regulate loaded shortening and power output in cardiac myocytes.* Circ Res, 2000. **87**(9): p. 768-73.
108. Edman, K.A. and A.R. Mattiazzi, *Effects of fatigue and altered pH on isometric force and velocity of shortening at zero load in frog muscle fibres.* J Muscle Res Cell Motil, 1981. **2**(3): p. 321-34.
109. Tong, C.W., et al., *Acceleration of crossbridge kinetics by protein kinase A phosphorylation of cardiac myosin binding protein C modulates cardiac function.* Circ Res, 2008. **103**(9): p. 974-82.
110. Stelzer, J.E., J.R. Patel, and R.L. Moss, *Protein kinase A-mediated acceleration of the stretch activation response in murine skinned myocardium is eliminated by ablation of cMyBP-C.* Circ Res, 2006. **99**(8): p. 884-90.
111. Steinberg, S.F., *Regulation of protein kinase D1 activity.* Mol Pharmacol, 2012. **81**(3): p. 284-91.
112. Tandon, M., et al., *A targeted library screen reveals a new inhibitor scaffold for protein kinase D.* PLoS One, 2012. **7**(9): p. e44653.
113. Swiderek, K., et al., *Sites phosphorylated in bovine cardiac troponin T and I. Characterization by 31P-NMR spectroscopy and phosphorylation by protein kinases.* Eur J Biochem, 1990. **190**(3): p. 575-82.
114. Hwang, H., et al., *Agonist activated PKCbetaII translocation and modulation of cardiac myocyte contractile function.* Sci Rep, 2013. **3**: p. 1971.
115. Schwoerer, A.P., et al., *Unloaded rat hearts in vivo express a hypertrophic phenotype of cardiac repolarization.* J Mol Cell Cardiol, 2008. **45**(5): p. 633-41.
116. Lu, Q.W., et al., *Phosphorylation of cardiac troponin I at protein kinase C site threonine 144 depresses cooperative activation of thin filaments.* J Biol Chem, 2010. **285**(16): p. 11810-7.
117. Howarth, J.W., et al., *Phosphorylation-dependent conformational transition of the cardiac specific N-extension of troponin I in cardiac troponin.* J Mol Biol, 2007. **373**(3): p. 706-22.
118. Sadayappan, S., et al., *Role of the acidic N' region of cardiac troponin I in regulating myocardial function.* FASEB J, 2008. **22**(4): p. 1246-57.
119. Manning, E.P., J.C. Tardiff, and S.D. Schwartz, *A model of calcium activation of the cardiac thin filament.* Biochemistry, 2011. **50**(34): p. 7405-13.
120. Chaudhri, V.K., et al., *Integration of a phosphatase cascade with the mitogen-activated protein kinase pathway provides for a novel signal processing function.* J Biol Chem, 2010. **285**(2): p. 1296-310.
121. Samoilov, M., S. Plyasunov, and A.P. Arkin, *Stochastic amplification and signaling in enzymatic futile cycles through noise-induced bistability with oscillations.* Proc Natl Acad Sci U S A, 2005. **102**(7): p. 2310-5.
122. Solaro RJ, W.M., *Physiology of the Myocardium*, in *Sabiston & Spencer Surgery of the Chest*, d.N.P. Selke FW, and Swanson SJ, Editor. 2010, Saunders Elsevier: Philadelphia. p. 725-737.
123. Kedzierski, R.M. and M. Yanagisawa, *Endothelin system: the double-edged sword in health and disease.* Annu Rev Pharmacol Toxicol, 2001. **41**: p. 851-76.
124. de Tombe, P.P. and R.J. Solaro, *Integration of cardiac myofilament activity and regulation with pathways signaling hypertrophy and failure.* Ann Biomed Eng, 2000. **28**(8): p. 991-1001.
125. Kooij, V., et al., *Characterization of the cardiac myosin binding protein-C phosphoproteome in healthy and failing human hearts.* J Mol Cell Cardiol, 2013. **60**: p. 116-20.
126. El-Armouche, A., et al., *Decreased phosphorylation levels of cardiac myosin-binding protein-C in human and experimental heart failure.* J Mol Cell Cardiol, 2007. **43**(2): p. 223-9.
127. Neumann, J., et al., *Increased expression of cardiac phosphatases in patients with end-stage heart failure.* J Mol Cell Cardiol, 1997. **29**(1): p. 265-72.
128. DeGrande, S.T., et al., *Molecular mechanisms underlying cardiac protein phosphatase 2A regulation in heart.* J Biol Chem, 2013. **288**(2): p. 1032-46.

129. Heijman, J., et al., *Function and regulation of serine/threonine phosphatases in the healthy and diseased heart.* J Mol Cell Cardiol, 2013. **64**: p. 90-8.
130. Brenner, B., et al., *Driving filament sliding: weak binding cross-bridge states, strong binding cross-bridge states, and the power stroke.* Adv Exp Med Biol, 2005. **565**: p. 75-91; discussion 371-7.
131. Lehrer, S.S., *The 3-state model of muscle regulation revisited: is a fourth state involved?* J Muscle Res Cell Motil, 2011. **32**(3): p. 203-8.
132. Nixon, B.R., et al., *AMP-activated protein kinase phosphorylates cardiac troponin I at Ser-150 to increase myofilament calcium sensitivity and blunt PKA-dependent function.* J Biol Chem, 2012. **287**(23): p. 19136-47.
133. Ge, Y., et al., *Top-down high-resolution mass spectrometry of cardiac myosin binding protein C revealed that truncation alters protein phosphorylation state.* Proc Natl Acad Sci U S A, 2009. **106**(31): p. 12658-63.
134. Westfall, M.V., *Post-translational modification of troponin*, in *Troponin: Regulator of Muscle Contraction*, J. J-P, Editor. 2013, Nova Science: New York.
135. Streng, A.S., et al., *Posttranslational modifications of cardiac troponin T: an overview.* J Mol Cell Cardiol, 2013. **63**: p. 47-56.
136. Gao, M., et al., *An altered expression of genes involved in the regulation of ion channels in atrial myocytes is correlated with the risk of atrial fibrillation in patients with heart failure.* Exp Ther Med, 2013. **5**(4): p. 1239-1243.
137. Ohtsuka, M., et al., *Role of Na+-Ca2+ exchanger in myocardial ischemia/reperfusion injury: evaluation using a heterozygous Na+-Ca2+ exchanger knockout mouse model.* Biochem Biophys Res Commun, 2004. **314**(3): p. 849-53.
138. Gautel, M., et al., *Phosphorylation switches specific for the cardiac isoform of myosin binding protein-C: a modulator of cardiac contraction?* EMBO J, 1995. **14**(9): p. 1952-60.
139. Dirkx, E., et al., *Protein kinase D increases maximal Ca2+-activated tension of cardiomyocyte contraction by phosphorylation of cMyBP-C-Ser315.* Am J Physiol Heart Circ Physiol, 2012. **303**(3): p. H323-31.
140. Bardswell, S.C., et al., *Distinct sarcomeric substrates are responsible for protein kinase D-mediated regulation of cardiac myofilament Ca2+ sensitivity and cross-bridge cycling.* J Biol Chem, 2010. **285**(8): p. 5674-82.
141. Braz, J.C., et al., *PKC-alpha regulates cardiac contractility and propensity toward heart failure.* Nat Med, 2004. **10**(3): p. 248-54.
142. Kass, D.A., *Heart failure: a PKGarious balancing act.* Circulation, 2012. **126**(7): p. 797-9.
143. Tsai, E.J. and D.A. Kass, *Cyclic GMP signaling in cardiovascular pathophysiology and therapeutics.* Pharmacol Ther, 2009. **122**(3): p. 216-38.
144. Spirito, P., et al., *The management of hypertrophic cardiomyopathy.* N Engl J Med, 1997. **336**(11): p. 775-85.
145. Scruggs, S.B., et al., *Partial replacement of cardiac troponin I with a non-phosphorylatable mutant at serines 43/45 attenuates the contractile dysfunction associated with PKCepsilon phosphorylation.* J Mol Cell Cardiol, 2006. **40**(4): p. 465-73.
146. Huang, X. and J.W. Walker, *Myofilament anchoring of protein kinase C-epsilon in cardiac myocytes.* J Cell Sci, 2004. **117**(Pt 10): p. 1971-8.
147. Mohamed, A.S., J.D. Dignam, and K.K. Schlender, *Cardiac myosin-binding protein C (MyBP-C): identification of protein kinase A and protein kinase C phosphorylation sites.* Arch Biochem Biophys, 1998. **358**(2): p. 313-9.
148. Xiao, L., et al., *PKCepsilon increases phosphorylation of the cardiac myosin binding protein C at serine 302 both in vitro and in vivo.* Biochemistry, 2007. **46**(23): p. 7054-61.
149. Haworth, R.S., et al., *Expression and activity of protein kinase D/protein kinase C mu in myocardium: evidence for alpha1-adrenergic receptor- and protein kinase C-mediated regulation.* J Mol Cell Cardiol, 2000. **32**(6): p. 1013-23.

150. Rybin, V.O., J. Guo, and S.F. Steinberg, *Protein kinase D1 autophosphorylation via distinct mechanisms at Ser744/Ser748 and Ser916.* J Biol Chem, 2009. **284**(4): p. 2332-43.
151. Deshmukh, P.A., B.C. Blunt, and P.A. Hofmann, *Acute modulation of PP2a and troponin I phosphorylation in ventricular myocytes: studies with a novel PP2a peptide inhibitor.* Am J Physiol Heart Circ Physiol, 2007. **292**(2): p. H792-9.
152. Bryant, J.C., R.S. Westphal, and B.E. Wadzinski, *Methylated C-terminal leucine residue of PP2A catalytic subunit is important for binding of regulatory Balpha subunit.* Biochem J, 1999. **339 (Pt 2)**: p. 241-6.
153. Wijnker, P.J., et al., *Protein phosphatase 2A affects myofilament contractility in non-failing but not in failing human myocardium.* J Muscle Res Cell Motil, 2011. **32**(3): p. 221-33.
154. Yin, X., et al., *Proteomics analysis of the cardiac myofilament subproteome reveals dynamic alterations in phosphatase subunit distribution.* Mol Cell Proteomics, 2010. **9**(3): p. 497-509.
155. Pan, J., et al., *PKC mediates cyclic stretch-induced cardiac hypertrophy through Rho family GTPases and mitogen-activated protein kinases in cardiomyocytes.* J Cell Physiol, 2005. **202**(2): p. 536-53.
156. Seko, Y., et al., *Pulsatile stretch activates mitogen-activated protein kinase (MAPK) family members and focal adhesion kinase (p125(FAK)) in cultured rat cardiac myocytes.* Biochem Biophys Res Commun, 1999. **259**(1): p. 8-14.
157. Shearer, F., C.C. Lang, and A.D. Struthers, *Renin-angiotensin-aldosterone system inhibitors in heart failure.* Clin Pharmacol Ther, 2013. **94**(4): p. 459-67.
158. Mundina-Weilenmann, C., et al., *Effects of acidosis on phosphorylation of phospholamban and troponin I in rat cardiac muscle.* Am J Physiol, 1996. **270**(1 Pt 1): p. C107-14.
159. Pyle, W.G., T.D. Smith, and P.A. Hofmann, *Cardioprotection with kappa-opioid receptor stimulation is associated with a slowing of cross-bridge cycling.* Am J Physiol Heart Circ Physiol, 2000. **279**(4): p. H1941-8.
160. Pyle, W.G., Y. Chen, and P.A. Hofmann, *Cardioprotection through a PKC-dependent decrease in myofilament ATPase.* Am J Physiol Heart Circ Physiol, 2003. **285**(3): p. H1220-8.
161. Avkiran, M., et al., *Protein kinase d in the cardiovascular system: emerging roles in health and disease.* Circ Res, 2008. **102**(2): p. 157-63.
162. Zhang, J., et al., *Phosphorylation, but not alternative splicing or proteolytic degradation, is conserved in human and mouse cardiac troponin T.* Biochemistry, 2011. **50**(27): p. 6081-92.
163. Kemp, B.E. and R.B. Pearson, *Protein kinase recognition sequence motifs.* Trends Biochem Sci, 1990. **15**(9): p. 342-6.
164. Galinska-Rakoczy, A., et al., *Structural basis for the regulation of muscle contraction by troponin and tropomyosin.* J Mol Biol, 2008. **379**(5): p. 929-35.
165. Obenauer, J.C., L.C. Cantley, and M.B. Yaffe, *Scansite 2.0: Proteome-wide prediction of cell signaling interactions using short sequence motifs.* Nucleic Acids Res, 2003. **31**(13): p. 3635-41.
166. Miller, M.L., et al., *Linear motif atlas for phosphorylation-dependent signaling.* Sci Signal, 2008. **1**(35): p. ra2.
167. Blom, N., et al., *Prediction of post-translational glycosylation and phosphorylation of proteins from the amino acid sequence.* Proteomics, 2004. **4**(6): p. 1633-49.
168. Ward, D.G., et al., *Additional PKA phosphorylation sites in human cardiac troponin I.* Eur J Biochem, 2001. **268**(1): p. 179-85.
169. Blumenthal, D.K., J.T. Stull, and G.N. Gill, *Phosphorylation of cardiac troponin by guanosine 3':5'-monophosphate-dependent protein kinase.* J Biol Chem, 1978. **253**(2): p. 324-6.
170. Stull, J.T. and J.E. Buss, *Phosphorylation of cardiac troponin by cyclic adenosine 3':5'-monophosphate-dependent protein kinase.* J Biol Chem, 1977. **252**(3): p. 851-7.
171. Vahebi, S., et al., *Functional effects of rho-kinase-dependent phosphorylation of specific sites on cardiac troponin.* Circ Res, 2005. **96**(7): p. 740-7.

172. Itoh, S., et al., *Role of p90 ribosomal S6 kinase (p90RSK) in reactive oxygen species and protein kinase C beta (PKC-beta)-mediated cardiac troponin I phosphorylation.* J Biol Chem, 2005. **280**(25): p. 24135-42.
173. Oliveira, S.M., et al., *AMP-activated protein kinase phosphorylates cardiac troponin I and alters contractility of murine ventricular myocytes.* Circ Res, 2012. **110**(9): p. 1192-201.
174. Jaquet, K., et al., *A site phosphorylated in bovine cardiac troponin T by cardiac CaM kinase II.* Biochim Biophys Acta, 1995. **1248**(2): p. 193-5.
175. Moir, A.J. and S.V. Perry, *Phosphorylation of rabbit cardiac-muscle troponin I by phosphorylase kinase. The effect of adrenaline.* Biochem J, 1980. **191**(2): p. 547-54.
176. Raggi, A., et al., *Structure-function relationships in cardiac troponin T.* Biochim Biophys Acta, 1989. **997**(1-2): p. 135-43.
177. McClellan, G., I. Kulikovskaya, and S. Winegrad, *Changes in cardiac contractility related to calcium-mediated changes in phosphorylation of myosin-binding protein C.* Biophys J, 2001. **81**(2): p. 1083-92.
178. Scruggs, S.B., et al., *Ablation of ventricular myosin regulatory light chain phosphorylation in mice causes cardiac dysfunction in situ and affects neighboring myofilament protein phosphorylation.* J Biol Chem, 2009. **284**(8): p. 5097-106.
179. Chang, A.N., et al., *Cardiac myosin is a substrate for zipper-interacting protein kinase (ZIPK).* J Biol Chem, 2010. **285**(8): p. 5122-6.